THE EFFECT OF MOISTURE ON CARBON DIOXIDE ADSORPTION OF A SOUTH AFRICAN COAL

Rosalind Dos Santos

A research report submitted to the Faculty of Engineering and the Built Environment, University of the Witwatersrand, Johannesburg, in partial fulfilment of the requirements for the degree of Master of Science in Engineering

Johannesburg, 2013

I declare that this research report is my own unaided work, except where stated and referenced otherwise. It is being submitted to the degree of Master of Science in Engineering by advanced coursework and research to the University of the Witwatersrand, Johannesburg. It has not been submitted before for any degree or examination to any other University.

R Dos Santos

____ (day) of _____ (month), _____(year)

Abstract

The CO_2 adsorption capacity of moist South African Coal was tested. The coal used in the research was a typical power generation coal from the Witbank coalfield. There is a deficiency of research into CO_2 adsorption capacity of large particles of South African coal with varying moisture content. Moisture in coal will decrease the available sites for adsorption. A volumetric adsorption system commissioned at the University of the Witwatersrand was used to determine CO_2 adsorption of South African coal. The results showed that moisture content in coal affected adsorption capacities for pressures up to 80 bar. Particle size also negatively affected adsorption capacity with large particles adsorbing less CO_2 than smaller ones. In addition, preliminary testing of CO_2 desorption from coal with adsorbed CO_2 into distilled water indicated that this should be explored further.

Key Words

CO_2 Adsorption Capacity, South African Coal, Moisture, Large Particles

Acknowledgements

The following people assisted greatly in the completion of this research report:

Professor Nikki Wagner

Prof Wagner supervised the completion of this Masters Research Report and the Coursework Component for this MSc Eng degree. She was available for consultation whenever guidance was needed and assisted greatly in all consumable items that were necessary for the completion of the research. Prof Wagner also completed all petrography work that has been presented in this report.

Mr Mulanga Maphada

Mr Maphada designed and commissioned the volumetric adsorption equipment at the University of the Witwatersrand for the completion of his MSc Eng degree. Without his work this research would not have been possible. He also started the process of automating the equipment.

Mr Tshifiwa Maphala

Mr Maphala, a PhD candidate at the University of the Witwatersrand, assisted in the training of all students needing to use the volumetric adsorption equipment. He also completed the automation of the equipment. Further he was always available for assistance and leak detection on the equipment which helped immeasurably.

Mr Alan Johns

Mr John, of ALS Laboratories, completed the moisture content determination on the as received sample free of charge for this project.

Mr Gregory Okolo

Mr Okolo, a PhD student of North West University, completed the surface area analysis on the samples used in this research.

Table of Contents

Acknowledgements 4
List of Figures 9
List of Tables 11
List of Symbols 14
Nomenclature 16
1 Introduction 17
2 Literature Review and Laboratory Adsorption Equipment Overview 20
2.1 Carbon Capture and Storage (CCS) 20
2.1.1 What is CCS? 20
2.1.2 CO_2 Storage 22
2.1.3 Carbon Capture and Storage (CCS) Potential in South Africa 24
2.1.4 Carbon Capture and Storage (CCS) in Unmineable Coal Seams 29
2.2 Moisture in Coal 30
2.2.1 Terminology 30
2.2.2 Location and Effect of Moisture in the Coal 31
2.2.3 International Standards for Coal Moisture Determination 33
2.3 CO_2 Adsorption on Coal 36
2.3.1 Principles of CO_2 Adsorption on Coal 36
2.3.2 Effects of Coal Properties on CO_2 Adsorption 37
2.3.3 Effect of Particle Size on Adsorption 39
2.3.4 Pressure Effects on Adsorption 39
2.3.5 Interactions of CO_2 with other Non-Coal Components 40
2.3.6 Models describing Adsorption 41
2.4 CO_2 Solubility in water 42
2.5 Chapter Summary 44
3 Hypothesis and Key Research Outcomes 45
3.1 Hypothesis 45

3.2 Key Research Outcomes 45
4 Methodology 46
4.1 Coal Preparation 46
4.2 As Received Coal Moisture Determination 47
4.3 Coal Characterisation 48
4.3.1 Petrography 48
4.3.2 Surface Area Analysis 49
4.3.3 TGA Analysis 49
4.4 Coal Particle Selection for Adsorption Experimentation 50
4.5 Coal Degassing and Moisturisation 50
4.6 True Volume Measurement 51
4.7 Adsorption Experimentation 52
4.7.1 Adsorption Capacity Testing Equipment 52
4.7.2 Equipment Details and Operation 53
4.7.3 Equipment Volume 58
4.7.4 Correcting for Leakage in the System 59
4.7.5 Adsorption calculations 60
4.8 Desorption of Added CO_2 into Distilled Water 64
4.9 Chapter Summary 65
5 Results 66
5.1 Coal Analyses 66
5.1.1 Coal Moisture Determination 66
5.1.2 Petrographic Analyses 66
5.1.3 Surface Area Analyses 69
5.1.4 TGA Analyses 69
5.2 Coal Moisturisation 71
5.3 True Volume Measurement 73

5.4 Calculation of the Equipment Volume 75

5.5 Adsorption 76

5.5.1 Preliminary Experimentation to Determine the Correct Equilibration Time for Samples 76

5.5.2 Adsorption Experimentation Results with 9.5 – 6.7 mm Size Class Particles .. 84

5.5.3 Adsorption Experimentation Results with 22.4 – 16 mm Size Class Particles and 3 hr Equilibration Times 92

5.6 Desorption 101

5.7 Chapter Summary 103

6 Discussion 104

6.1 Coal Analyses 104

6.1.1. Coal Moisture Determination 104

6.1.2 Surface Area Analysis 104

6.1.3 TGA Analysis and Petrographic Analysis 105

6.2 Coal Particle Selection 106

6.3 Coal Moisturisation 106

6.4 True Volume Measurement 108

6.5 Equipment Volume 108

6.6 Adsorption Testing 109

6.6.1 Volumetric Adsorption Equipment 109

6.6.2 Experiment Design 110

6.6.3 Impact of Equilibration Time on Adsorption Capacity 111

6.6.4 Adsorption Experimentation Results with 9.5 – 6.7 mm Size Class Particles 115

6.6.5 Adsorption Experimentation Results with 22.4 – 16 mm Size Class Particles 116

6.6.6 Impact of Moisture on Adsorption Capacity 117

6.6.7 Impact of Particle Size on Adsorption 120

6.6.8 Comparison with Published Results 121

6.7 Desorption 125

6.8 Chapter Summary 126

7 Conclusions 127

8 Recommendations 129

References 131

Appendix A – Compressibility Factors used in the Calculation of CO_2 Adsorption..... 136

Appendix B– Derivation of He Stereo Pycnometer Equation 145

Appendix C– Coal Analyses Results..... 147

Appendix D – Results of Blank Runs to Quantify Equipment Leakage..... 148

List of Figures

Figure 1: Phase diagram of CO_2 (CO_2 Info, 2006) 22
Figure 2: Long Term Mitigation Scenarios for South Africa (Energy Research Centre, 2007) 25
Figure 3: Work plan and timeline of the SACCCS (SACCCS, 2012) 26
Figure 4: Coal fields of South Africa (Falcon, 1989) 27
Figure 5: Image from the *Atlas on Geological Storage in South Africa* (Cloete, 2010) showing all identified storage sites in South Africa 28
Figure 6: CO_2 Emissions and their intensity across South Africa (Cloete, 2010) 29
Figure 7: Adsorption of water vapour on coal with increasing relative pressure (Charrière&Behra, 2010) 32
Figure 8: Core aspects of the laboratory CO_2 adsorption equipment 54
Figure 9: Picture of the laboratory adsorption equipment showing the pump, oven, degassing system, and the data logging system (see text for annotations) 54
Figure 10: Top View of Pressure Vessel/Reactor B used in the adsorption capacity testing 56
Figure 11: Internal view of the pressure vessel/reactor used to hold the coal samples .. 56
Figure 12: Reactive and inert semifusinite (oil immersion lense, reflected light petrographic image) 67
Figure 13: Picture of the vitrinite component in the coal (oil immersion lense, reflected light petrographic image) 68
Figure 14: Carbonate minerals (grey/brown) distributed in the coal (Light Grey) [oil immersion lense, reflected light petrographic image] 68
Figure 15: Proximate analysis data - mass loss during heating of the coal sample representing size class 9.5 – 6.7 mm 70
Figure 16: Data sheet from true volume measurement of a coal particle in the He Pycnometer 74
Figure 17: Plot of the pressure steps used in experimentation on the CO_2 adsorptive capacity of coal used in this research 77
Figure 18: Gradual pressure decrease for a single pressure step as adsorption occurs in the sample cell 78
Figure 19: Cumulative moles of CO_2 adsorbed for preliminary testing of 9.5 -6.7 mm samples in the Volumetric Adsorption Equipment 83
Figure 20: Volume of CO_2 adsorbed per ton for preliminary testing of the 9.5 -6.7 mm samples that were placed in the Volumetric Adsorption Equipment 84
Figure 21: Cumulative moles of CO_2 adsorbed by 9.5 – 6.7 mm size class particles 91
Figure 22: Specific Adsorption Capacity of the 9.5 – 6.7 mm size class particles 92
Figure 23: Screenshot of the error logs from the volumetric adsorption equipment 95
Figure 24: Cumulative moles of CO_2 adsorbed by 22.4 - 16 mm size class particles 100
Figure 25: Specific Adsorption Capacity of the 22.4 to 16 mm size class particles 100
Figure 26: 22.4 – 16 mm particle placed in distilled water after removal from the Volumetric Adsorption Equipment 102

Figure 27: Sheared and snapped bolt from the pressure vessels/reactors 109
Figure 28: Difference in specific adsorption capacities with 9.5 – 6.7 mm size class particles where different adsorption equilibration times were used..... 113
Figure 29: Comparison of 9.5 – 6.7 mm particles to determine whether the equipment was leaking during preliminary testing to determine the correct equilibration time 114
Figure 30: Pressure decrease with adsorption on Sample 3 (14.45%, 3hrs) in the second pressure step..... 115
Figure 31: Specific Adsorption Capacity of particles S3 to S5 from the 9.5 – 6.7 mm size class particles 116
Figure 32: Specific Adsorption Capacity of particles L1, L2, L3, L4 and L6 from the 22.4 – 16 mm size class particles 117
Figure 33: Differing adsorption capacities between dry and moisturized 9.5 – 6.7 mm size class samples..... 118
Figure 34: Specific Adsorption capacity of different size class particles (S3, S4, S5, L1, L2, L3, L4, L6) 120
Figure 35: Specific Adsorption capacity of different size class particles (S3, S4, S5, L1, L2, L3, L4) 121
Figure 36: Adsorption curves generated in research on South African coal by Saghafi *et al*. (2008) 123
Figure 37: CO_2 and CH_4 adsorption capacities of low rank South African Coal 124
Figure 38: ALS laboratory group coal moisture determination analysis results 147

List of Tables

Table 1: Increasing solubility of CO_2 with increasing pressure 43
Table 2: Size classification of sample and distribution of particles in different size classes 47
Table 3: Further size classification of 2.36 – 9.5 mm size fraction 47
Table 4: CO_2 Compressibility factors at different pressures and temperatures (Perry *et al.*, 1997) 62
Table 5: Compressibility factors for CO_2 that were used in the calculation of the results of this research 63
Table 6: Summary of Adsorption Experimentation, Particles, Size Classes and Sample IDs 66
Table 7: Maceral groups and the volume percentages in which they occur in the 9.5 – 6.7 mm and 22.4 – 16 mm size class representative samples 67
Table 8: Surface area analysis results for the 22.4 – 16 mm size class sample and the two 9.5 - 6.7 mm particles 69
Table 9: Proximate analysis on 9.5 – 6.7 mm and 22.4 – 16 mm size class coal used in experimentation 70
Table 10: Moisture addition to particles in the 9.5 – 6.7 mm size class 71
Table 11: Change in mass of particles from the 9.5 – 6.7 mm size class with evaporation of adsorbed water 72
Table 12: Change in mass of particle L7 from the 22.4 – 16 mm size class with evaporation of adsorbed water 73
Table 13: Volume particles measured in the He Pycnometer 75
Table 14: Determination of the Volume of the Sample Cell through Helium Expansion in the constant volume system 76
Table 15: Recorded pressures and temperatures and calculated CO_2 adsorption for Sample 1 79
Table 16: CO_2 adsorption quantified in terms of Sample 1 mass 79
Table 17: Recorded pressures and temperatures and calculated CO_2 adsorption for Sample 2 80
Table 18: CO_2 adsorption quantified in terms of Sample 2 mass 80
Table 19: Recorded pressures and temperatures and calculated CO_2 adsorption for Sample 3 81
Table 20: CO_2 adsorption quantified in terms of Sample 3 mass 81
Table 21: Recorded pressures and temperatures and calculated CO_2 adsorption for Sample 4 82
Table 22: CO_2 adsorption quantified in terms of Sample 4 mass 82
Table 23: New sample identifications for ease of comparison of results 83
Table 24: Recorded pressures and temperatures and calculated CO_2 adsorption for S1 85
Table 25: CO_2 adsorption quantified in terms of Sample S1 mass 86
Table 26: Recorded pressures and temperatures and calculated CO_2 adsorption for S2 87
Table 27: CO_2 adsorption quantified in terms of Sample S2 mass 87
Table 28: Recorded pressures and temperatures and calculated CO_2 adsorption for S3 88

Table 29: CO_2 adsorption quantified in terms of Sample S3 mass 88
Table 30: Recorded pressures and temperatures and calculated CO_2 adsorption for S4 89
Table 31: CO_2 adsorption quantified in terms of Sample S4 mass 89
Table 32: Recorded pressures and temperatures and calculated CO_2 adsorption for S5 90
Table 33: CO_2 adsorption quantified in terms of Sample S5 mass 90
Table 34: Recorded pressures and temperatures and calculated CO_2 adsorption for L1 93
Table 35: CO_2 adsorption quantified in terms of Sample L1 mass 93
Table 36: Recorded pressures and temperatures and calculated CO_2 adsorption for L2 94
Table 37: CO_2 adsorption quantified in terms of Sample L2 mass 94
Table 38: Recorded pressures and temperatures and calculated CO_2 adsorption for L3 95
Table 39: CO_2 adsorption quantified in terms of Sample L3 mass 96
Table 40: Recorded pressures and temperatures and calculated CO_2 adsorption for L4 96
Table 41: CO_2 adsorption quantified in terms of Sample L4 mass 97
Table 42: Recorded pressures and temperatures and calculated CO_2 adsorption for L5 97
Table 43: CO_2 adsorption quantified in terms of Sample L5 mass 98
Table 44: Recorded pressures and temperatures and calculated CO_2 adsorption for L6 99
Table 45: CO_2 adsorption quantified in terms of Sample L6 mass 99
Table 46: pH readings of distilled water in which the samples used for preliminary experimentation were placed after adsorption experimentation 101
Table 47: pH readings of distilled water in which the samples from the 9.5 – 6.7 mm size class were placed after adsorption experimentation 101
Table 48: pH readings of distilled water in which the samples from the 22.4 - 16 mm size class were placed after adsorption experimentation 102
Table 49: pH of distilled water used to moisturise coal particles after removal of the particle 103
Table 50: Dry Masses of all Particles used in Adsorption Experimentation 110
Table 51: Proximate analyses of samples from Saghafi *et al*. (2008) 122
Table 52: Compressibility Factors used in the Calculation of the Results for Sample 2 . 136
Table 53: Compressibility Factors used in the Calculation of the Results for Sample 3 . 137
Table 54: Compressibility Factors used in the Calculation of the Results for Sample 4 . 137
Table 55: Compressibility Factors used in the Calculation of the Results for S1 138
Table 56: Compressibility Factors used in the Calculation of the Results for S2 138
Table 57: Compressibility Factors used in the Calculation of the Results for S3 139
Table 58: Compressibility Factors used in the Calculation of the Results for S4 139
Table 59: Compressibility Factors used in the Calculation of the Results for S5 140
Table 60: Compressibility Factors used in the Calculation of the Results for L1 141
Table 61: Compressibility Factors used in the Calculation of the Results for L2 141
Table 62: Compressibility Factors used in the Calculation of the Results for L3 142
Table 63: Compressibility Factors used in the Calculation of the Results for L4 143
Table 64: Compressibility Factors used in the Calculation of the Results for L5 143
Table 65: Compressibility Factors used in the Calculation of the Results for L6 144
Table 66: Blank Run to quantify leakage of the adsorption experimentation on particle S1 148

Table 67: Leakage testing of the adsorption equipment from the 11th to 13th September 2012 148
Table 68: Blank run to quantify leakage of the adsorption equipment conducted from 21st to 22nd September 2012 149
Table 69: Blank run to quantify leakage of the adsorption equipment during experimentation conducted from 30th October to 4th November 2012 149

List of Symbols

a	weight of the weighing bottle (g)
A	air-dry-loss (%)
B	weight of the weighing bottle and wet coal (g)
c	weight of the weighing bottle and dried coal (g)
^{o}C	degrees Celsius
cm	centimetre
G	weight of the gross sample
K	Henry's Law Constant (taken from Brown *et al*., 2003)
L	loss in weight in air-drying
m	metres
M	total moisture (%)
N_{ads}	number of moles of CO_2 that have adsorbed on the coal (mol)
N_{Final}	number of moles of CO_2 that are present in the void space in the sample cell at the end of the current pressure step (mol)
$N_{Initial}$	number of moles of CO_2 that are present in the void space in the sample cell at the start of the current pressure step (mol)
P	Pressure (bar)
P_2	pressure in the sample cell after equilibrium is achieved between the sample and the He subsequent to the initial pressurization with He (bar)
P_3	pressure in the sample cell after the addition of V_A and the expansion of the He (bar)
P_{Final}	pressure in the void space of the sample cell at the end of the pressure step (bar)
P_g	partial pressure of the gas over the solution
$P_{Initial}$	pressure in the void space of the sample cell at the start of the pressure step (bar)
P_i	initial pressure in the system before the expansion of the He (bar)
P_j	pressure in the entire system when the He can move freely between the reference and sample cells (bar)
P_k	initial pressure in the system when a sample of known volume is in the sample cell before the expansion of the He out of the reference cell and into the whole system (bar)
P_l	pressure in the entire system when the He can move freely between the reference cell and sample cell containing the sample of known volume (bar)
r	residual moisture (%)
R	ideal gas constant (0.08314472 L bar/K mol)
S_g	Solubility of the Gas in Water
T_{Final}	temperature in the void space of the sample cell at the end of the pressure step (K)
$T_{Initial}$	temperature in the void space of the sample cell at the start of the pressure step (K)
V	volume of the sample cell and all tubing between V2 and V3, less the volume of the coal sample used for experimentation (mL)
V_A	added volume available for the expansion of the He into the adjoining cell of the Pycnometer (cm^3)
V_C	volume of the sample cell of the Pycnometer (cm^3)
V_K	a sample of known volume (cm^3)

V_P	volume of the particle placed in the Pycnomter (cm^3)
V_R	volume of the reference cell and all tubing from the valve after the pump to the valve before the sample cell (mL)
V_S	volume of the sample cell and all tubing from the after the valve before the sample cell valve after at the system exit (mL)
µm	micrometers/microns
Z_{Final}	compressibility factor used to cater for the non ideality of the system for the pressure and temperature in the sample cell at the end of the pressure step
$Z_{Initial}$	compressibility factor used to cater for the non ideality of the system for the pressure and temperature in the sample cell at the start of the pressure step

Nomenclature

Ar	Argon
C	Carbon
CBM	Coal Bed Methane
CCS	Carbon Capture and Storage
CH_4	Methane
CO	Carbon Monoxide
COP	Conference of the Parties
CO_2	Carbon Dioxide
daf	dry ash free
DR	Dubinin Radushkevich
DVS	Dynamic Vapour Sorption
ECBM	Enhanced Coal Bed Methane
EOR	Enhanced Oil Recovery
GHG	Greenhouse Gas
GWP	Global Warming Potential
H^+	Hydrogen Ions
H_2	Hydrogen
He	Helium
Hg	Mercury
H_2O	Water
ID	Identification
ISO	International Standards Organisation
IUPAC	International Union of Pure and Applied Chemistry
K_2SO_4	Potassium Sulphate
LTMS	Long Term Mitigation Scenarios
N_2	Nitrogen
N_2O	Nitrous Oxide
SACROC	Scurry Area Canyon Reef Operators
SACCCS	South African Centre for Carbon Capture and Storage
sg	Specific Gravity
Temp	Temperature
TGA	Thermo Gravimetric Analysis
UCG	Underground Coal Gasification
USA	United States of America

1 Introduction

The Carbon Dioxide (CO_2) adsorption capacity of coal is of interest as the storage of CO_2 in unmineable coal seams has been identified as a possible mitigation option for climate change (Day *et al*., 2008b). Anthropogenic greenhouse gases (GHGs), of which CO_2 is the majority contributor, are widely believed to be the cause of climate change (White *et al*., 2003). CO_2 is emitted largely through fossil fuel combustion, and land use changes, such as deforestation. Other GHG contributors include the rotting of organic waste which releases methane (CH_4) and the application and production of inorganic fertilizer which releases nitrous oxide (N_2O). This research will focus on CO_2 as it is the gas that will be sequestered in all carbon capture and storage (CCS) initiatives.

Carbon Capture and Storage (CCS) is the process of separation of CO_2 from flue gas, compression to supercritical conditions, transportation to appropriate storage sites, injection into the storage site, and monitoring to confirm that the gas does not escape or migrate (Beck, 2011). There are many storage options and separation (also called capture) options, some of which are discussed below. This research project focuses on the CO_2 storage capacity of coal, and the effect that coal moisture has on the CO_2 adsorption capacity of coal.

South Africa meets 94% of its electricity demand with coal fired power stations as well as roughly 30% of its fuel oil demands from fossil fuel conversion (Beck *et al*., 2011). This dependence on coal places South Africa as the 13th largest CO_2 emitter in the world.

Coal is a porous substance and as such has a large surface area for adsorption. CH_4 is often found adsorbed in coal in underground seams and this demonstrates the long term storage capacity of coal seams as a potential CCS option (Krooss *et al*., 2002). Coal is however, an important energy source in the current world economy, and therefore this option could only be used on coal seams that are uneconomical to mine, due to factors such as depth, seam thickness (Viljoen *et al*., 2010) and coal quality[1]. Furthermore, in the South African situation, coal fields are the only storage options that would not require large investment in a CO_2 pipeline. The reason for this is that most large CO_2 emitters in the country are near the coal basins, and hence large CO_2 transportation costs would be avoided.

Carbon Capture and Storage (CCS) in coal is seen as the less favourable option when compared to storage options such as deep geological basins, saline aquifers, depleted oil and gas wells (Cloete, 2010; Viljoen *et al*., 2010). Some of the reasons for this include not wanting to sterilize coal reserves, and the competition of the storage technology

[1] The definition of unmineable may change with time and technology advances. What may in the past have been unmineable, may become an economically feasible mine.

with Underground Coal Gasification (UCG) which allows deep coal reserves to be gasified *in situ* and therefore allows recovery of the energy without deep mining. However, the establishment of a Coal Bed Methane (CBM) industry where the CH_4 is extracted from the coal seam may promote this storage mechanism. In Enhanced Coal Bed Methane (ECBM) Recovery, CO_2 will displace the CH_4 in the pores of the coal, and the CH_4 can then be collected and used for energy generation. Thus there is some energy yield from the process and the CO_2 may be stored for geological significant periods of time (White *et al*., 2005).

Before large scale storage in unmineable coal seams can be attempted, research must be completed to determine the capacity of the coal to store CO_2, and the factors that will affect this capacity. As stated by Viljoen *et al*. (2010): "*CO_2 adsorption capacity data for South African coals is very scarce"*. Consequently, there is little research into CCS on moist South African coal, even though underground coal is likely to have high moisture content (Day *et al*., 2008b). Most research concerns dry powdered coal. Limited research has been found to date on the permanence of underground storage of CO_2 in coal in the event there is water ingress in areas of the coal seam where CO_2 has been stored. Viljoen *et al*. (2010) state that the presence of potable ground water is a concern as CO_2 storage can contaminate groundwater. Further, the holes drilled into the coal seam to allow the CO_2 to be stored in the coal may provide opportunities for water ingress into the coal seams. Therefore, this research project will generate data on the adsorption of CO_2 on moist coal, and aims to provide an indication of whether adsorbed CO_2 dissolution into water will be an important factor in underground coal CO_2 storage.

Another aspect where there is minimal data is on storage of CO_2 in large particles. Underground storage of CO_2 in coal seams, in the event that it is ever conducted, will be in coal seams which would be difficult and expensive to fracture to small particles; the difficulty would increase with increasing depth of the coal seams. Currently research on coal storage capacity is on dry, powdered coal or very small particle sizes for logistical reasons (Day *et al*., 2008b; Goodman *et al*., 2004; Krooss *et al*., 2002; Ozdemir and Schroeder, 2009; Mastalerz *et al*., 2004). Particles in the size range of 9.5 – 6.7 mm and 22.4 – 16 mm in diameter were used in adsorption experimentation in this research.

The research work was conducted on a typical South African power generation coal from the Witbank coal field using high pressure adsorption equipment that was designed at the University of the Witwatersrand (Maphada, 2012). The equipment uses liquid CO_2 and measures the change in pressure in a vessel and piping of known volume as the gas/supercritical CO_2 adsorbs onto the coal samples. Submersion of samples in distilled water was used in the moisturisation of the coal. This was done as submersion in water would be responsible for high surface moisture content of coals in underground coal seams near an underground water source or with natural/man made water ingress. This research does not cater for different residual moisture contents as a single coal was

used in experimentation. Therefore the residual moisture content of this coal should be the same in all experimentation.

A brief overview of the coal reserves in South Africa and those that could be used for CO_2 storage follows, as well as further information on international standards and work that has been done on CO_2 adsorption potential of coal. The experimentation is discussed, as well as all analyses that were conducted on the coal. The results are compared with published literature on the storage capacity of CO_2 in coal.

2 Literature Review and Laboratory Adsorption Equipment Overview

In order to address the research aims and objectives, literature was consulted to provide an understanding of CCS in South Africa, moisture in coal, CO_2 adsorption on coal and CO_2 adsorption in H_2O.

2.1 Carbon Capture and Storage (CCS)

2.1.1 What is CCS?

Carbon Capture and Storage (CCS) is the separation of CO_2 from industrial waste/flue gas into a high purity stream, compression to beyond supercritical conditions, transportation (if needed) by pipeline, ship, land vehicles etc. to a geological storage site, injection of the supercritical CO_2 into the storage basin/area and finally the monitoring of the supercritical fluid to ensure it remains in storage (Beck, 2011). Carbon Capture and Storage (CCS) has arisen out of a global need to reduce GHG emissions, as these emissions have been linked to climate change.

Bolland (2012) cites three basic principles for separating, or capturing, CO_2 from power plants as:

1. Post-combustion CO_2 capture
2. Pre-combustion CO_2 capture; and
3. Oxy-combustion CO_2capture.

Currently the major capture technologies in operation are oxy-combustion capture and post combustion capture (Alstom, 2009).

Post-combustion CO_2 capture

Post-combustion CO_2 capture refers to the capture of CO_2 from flue gas after combustion with the use of separation equipment to remove most of the CO_2 from the gas (Bolland, 2012). Post-combustion capture at an implementation scale is currently the chilled ammonia or the advanced amine process (Alstom, 2009). Ammonia and amines are both used as solvents into which CO_2 is adsorbed from the flue gas, thus separating out the CO_2. The CO_2 is then released from the solvent and the solvent is regenerated. Membrane separation can be used in post-combustion capture. It can however also be used in pre-combustion and oxy-combustion capture for the oxygen separations. Membranes can be designed to affect a number of separations and thus are suited for multiple separation applications.

Pre-combustion CO_2 capture

Pre-combustion CO_2 capture involves producing a syngas of Hydrogen (H_2) and Carbon Monoxide (CO) and then the use of the water-gas shift reaction to form H_2 and CO_2. Thus the heating value of the fuel is converted to molecular H_2 that can then be used for fuel in a power plant (Bolland, 2012).

Oxy-combustion CO_2 capture

Oxy-combustion is the use of pure oxygen for combustion of fossil fuels therefore minimising separation that needs to be done to obtain a pure CO_2 stream that can be pressurised and stored. The CO_2 that has been separated from the flue gas is then pressurised, injected and stored.

The compression and transportation stages are unlikely to pose problems in the overall chain of activities for CCS. This is because compression and transportation of gasses has occurred in the natural gas industry (amongst other industries) for many years. The phase diagram for CO_2 can be found in Figure 1. The critical pressure of CO_2 is 73.8bar. This pressure is high, and therefore energy is expended in getting the pure CO_2 to supercritical state from atmospheric pressure following extraction from the flue gas. This high pressure also has to be maintained during the transportation of the gas as the containers used to hold the gas will have to be able to withstand this pressure. If a pipeline for CO_2 is constructed, care must be taken not to let the gas drop below the critical pressure due to friction losses or temperature changes, for example. If the CO_2 changes from the supercritical state to the gas phase then the specific volume will change drastically and may result in operational difficulties to the pipeline. However, while improvements and efficiency increases may be required, compression and transportation of compressed gasses has occurred for many years. Therefore most of the current research globally focuses on the capture and storage aspects of the CCS chain of activities.

Further discussion on capture technologies is beyond the scope of this research report. A discussion on options for CO_2 storage follows.

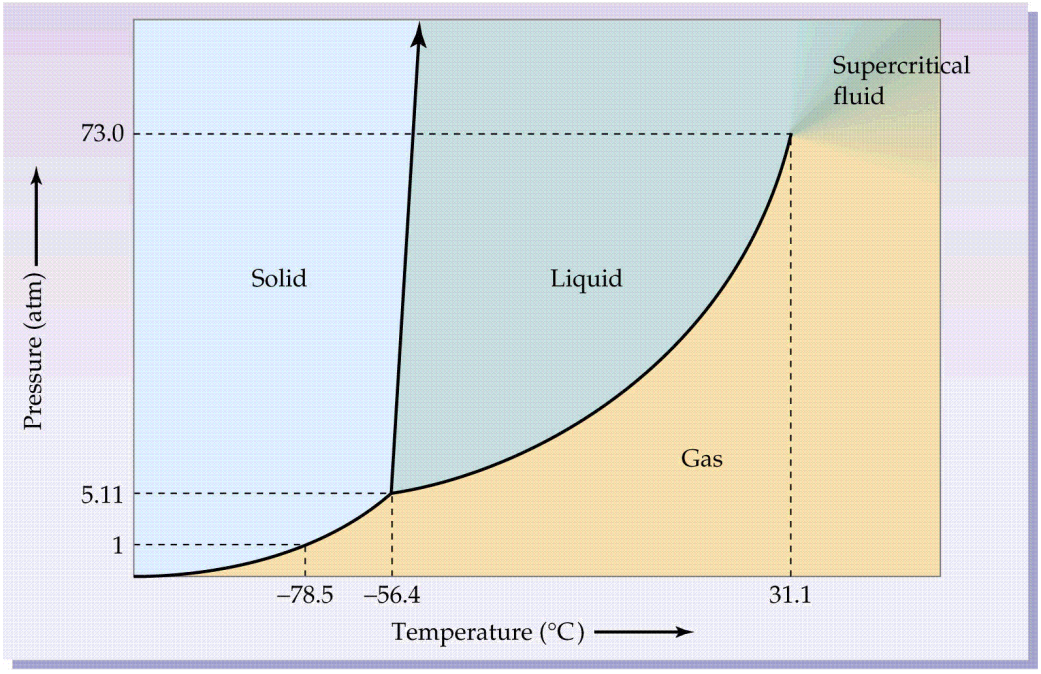

Figure 1: Phase diagram of CO_2 (CO_2 Info, 2006)

2.1.2 CO_2 Storage

The storage options for CO_2 sequestration include deep geological formations, saline aquifers, marine sequestration, depleted oil and gas reservoirs, ECBM recovery, and unmineable coal seams. The trapping mechanisms for CO_2 are listed by Gibson-Poole *et al*. (2006) as:

- Structural or Stratigraphic trapping
  - This is the trapping of CO_2 below low permeability caprock, similar to a hydrocarbon accumulation (Viljoen *et al*., 2010)
- Hydrodynamic trapping
  - This is the migration of dissolved and immiscible CO_2 with formation water over period of time in the order of thousands to millions of years (Viljoen *et al*., 2010).
- Residual Gas trapping
  - At saturation values of 5 to 30% CO_2 is trapped in pore spaces by capillary action (Viljoen *et al*., 2010).
- Solubility trapping
  - This is the dissolution of CO_2 in formation waters through diffusion, dispersion and convection (Viljoen *et al*., 2010).
- Mineral trapping; and

    - This mechanism is permanent, but occurs slowly over thousands of years. CO_2 interacts with formation minerals to form carbonates (Viljoen *et al*., 2010).
- Adsorption trapping.
    - This is the key trapping mechanism for CO_2 storage in unmineable coal or ECBM Recovery. CO_2 adsorbs onto the surface of coal and/or organic material (Viljoen *et al*., 2010).

The storage options for CO_2 in unmineable coal seams range from a depth of 300 – 800 m. Bachu (2007), Solomon *et al*. (2008) and Viljoen *et al*. (2010) all state storage in reservoirs at depths less than approximately 800 m may be technically and economically feasible, but the low storage capacity of shallow reservoirs where CO_2 may be in the gas phase could be problematic. At depths of 800 m and below the pressure should be sufficient to keep the CO_2 in place. However at lower depths the CO_2 may be held in the coal matrix through the Van der Waals forces of adsorption. Engelbrecht *et al*. (2004) suggest a depth of 1500 m in marine sequestration not only to keep the CO_2 in supercritical state but to prevent effects on the surface eco system.

The operational storage projects currently use depleted oil and gas reservoirs and saline aquifers for storage (Alstom, 2009; Bureau of Economic Geology, 2012; Statoil, 2011). There are currently CO_2 storage sites in operation worldwide namely: In Salah in Algeria, Sleipner and Snøhvit in Norway, Weyburn operations in Canada, Scurry Area Canyon Reef Operators (SACROC), Cranfield and Salt Creek Enhanced Oil Recovery in the United States of America. Weyburn and Salt Creek sites are Enhanced Oil Recovery (EOR) sites as this technology is currently financially feasible (Changbing, 2011). Not all CO_2 that is used in EOR remains underground, but the purpose of EOR is to increase oil yield not to permanently store CO_2. Sleipner and Snøhvit are Norwegian CO_2 storage sites. Norway has implemented strict GHG taxation and therefore the process is economically feasible as it allows organisations to avoid paying the tax for emitting the GHGs into the atmosphere. Therefore, Norwegian natural gas producers separate the CO_2 from the natural gas and re-inject the CO_2 under the gas reservoir in saline aquifers (Statoil, 2011). There is minimal risk of escape as the CO_2 is stored under an 800 m thick layer of gas-tight cap rock in Utsira formation for Sleipner, and 2500 m beneath the seabed and in a geological layer of porous sandstone called the Tubåen formation in Snøhvit (Statoil, 2011).

Potential for CO_2 storage exists in CBM recovery, and in storage of CO_2 in unmineable coal seams (Cloete, 2010). Both of these technologies work on the principle that coal has a large surface area and therefore gas easily adsorbs onto the coal structure (Busch *et al*., 2004; Crosdale *et al*., 1998). A gas will adsorb to a surface when the intermolecular forces between the solid and the gas are stronger than those between the gas molecules themselves (Treybal, 1981).

In CH_4 bearing coal seams, the CH_4 can be recovered with the injection of CO_2 into the seam. The CO_2 adsorbs to the coal surface thereby displacing the CH_4 from the coal

matrix, and thus CH_4 can be collected for uses such as power generation. During this process the CO_2 will be permanently stored in the coal seam (Krooss *et al*., 2002) if the coal is never combusted for energy. Day *et al*. (2008b) list the advantages of CO_2 storage in unmineable coal seams as the ability for coal to adsorb large quantities of gas due to its microporous nature and the displacement of any CH_4 that is adsorbed in the coal seam, which can be collected and used for energy purposes.

2.1.3 Carbon Capture and Storage (CCS) Potential in South Africa

South Africa's economy is fossil fuel driven and emissions intensive (Beck *et al*., 2011). Further the demand on electricity outstrips supply and as a result of this large, coal fired power stations are currently being commissioned. The Integrated Resources Plan sets out a path for future energy generation in South Africa to reduce GHG emissions and increase the share of renewable energy generation on the South African electricity grid (Department of Energy, 2011). However, the coal fired power stations that are currently in construction phase will be operational for another 50 to 60 years (Beck *et al*., 2011). South Africa also has high GHG emission reduction targets that were made at the Conference of the Parties (COP) in Copenhagen in 2009. These targets are: 34% below the business as usual emissions trajectory by 2020 and 42% by 2025 (Beck *et al*., 2004; Paton, 2010).

In 2000, the South African GHG emissions were 435 million tons of CO_2 equivalent (Department of Environmental Affairs and Tourism, 2009; Letete *et al*., 2009); more current data has not been found. CO_2 equivalent is the total amount of GHG released including gases such as CO_2, CH_4 and N_20. These gases are converted to CO_2 equivalent by a factor known as the Global Warming Potential (GWP). The GWP converts the time that the GHGs are in the atmosphere and causing warming effects to an amount of CO_2 that would be equivalent to that. Hence, CO_2 equivalent is the unit that most country GHG inventories are measured in.

The Long Term Mitigation Scenarios were released by the Department of Environmental Affairs and Tourism (2007) and reflect options available to South Africa to meet a number of emission trajectories. These emissions paths were given names for ease of discussion and referral, and are mentioned in order of decreasing country emissions below:

- growth in emissions without constraints,
- following the current[2] development plans,
- what South Africa can do,

[2]Report was released in 2007. Thus 'current' will refer to the planning framework of that time

- what South Africa could do [could do refers to the option that reduces more GHGs], and
- the emission path required by science.

These scenarios are illustrated in Figure 2. As can be seen in the Figure these emissions paths are listed in decreasing national emissions levels. All scenarios approach a forecast growth in emissions, then emissions plateau and decline in all scenarios with the exception of the growth without constraints. The required by science path is the emissions level that has been determined in line with climate targets (Energy Research Centre, 2007). This emissions path peaks the earliest, 2020, and then starts to decline (Energy Research Centre, 2007).

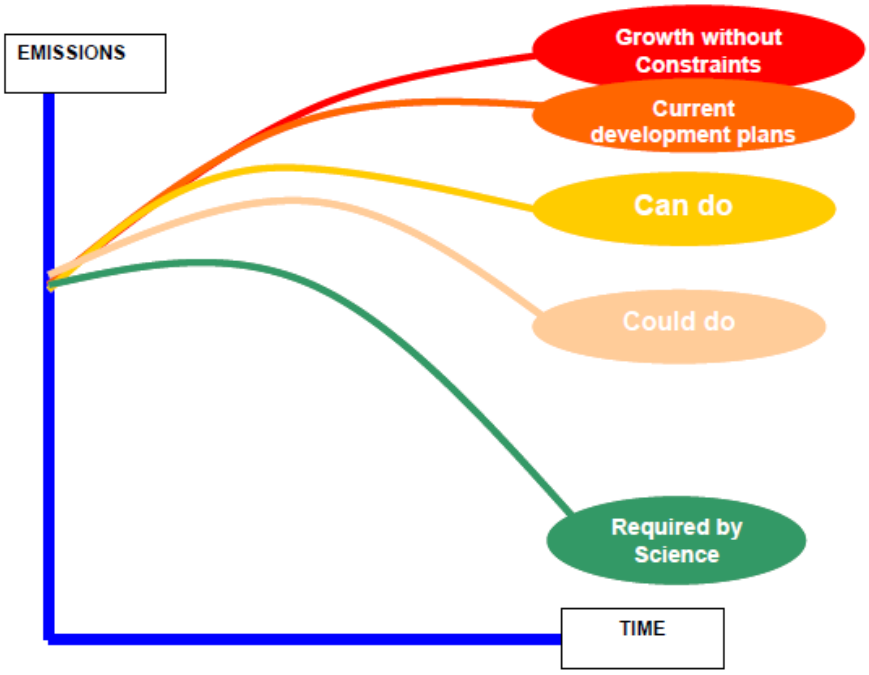

Figure 2: Long Term Mitigation Scenarios for South Africa (Energy Research Centre, 2007)

Time has shown that the "required by science path" is the one that the South African government will aim for. This path refers to 30 to 40% reduction from 2003 emission levels by 2050. Considering the targets put forward at COP15 of 34% below the business as usual emissions trajectory by 2020 and 42% by 2025 (Beck *et al.*, 2004; Paton, 2010; South Africa Climate Change, 2012). South Africa has elected to follow a more stringent path; however these targets are highly conditional on funding and technology transfer from the developed world (Paton, 2010). CCS has always been part of the strategy for

emission reductions of the order needed to meet the required by science scenario. Thus, CCS should be increasingly important going forward if these national emission reduction targets are to be met.

The South African Centre for Carbon Capture and Storage (SACCCS) has been established to roll out CCS in South Africa. Figure 3 shows the goals and timeline of the SACCCS (SACCCS, 2012). The centre is currently preparing for the test injection.

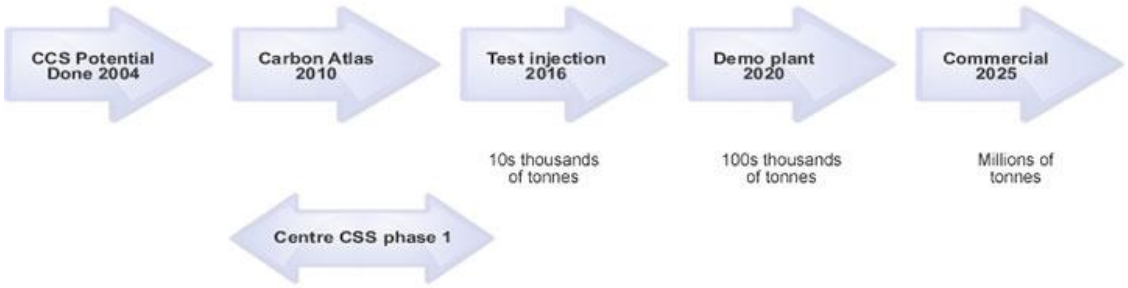

Figure 3: Work plan and timeline of the SACCCS (SACCCS, 2012)

The Council for Geoscience (Cloete, 2010; Viljoen *et al*., 2010) has estimated the storage potential in South Africa to be 150 Gt of CO_2. The majority of this storage potential is offshore in saline formations, and less than 2% is onshore. Of this 2%, 58% is in coal seams (this is 1.2% of total storage capacity in South Africa). However, with the development of a CBM industry in South Africa, the onshore storage potential in coal could be increased. CO_2 storage in unmineable coal seams could be in competition with UCG technology. The reason for this is that once the CO_2 is stored in coal it cannot be gasified as all the CO_2 would be released again. Nevertheless, the ~1.2 Gt potential for CO_2 storage in coalfields in South Africa is still substantial and further research is needed in this field.

A map of the South African coal fields are represented in Figure 4 (Falcon, 1989). Lesotho and Swaziland are not delineated in this figure which allows the extent of the Karoo Basin and the coal fields in the basin to be clearly seen. Figure 5 is from the *Atlas on Geological Storage of Carbon Dioxide in South Africa* (Cloete, 2010) and shows the potential storage capacity through the size of the black dots on the yellow areas indicating the coal fields of South Africa[3]. The agreement in the shape and situation of the coal fields can easily be seen on both maps and some storage potential exists in most of the countries coal fields.

[3] In the event that only a black and white copy of this report is available, it is suggested that Figure 4 and Figure 5 are compared for the situation of the coalfields in South Africa.

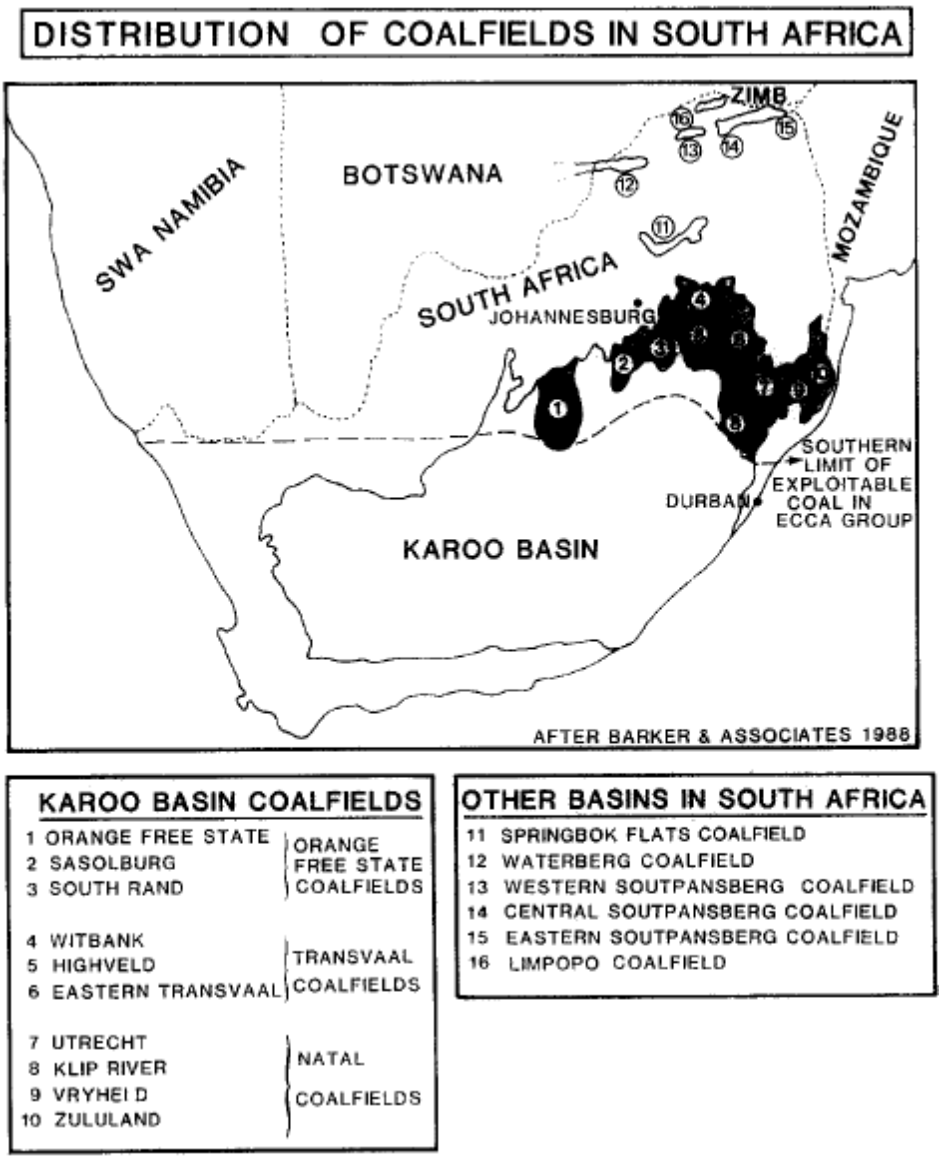

Figure 4: Coal fields of South Africa (Falcon, 1989)

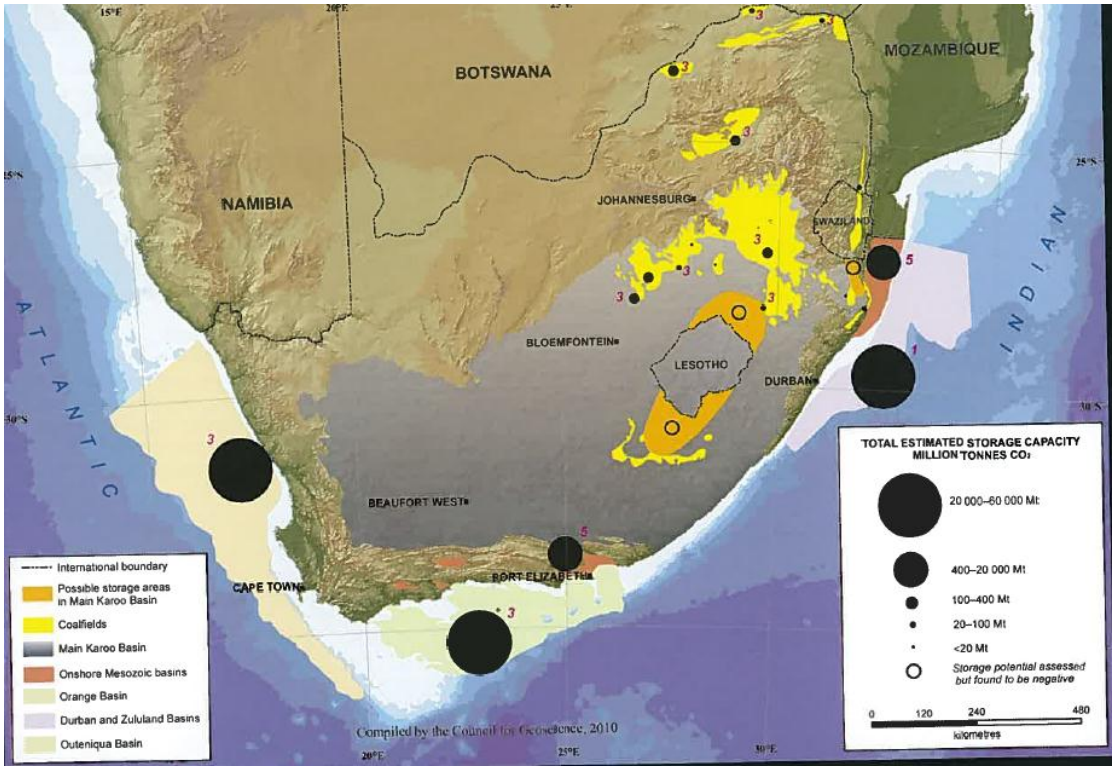

Figure 5: Image from the *Atlas on Geological Storage in South Africa* (Cloete, 2010) showing all identified storage sites in South Africa

The proximity of the potential coal storage sites to the major sources of CO_2 emissions in the country is apparent when considering Figure 5 and Figure 6, both from Cloete (2010). Therefore, in the South African context, storage in unmineable coal seams needs further research to fully explore the option. Transportation of CO_2 will add difficulty and cost to any storage process, and therefore the storage in offshore geological basins, while the most promising in terms of the work of Cloete (2010) and Viljoen *et al*. (2010) should not be considered as the only option for South Africa.

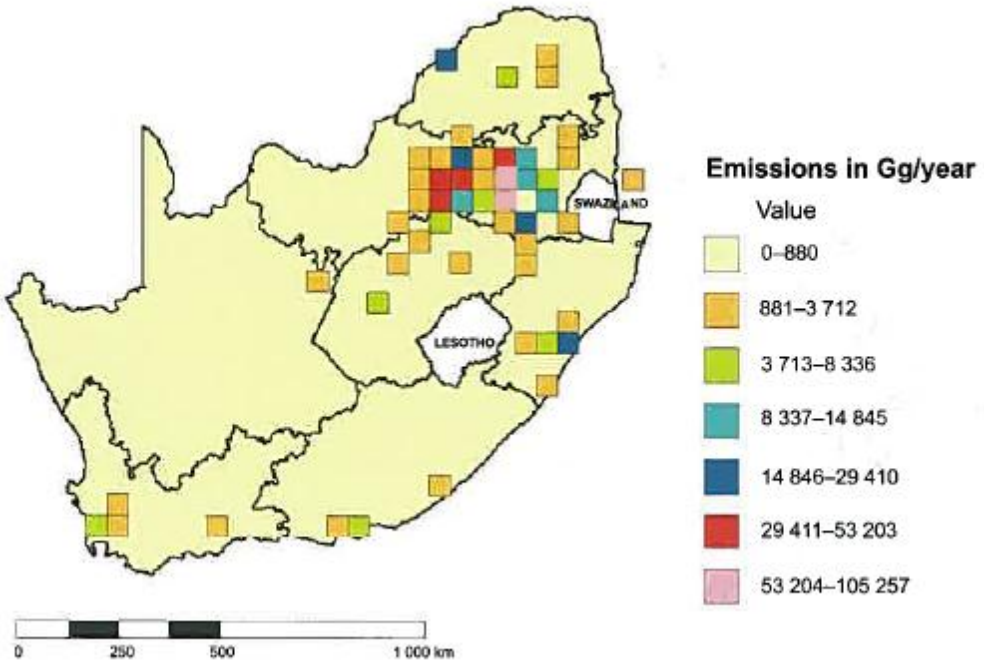

Figure 6: CO_2 Emissions and their intensity across South Africa (Cloete, 2010)

Saghafi *et al*. (2008) suggest that CO_2 storage should be considered in the vicinity of dolerite intrusions in South African coal mines. This is suggested as they found that the gas diffusivity of heat affected coals near dykes was greater by a factor of two and thus increases the CO_2 storage potential. Section 2.3.2.1 that considers the effect of coal rank on CO_2 storage potential should also be consulted with regards to storage capacity of metamorphosed coal.

2.1.4 Carbon Capture and Storage (CCS) in Unmineable Coal Seams

To store CO_2 in unmineable coal seams, drilling is required. During drilling there may be some fracturing of the coal. If there is sufficient fracturing to allow the CO_2 to access the entire coal reservoir, then injection could start. Alternatively, the coal seam shall have to be fractured to allow the CO_2 to move through the coal reservoir. Opening pathways for the gas to move through the reservoir will also allow other gases and liquids that may be present to move through the coal. Storage capacity in coals is a function of depth, thickness, permeability, extent and continuity, rank, ash content and lithotype of the coal (White *et al*., 2005). Viljoen *et al*. (2010) note that the tendency of coal to swell during injection of CO_2 may limit the rate of injectivity. If there is ground water in the area, the possible contamination effects are currently unknown. Viljoen *et al*. (2010)

state that the presence of potable ground water is a concern as CO_2 storage can contaminate groundwater.

On injection in the coal seam at supercritical pressure, the CO_2, may adsorb to the coal and displace any CH_4 that is currently adsorbed in the pores. CH_4 may be collected and used for power generation. The many factors that influence the adsorption of the CO_2 on the coal are discussed further in this Chapter.

After storage in the coal seam is complete the borehole through which the CO_2 was injected should be closed and sealed, and the site should be monitored to ensure there is no leakage. Adsorption on coal is considered a safe means of CO_2 storage as CH_4 has remained absorbed in some coal seams for geological time periods (Krooss *et al*., 2002).

2.2 Moisture in Coal

2.2.1 Terminology

There are different quantities of water that may be present in a coal sample/deposit depending on the amount of water the coal has been in contact with, and the contact time. Johns (2011) provided a breakdown of coal moisture from a laboratory analyst's view, according to the International Standards Organisation (ISO) standards for coal moisture determination. Moisture in coal has many differing terms and thus one has to be sure that in different countries and contexts the same term does not refer to different moisture contents. For example, the bed moisture of the coal is correlated to the as received or total moisture. Storage or transport conditions could result in changes in the bed moisture and the as received or total moisture content. Some commonly used terms for moisture in coal from Johns (2011) are:

- As received moisture/Total moisture
    - *This is the moisture in the coal that is delivered to the coal consumer*
- Free moisture/Surface moisture/Superficial moisture
    - *This is the moisture on the surface of the coal that will be lost by air drying the coal at 40^oC*
- Air Drying Moisture
    - *This is the moisture that remains in the sample after it has been air dried*
- Combined Moisture/Residual Moisture
    - *This is the moisture that remains in the coal sample after air drying and drying at 110^oC*
- Bed Moisture
    - *This is the moisture of the coal in situ*
- Equilibrium Moisture

    - *This is the moisture in a sample that is in equilibrium with a certain environment. This moisture quantity will depend on the moisture in the environment that the coal is in equilibrium with.*
- Inherent Moisture
    - *In South Africa this is the moisture that is in an analysis sample*
    - *In the United State of America (USA) it is used for either the bed moisture or the equilibrium moisture of a sample.*
- Water of Crystallisation
    - *This water is bound in the coal components and will only be released in the combustion of the coal.*
- Moisture Holding Capacity
    - *This is the moisture that the coal contains after equilibrium with K_2SO_4 in 97% humidity*

Although this extensive list is useful, it is evident that different researchers still use the same terms to mean different moisture contents. ASTM D3302-74 also defines many of these moisture terms differently. Unsworth *et al*. (1989), for example, defined water saturated coal as coal with all accessible pores filled with water and the inherent moisture in coal as coal with all pores smaller than 10 µm filled with water. The additional moisture that shall be discussed further in the report is the mass percentage of water that is added to the coal samples through submersion in distilled water. Through experimentation where these coal samples were left in open conditions to dry – this additional moisture is free moisture/surface moisture or superficial moisture.

2.2.2 Location and Effect of Moisture in the Coal

The effects of moisture in coal are that of a swelling agent. Suuberg *et al*. (1993) found that shrinkage of coals during drying is significant and can be directly correlated with mass loss of moisture from coal. The results were confirmed by Ozdemir and Schroeder (2009) and ASTM D1412-07, who determined that the degree of shrinkage of wet coals during drying is larger than the volume of water removed. When low rank coals are dried, less CO_2 is able to occupy the pores of the coal than the amount of water that was previously in the pores (Ozdemir and Schroeder, 2009). Ozdemir and Schroeder (2009) believe this is due to relaxing of the pores that were previously held open by water during drying. This is not observed in high rank coals as they have a more rigid structure and do not shrink during drying. Therefore, the structure of coal changes with differing moisture contents, and competition of water and gas for storage sites may not be the only mechanism by which water content in coals affects adsorption.

Charrière and Behra (2010) studied the adsorption and desorption of water vapour from high volatile bituminous coal and lignite. The method of adding the moisture was with the use of a Dynamic Vapour Sorption (DVS) analyzer. The DVS removes all moisture from the initial sample in a closed system and then keeps the sample in an environment of N_2 and H_2O vapour. Moisture then adsorbs to the coal sample and the amount of moisture in the system is either increased if data for the adsorption side of the isotherm is currently being generated, or decreased in the case of data for desorption. The moisture adsorbed to the coal is measured by a change in mass of the sample. Although the method of moisture addition to the coal differs from the one used in this research, the results generated reflect the adsorption of water onto coal and the most likely situation of the water molecules in the coal.

Figure 7 shows the results generated by Charrière and Behra (2010) on the likely sites for adsorption of H_2O to coal. The first stage, marked I in Figure 7, refers to the adsorption of the H_2O on the carboxyl and hydroxyl groups in the coal. The second stage, II, refers to the H bonding between H_2O molecules that will occur when there are already some adsorbed H_2O molecules. This is also referred to as adsorption of H_20 molecules onto secondary sites. The third stage, III, occurs when the concentration of H_20 molecules around functional groups is high enough and H_2O clusters are formed around the adsorption site. In the final stage, IV, micropore filling and capillary condensation in narrow pores occurs and is indicated by the slower rate of adsorption.

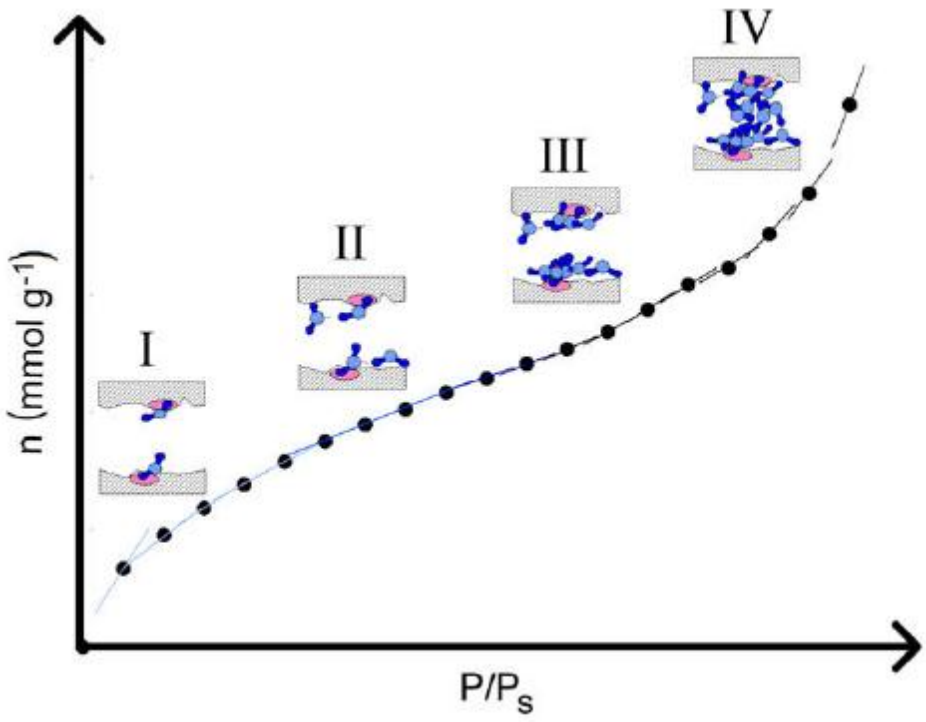

Figure 7: Adsorption of water vapour on coal with increasing relative pressure (Charrière&Behra, 2010)

Ozdemir and Schroeder (2009) recognize the tendency for water in moist coals to occupy the pore spaces, which are the active sites for CO_2 adsorption, and block transport pathways to the pore spaces and thus significantly reduce adsorption capacity when compared to the dry coal. Therefore moisture of coal should be taken into account in CO_2 adsorption experimentation.

2.2.3 International Standards for Coal Moisture Determination

ASTM D1412-07, *Standard Test Method for Equilibrium Moisture of Coal at 96 to 97 Percent relative Humidity and 30°C*

ASTM D1412-07, *Standard Test Method for Equilibrium Moisture of Coal at 96 to 97 Percent relative Humidity and 30°C*, was consulted for further information on the determination of moisture content in coal. A summarised account of this standard is presented followed by a discussion regarding the suitability of use of the standard in this research.

The use of this standard involves placing a sample of crushed coal (4.75µm in accordance with ASTM Practice D2013) in 100 mL of distilled water that has been recently boiled and cooled for 3.5 hours. This water is then filtered from the coal and the coal is placed in a weighing bottle of known weight in a desiccator under 30 mm Mercury (Hg) absolute pressure with a saturated solution of Potassium Sulphate (K_2SO_4) used to maintain the 96 to 97% humidity environment. After equilibration (this may be as long at 72 hours for lignitic coals) the weighing bottle is returned to atmospheric pressure, sealed and the weight is recorded. When a constant temperature oven has reached 105°C uncover and place the weighing bottle in the oven for 1.5 hours. After this time remove the bottle from the oven and cool for 30 minutes over either: Anhydrous Calcium Sulphate, Silica Gel, Magnesium Perchlorate or Concentrated Sulphuric Acid. After 30 minutes weigh the sample. The percentage equilibrium moisture in the analysis sample can then be calculated as:

$$Equilibrium\ Moisture\ in\ Analysis\ Sample, \% = \frac{(B-c)}{(B-a)} * 100 \qquad 1$$

Where:
a is the weight of the weighing bottle (g)[4]
B is the weight of the weighing bottle and wet coal (g)
c is the weight of the weighing bottle and dried coal (g)[5]

[4] 'a' is annotated as 'A' in ASTM D1412-07 however 'a' has been used in this report to avoid confusion with the 'A' in ASTM 3302-74

[5] 'c' is annotated as 'C' in ASTM D1412-07 however 'c' has been used in this report to avoid confusion with the abbreviation for elemental Carbon

Not all the equipment needed to complete this ASTM D1412-07 was on hand at the University of the Witwatersrand, and although it could be obtained the decision was made to determine the moisture content of coal used in the experimentation through weight difference between the dry and moisturised coal samples, as suggested in the standard, but not to use the K_2SO_4 humid environment to add the moisture to the coal or a constant temperature oven to dry the coal. This decision was made as this test could not be conducted before experimentation started as the coal would then need to be moisturised again. Nor could it be conducted after the experimentation as the moisture content of the coal is likely to change during adsorption experimentation. This is the case as the adsorption experimentation was carried out at a constant temperature of 40^{o}C to ensure that supercritical conditions of $CO_2$are reached during each successive pressure step. The method of using a reference cell to expand CO_2 into the sample cell, results in pressure fluctuations with the changing pressure of gases. As the pressure is released into the sample cell there is cooling due to the constant volume expansion of the gas. Thus, a temperature higher than the supercritical temperature of CO_2 is used for the constant temperature oven. Thus, the ASTM D1412-07 test was not suited to this research as surface moisture dries from coal at 40^{o}C, the temperature of experimentation.

ASTM 3302-74, *Standard Test Method for Total Moisture in Coal*

ASTM 3302-74, *Standard Test Method for Total Moisture in Coal*, is used for large quantities of coal such as shipments. If the sample is too large, too wet to handle or transport without loss of moisture; the first step in ASTM 3302-74 is to spread the sample out on a drying floor, and to stir and weigh until the mass loss is less than 0.1% per hour. Excess drying of the sample should be avoided and the gross weight of the sample should be recorded before division in accordance with ASTM D2013 (*Preparing Coal Samples for Analysis*). The smaller sample is then divided over a number of pans and placed in an air drying oven at a temperature of 10 to 15^{o}C above room temperature with at least one air exchange in the oven per minute. When the surface of the coal appears to be dry the sample pans should be removed and weighed. Drying should continue until the weight loss of the sample is less than 0.1% per hour. When the final air dry weight of the sample is recorded time should be allowed such that the sample is in equilibrium with the temperature and humidity of the room in which the analysis is conducted.

To determine the residual moisture on a prepared sample, two methods are provided in ASTM 3302-74 depending on the top particle size of the samples. Residual moisture as defined in ASTM 3302-74 is '*the moisture remaining in the sample after determining the air-dry-loss*'. Detail will not be provided on each method for the different particle sizes, as ASTM 3302-74 can be consulted. The difference in methods stems from smaller

particle sizes being more manageable and therefore smaller containers are needed for a representative sample. The commonality in the methods is that the samples are dried in an oven at a temperature of 107°C ±3°C and after several hours the samples are weighed again to determine their moisture loss.

The % total moisture, air-dry-loss and % residual moisture (according to ASTM 3302-74) are calculated as follows:

$$M = [r(100 - A)/100] + A \quad (2)$$

Where:
M is the total moisture (%)
A is the air-dry-loss (%)
r is the residual moisture (%)[6]

A is calculated as follows:

$$A = (L/G) * 100 \quad (3)$$

Where:
L is the loss in weight in air-drying
G is the weight of the gross sample

r is calculated as follows:

$$r = [(W - H)/W] * 100 \quad (4)$$

Where:
W is the weight of the sample used
H is the weight of the sample after heating

ASTM 3302-74 for coal moisture determination is not useful for this project for the same reason as the previous standard. Namely, the sample is dried during the moisture determination. Therefore the moisture added to the sample, which in this research is a single large particle, could not be determined from the particle before experimentation as the particle would then be dried. Further, as moisture is a changing property of coal, a large amount of moisturised coal cannot be prepared in advance from which a representative sample is tested and the remainder used in experimentation. Even if stored in a well sealed container there will be air in the container and a new equilibrium

[6] 'r' is annotated as 'R' in ASTM 3302-74 however 'r' has been used in this report to avoid confusion with the ideal gas constant

will be obtained with the environment in the container. The same argument will apply to a container filled with either moist air or dry air.

However, what has been taken from both standards in terms of moisture determination on coal is that, moisture determination is done based on a change in mass of the sample. Provided no other change has occurred to the coal a simple change in mass can be used to estimate the moisture content of a sample. Therefore the amount of moisture that was added to the samples for CO_2 adsorption experimentation was determined in this way prior to starting the adsorption experimentation.

2.3 CO_2 Adsorption on Coal

Theory behind the mechanisms of adsorption and application of this to CO_2 adsorption in coal is discussed further below. The literature that was consulted allowed a more balanced view to be formed on the results and outcomes of this research.

2.3.1 Principles of CO_2 Adsorption on Coal

2.3.1.1 Adsorption

Adsorption is the adherence of molecules to a surface (Brown *et al*., 2003). There are two types of adsorption: physical and chemical adsorption. Physical adsorption is the type of adsorption that occurs between CO_2 and coal. Physical adsorption is also known as van der Waals adsorption, as it is a result of the van der Waals forces of attraction between the molecules of the solid and the substance adsorbed (Treybal, 1981). When the intermolecular attractive forces between a solid and a gas are greater than the intermolecular attractive forces between the molecules of the gas, the gas will adsorb on the surface of the solid (Treybal, 1981). Gas adsorption on the internal surface area is considered to be the most important mechanism for retaining gas in coal (Mares *et al*., 2009).

2.3.1.2 Coal Pores and Structure

The International Union of Pure and Applied Chemistry (IUPAC) has divided the pores in porous materials into three categories based on pore diameter, namely: micropores (diameters <2 nm), mesopores (diameter 2 nm – 150 nm) (McCusker *et al*., 2001) and macropores (diameter >150 nm). Other classifications are used in literature and will be stated in the event that they differ from the IUPAC classifications listed above. Crosdale

et al. (1998) use the IUPAC classification of micropores being those less than 2nm in diameter.

Unsworth *et al*. (1989) found that the macropore volume increases with decreasing coal rank, whilst mesoporosity was closely related to inherent moisture content and differed with vitrinite and inertinite. Unsworth *et al*. (1989) also found that microporosity varied widely in low rank bituminous coals.

Gamson *et al*. (1993) recognise three types of coal porosity in their research, namely: fracture porosity, phyteral porosity and matrix porosity. The difference in porosity classifications is due to the fact that Gamson *et al*. (1993) were looking at CH_4 recovery from coal reserves and therefore were using large coal particles [~1 cm^3 cut from seam cores] and not crushed and sized coal. Fracture porosity refers to macro- and microfractures in the coal, phyteral porosity refers to the cavities in coal associated with organic compounds and matrix porosity refers to the pores in between maceral fragments, minute particles and clays. Crosdale *et al*. (1998) found that with development of extensive unmineralised fracture systems desorption may be rapid even in vitrinite rich coals which usually have slow desorption rates due to the microporous nature.

The porosity of coal is also important in adsorption experimentation, as porosity is often used as an indicator of the adsorption potential of coals as the CO_2 that adsorbs to coal is generally found in the pores. Thus porosity may be a method of correlation of the results that will allow application to other coals. Porosity can be measured with a Hg porosimeter, but Day *et al*. (2008b) suggest that porosity is not a reliable indicator of adsorption.

Day *et al*. (2008b) found that weathered coal, which exhibited higher porosity to other coal samples, had higher CO_2 adsorption capacity.

2.3.2 Effects of Coal Properties on CO_2 Adsorption

2.3.2.1 Rank Effects on Adsorption

The porosity and inherent moisture in coal is determined primarily by rank effects (Unsworth *et al*., 1989). Unsworth *et al*. (1989) found that inherent moisture increases with decreasing carbon content. Therefore inherent moisture is higher in low rank coals. This is significant as water has been found to reduce CO_2 adsorption capacity of coal as it blocks access to the pores (Mares *et al*., 2009) and infers that low rank coals may have lower CO_2 adsorption capacities than higher rank coals.

Saghafi *et al*. (2006) found that adsorption capacity increases with the rank of coal. This may be problematic as coal that is not economical to mine that could be used for CCS in

South Africa is likely to be low rank. Day *et al*. (2008b) found that sorption capacity of coal reduced with rank to a minimum at a vitrinite reflectance of 1.2% (85% C on a daf basis) and then increased from there. A dry ash free basis excludes all moisture and ash content of the sample (World Coal Institute, 2007). Day *et al*. (2008b) tested 30 coals of various rank and origin and therefore this result is presumed to be reliable.

Lignites have better CO_2 adsorption capacities due to CO_2 dissolution into the moisture (Viljoen *et al*., 2010). Lignitic coals are low rank and thus have higher moisture content.

Authors such as Engelbrecht *et al*. (2004) that wrote specifically on South African coals, claim that the 2:1 ratio of preferential adsorption of CO_2 over CH_4 may be even better in low rank coals. However this refers to a ratio of CO_2 to CH_4 adsorption and not to the actual volume or quantity of gas adsorbed.

There is some disparity on the differences in CO_2 adsorption in different rank coal, as researchers are observing contrasting trends. Bhebhe (2008) found that coal of a higher rank has higher adsorption capacities. However, it was also mentioned that the vitrinite contents of the different rank coals varied considerably and that this may be the determining factor for the adsorption content and not the rank of the coal.

Day *et al*. (2008a) found that moisture negatively effects the adsorption capacity of all coals however the degree of effect is dependent on the rank or the coal. Higher rank coals had adsorption capacities that were less changed with moisture than lower rank coals.

2.3.2.2 Maceral and Mineral Matter Effects on Adsorption

The porosity that is predominant in the different coal macerals will be discussed below as porosity is a good indicator of the CO_2 storage capacity of coals. Adsorption should occur in meso- and micropores (Unsworth *et al*., 1989). Dutta *et al*. (2008) found that CO_2 injected into coal is competitively adsorbed in the micropores.

In x-ray and neutron testing of the microstructure of low rank coals, telovitrinite has been found to have a strong association with macroporosity, and an association with meso- and micro-porosity (Mares *et al*., 2009). Vitrinite was found to have good correlations with specific surface area (Mares *et al*., 2009). Unsworth *et al*. (1989) found that inertinite contains more macroporosity (30nm – 10 µm) and less microporosity than vitrinite. Their work also found that in coals of the same rank, inherent moisture did not differ in vitrinite and inertinite. Crosdale *et al*. (1998) found that vitrinite rich coals had a higher adsorption capacity than inertinite rich coals.

While conducting experiments on the mechanisms through which CH_4 can flow through coal, Gamson *et al*. (1993) found that mineral matter will block transport pathways in

larger coal particles. Crosdale *et al*. (1998) found that mineral matter is non adsorbent and acts as a simple diluent.

2.3.3 Effect of Particle Size on Adsorption

Adsorption increases with decreasing particle size as crushing coal opens further pores (Busch *et al*., 2004). Coal is a heterogeneous microporous material and the movement of gases and fluid through the coal is through the pore network (Mares *et al*., 2009). Therefore adsorption is dependent on surface area, pore size distribution and porosity of coal.

Airey (1968), when examining the rate of release of CH_4 from coal, found that the theory for gas flow through a cracked solid had better agreement with experimental data generated than the theory for gas flow through a homogeneous solid. Thus, in large coal particles, gas diffusion may be controlled by the presence of cracks and cleats. This agrees with the work of Crosdale *et al*. (1998) who found that gas desorption that occurs at a greater speed than literature predicts for vitrinite rich coals, may be controlled by unmineralised fracture systems.

Sabir and Chalaturnyk (2009) suggest that the phenomena of swelling and shrinkage in coal with variable adsorbed gas contents can be modelled with adsorption testing on intact particles. This confirms the need to conduct adsorption experiments on large particles. Furthermore, in the seam coal is under the influence of overburden pressure. Bringing the coal to the surface opens the fractures in the coal and increases the surface area available for adsorption (Sabir and Chalaturnyk, 2009). Therefore, it must be noted that adsorption experiments carried out at surface may yield results reflecting larger adsorption capacities than can be achieved in underground CO_2 storage in coal. Overburden pressure can be simulated in the laboratory, if large particles are used in adsorption testing, with constant-pressure adsorption testing (as opposed to constant-volume adsorption testing that is currently widely used).

2.3.4 Pressure Effects on Adsorption

All adsorption isotherms produced in CO_2 storage capacity on coal (amongst other porous media) display the trend of increased adsorption at increased pressure. At very high pressures large volumes of gas can be stored in the free phase, and gas in free phase may have comparable volumes to the gas in the adsorbed phase if the porosity is not significantly reduced (Saghafi *et al*., 2008). Therefore, adsorption is dominant at low pressures and at high pressures gas will be stored in the macropores and large fractures in the coal. The quantity of gas stored in the free phase is dependent on temperature,

pressure and the porosity of the coal (Saghafi *et al*., 2008), and thus a quantification on the pressure values for low and high pressure is not provided.

Researchers such as Saghafi *et al*. (2008) caution on the storage of CO_2 in free space in coal as the release of this gas may occur with seismic changes. Krooss *et al*. (2004) discuss the permanence of CO_2 adsorption as a storage mechanism. However, when CO_2 is not adsorbed to the pores of coal, the permanence of the storage will rest in pressure gradients and permeability of the coal basin and surrounding strata. Thus, while large amounts of CO_2 can be stored in coal at high pressures (such as the pressure of underground coal seams), the amount of adsorbed CO_2 versus the CO_2 in macropores and fractures should be considered.

2.3.5 Interactions of CO_2 with other Non-Coal Components

2.3.5.1 CH_4 and CO_2 Interactions in Coal

Laboratory tests and field experiments show that when two CO_2 molecules are adsorbed, one CH_4 molecule is released (Krooss *et al*., 2002; Saghafi *et al*., 2007; Mares *et al*., 2009). Data has been generated with New Zealand coals that shows that on average 6.7 times more CO_2 can be stored than CH_4 (Mares *et al*., 2009). Another view published in Cloete (2010) is that 3 to 13 molecules of CO_2 are preferentially adsorbed onto South African coal (depending on the rank of the coal) for each molecule of CH_4 that is released.

This phenomenon is observed in wet and dry coals. Busch *et al*. (2004) observed that in dry coals CO_2 adsorption rates are consistently higher (2 – 3 times) than CH_4 adsorption rates; and CO_2 adsorption rates are 5-6 times higher than CH_4 adsorption rates in wet coals.

2.3.5.2 H_2O, CH_4 and CO_2 Interactions in Coal

Busch *et al*. (2004) recommend that moisture effects have to be taken into account in coal experimentation because of the natural moisture content of coals. Charrière and Behra (2010) state that H_20 interactions with coal are different to CO_2, CH_4 and N_2 interactions as a result of strong H_2O-H_2O interactions as opposed to weak H_20-coal interactions. In further detail, the H-bonding intermolecular forces between H_2O molecules are different to the weak intermolecular forces between gas molecules; and the H_2O-coal interactions are weaker than the gas-coal interactions.

Joubert *et al*. (1974) conducted experiments on CH_4 sorption on wet bituminous coal and found that moisture content in coal decreased adsorption capacity up to the

adsorbed water saturation capacity of the coal; and after that moisture content had no further effects on the CH_4 adsorption capacity. These results were interpreted as the excess moisture remaining on the surface of the coal and not blocking access to the pores where adsorption occurs.

Day *et al*. (2008a) found that beyond a certain moisture content there were no further effects on adsorption. This moisture content for the Australian and Chinese coals analysed in their research was the equilibrium moisture content attained after exposure of these coals to a 40 – 80% humidity environment.

Mares *et al*. (2009) adsorbed CO_2 on 'dry ash free' and 'as analysed'[7] New Zealand coals. The moisture effects on adsorption that were observed between these two conditions were that moisture condenses in pores and blocks access to micropores by gases. Airey (1968) states that the moisture content of coal is known to affect its CH_4 adsorption capacity. It can be supposed that moisture content will affect CO_2 adsorption as well. Busch *et al*. (2004) found that sorption rates of CO_2 in wet coals were reduced by a factor of more than 2 when compared to dry coals.

Day *et al*. (2008b) state the general consensus is that sorption capacity decreases with the presence of moisture. Day *et al*. (2008b) also state that storage capacity will be more than that of adsorption alone as CO_2 dissolution into the water will occur.

Contrary to this Viljoen *et al*. (2010) found that lignitic coals have higher adsorption capacity due to dissolution of the CO_2 in the moisture of the coal. This may require extensive treatment and disposal of acidic ground water (Viljoen *et al*., 2010).

2.3.6 Models describing Adsorption

A brief discussion on the calculation methods that were used in the surface area analysis that was conducted on the samples follows.

Langmuir Adsorption Isotherms

The Langmuir adsorption isotherm for microporous materials displays a steep increase in adsorbed volume at low pressures and flattens out at higher pressures once a monolayer of adsorbed gas is achieved. The Langmuir model assumes dynamic equilibrium between the adsorbate and the adsorbant and thus adsorption is restricted to a single monolayer (Dutta *et al*.,2008). The Langmuir model underestimated adsorption at pressures over supercritical conditions (Day *et al*., 2008b).

[7]As analysed coals included mineral matter and moisture

BET Theory

The Brunauer-Emmett-Teller (BET) model is often used for vapour adsorption and caters for multiple adsorbed layers (Charrière and Behra, 2010). Molecules that are already adsorbed in a monolayer at the surface, as with Langmuir, provide sites for further adsorption and the molecules are assumed to condensate at the solid surface. The monolayer adsorption capacity and the surface area of solids can be estimated using a fixed number of points on the coal surface and the inflexion point in the mathematical model that corresponds to the formation of a second adsorbed layer (Charrière and Behra, 2010).

Dubinin-Radushkevich (DR)

The DR equation, similar to the others discussed above is used for determining sorption capacity of materials. The DR adsorption isotherm is a pore filling model that does not assume monolayer surface coverage (Sakurovs *et al*., 2007). However with some assumptions it can be used to determine surface area (Sakurovs *et al*., 2007).

In summary, the differences between these methods are that Langmuir assumes a single layer of adsorption, BET allows for multiple layers of adsorption, and DR caters specifically for adsorption where pores of a substance are filled. The focus of this study is not modelling adsorption of CO_2 on coal and therefore these equations will not be discussed further; an awareness was however necessary for understanding of other researcher's work.

2.4 CO_2 Solubility in water

The solubility of gases in water is affected by temperature and pressure. As pressure increases, the solubility of a gas increases (Brown *et al*., 2003). In contrast, as temperature increases the solubility of a gas in solution decreases (Brown *et al*., 2003). Therefore the CO_2 solubility in water is at the highest at high pressures and low temperatures.

Extending this line of thought to storage of CO_2 in unmineable coal seams, the pressure effects on solubility should have more impact than the temperature effects. This is because CO_2 is stored below ground and therefore both the temperature and the pressure are higher than surface conditions. The increased pressure results in greater gas solubility in water and therefore may impact on the long term storage in coal seams that have water ingress. Solubility of gases in water can be predicted using Henry's law:

$$\mathbf{S_g = kP_g} \qquad 5$$

Where:
S_g is the Solubility of the Gas in Water
k is the Henry's Law Constant (taken from Brown *et al*., 2003)
P_g is the partial pressure of the gas over the solution

Equation 5 has been applied to a range of pressures to demonstrate the increasing solubility of CO_2 at higher pressures. Day *et al*. (2008b) used the Henry's law constant in the modification of the Dubinin-Radushkevich equation for use beyond supercritical pressures. While they note that k is strongly affected by errors in cell volume and coal density, it proves that Henry's law can be used for sorption of CO_2 on coal beyond supercritical pressures. The results of the calculations with Equation 5 are in Table 1.

Table 1: Increasing solubility of CO_2 with increasing pressure

CO_2 Partial Pressure (atm)	Henry's Law Constant for CO_2 (mol/L atm)	Solubility of CO_2 in Water (mol/L)
10	0.031	0.31
20	0.031	0.62
30	0.031	0.93
40	0.031	1.24
50	0.031	1.55
60	0.031	1.86
70	0.031	2.17
80	0.031	2.48
90	0.031	2.79
100	0.031	3.1

No monitoring data has been found on the dissolution of adsorbed CO_2 from coal into groundwater as unfortunately no sites worldwide where CO_2 has been stored in unmineable coal seams, without ECBM Recovery have been found. Day *et al*. (2008b) cite the dissolution of CO_2 into pure water at 50^{o}C and 100 bar is one mole per kilogram. These conditions could easily be found in an unmineable coal seam. Day *et al*. (2008b) acknowledge that CO_2 dissolution would be lower in saline water but expect dissolution to occur, as is the case with storage in saline aquifers.

At the Sixth Conference on Carbon Capture and Storage in Trondheim, Norway, monitoring data on storage in saline aquifers has indicated that a small portion of injected CO_2 has dissolved in the surrounding water in the Cranfield aquifer (Changbing, 2011). This is in opposition with the SACROC EOR field where no pH or HCO_3^- changes have been noticed. The SACROC EOR field has been in operation since 1972 and over 175 million tons of CO_2 have been injected (Bureau of Economic Geology, 2012). Roughly half of the CO_2 injected is co-produced with the oil and then separated and

recycled back into the well. The other half is presumed to be sequestered at 6,000 – 7,000 ft below the surface (Bureau of Economic Geology, 2012).

The reasons behind the disparity in the Cranfield and SACROC data are unknown, thus reinforcing the importance of water dissolution research. The literature consulted demonstrates that the dissolution of supercritical CO_2 into surrounding water is possible, but it cannot be used to imply that this will happen with storage in unmineable coal seams, as these are geologically different storage options.

Krooss *et al*. (2002) consider the future release of CO_2 stored in unmineable coal unlikely as the process of gas adsorption has proven its stability over geological time periods. This research however focussed on adsorption of CO_2 and CH_4 and not gas desorption. Desorption and dissolution into water was not considered by Krooss *et al*. (2002).

Research on desorption of CO_2 from coal and dissolution into water has not been found as yet. Preliminary experiments that may provide an indication on whether water ingress in CO_2 bearing coal seams is a concern for storage of CO_2 in unmineable coal seams shall be conducted with the CO_2 saturated coal from this research.

2.5 Chapter Summary

This chapter has addressed a number of published works on CCS, coal properties and coal structure, gas adsorption in coal, water sorption on coal and desorption from coal. This theory will be applied in the following sections in the development of a methodology for the research, and in the discussion to interpret the results.

3 Hypothesis and Key Research Outcomes

The questions that this research proposed to answer are set out in this section.

3.1 Hypothesis

Wet, large coal particles will store less CO_2 than dry, crushed coal particles at all pressures above atmospheric pressure.

3.2 Key Research Outcomes

1. *What will be the effect of different moisture contents on the CO_2 adsorption onto the coal?* Globally it is the norm to conduct CO_2 adsorption experimentation on dry coal. It is highly unlikely that all the coal underground will be dry and therefore research is needed on wet coal with varying moisture contents to determine the CO_2 storage capacity of coal more accurately.
2. *How will adsorption capacity change when large coal particles are used in experimentation?* Underground coal will not be crushed/powdered, and therefore data on the CO_2 adsorption capacity of large particles is necessary to further work from laboratory scale to small scale pilot project implementation (in the event that the laboratory tests that strive for more realistic conditions prove successful).
3. *Once CO_2 is adsorbed onto the coal, will dissolution into surrounding water occur?* The permanence of CO_2 storage is important, as a solution to reduce the release of anthropogenic CO_2 into the environment is needed and not a temporary store of CO_2 which may later escape.
4. *Can the CO_2 adsorption results generated on dry coal be adjusted to compensate for moisture in coal?* The results generated by this project will be compared with published results on CO_2 adsorption of South African coals.

4 Methodology

The preparation of the coal samples used in the research, the analyses conducted on the coal, the true volume determination of the samples used in the adsorption experimentation, and the procedure used to determine the CO_2 adsorption potential of these coal samples is discussed in this chapter.

4.1 Coal Preparation

An initial sample of typical South African power generation coal from the Witbank coal field was obtained. Power generation coal is lower quality, in terms of the lower vitrinite content and ash, than export quality coal and therefore is presumed to approximate coal that may be used for CCS more accurately. The starting sample mass used in the project was 41.7 kg[8]. This coal was coned and quartered to ensure that the sample on which experimentation would be done was representative. The process of coning and quartering involved thoroughly mixing the coal so that particle sizes and relative densities were evenly mixed. Then the coal pile was flattened and a smaller representative sample for crushing was removed. This sample was screened and hand crushed such that no particles were larger than 23 mm in diameter. This size was chosen as a spherical coal particle that is not larger than 23 mm in diameter will fit in the high pressure adsorption equipment. The other size classes were separated to avoid reclassification if a smaller particle size had to be used in experimentation due to poor results with the large particles.

The mass of each fraction into which the coal was screened is tabulated below. While care was taken to avoid loss of sample mass, some did occur. Around 130 g of coal was lost. This amount may actually be smaller or larger as different equipment was used to weigh the smaller amounts of coal. The error bands of these scales are not known as the equipment has been in use for extended periods. The particle size range that was desired for the experiments was the largest size class, namely 22.4 - 16 mm.

[8]The sample sent to ALS Laboratory for moisture content analysis was taken from this initial sample.

Table 2: Size classification of sample and distribution of particles in different size classes

Size Class (mm)	Mass of Coal in Size Class (kg)
22.4 - 16	4.130
16 - 9.5	3.195
9.5 - 2.36	5.125
2.36 and below	3.430

During experimentation it became necessary to produce another size class of smaller particles for use with different pressure vessels in the high pressure adsorption equipment. Therefore a size class of 9.5 – 6.7 mm was screened from the 9.5 – 2.36 mm size class The mass of coal in the new size classes created is tabulated below.

Table 3: Further size classification of 2.36 – 9.5 mm size fraction

Size Class (mm)	Mass of Coal in Size Class (kg)
9.5 - 6.7	1.345
6.7 - 2.36	3.765

Thus, CO_2 adsorption experimentation was conducted both on the 22.4 – 16 mm and the 9.5 – 6.7 mm size classes. Both size classes were crushed further for characterisation analyses. The characterisation analyses and adsorption methodology used in this research is discussed further below.

4.2 As Received Coal Moisture Determination

As a large focus of this research is the moisture content of coal, the first analysis that was conducted was a moisture content determination of the as received Witbank power generation coal. The moisture content determination was conducted to understand the baseline moisture content of the coal before any moisture was added to the coal samples.

25 kg of coal was sent to ALS Laboratory group, Witbank, based on the diameter of the largest particles in the original coal sample received. ALS laboratory then obtained representative samples from the 25 kg of coal and conducted the moisture testing. This procedure was followed so ALS laboratory could have confidence in the moisture determination results. As the sample preparation was performed in house there was confidence that the results were representative of the coal that was received.

4.3 Coal Characterisation

A moisture content determination, petrographic analysis, thermogravimetric analysis (TGA), and surface area analysis to determine available surface area for adsorption, were conducted. The sample preparation and methodology for the petrographic, TGA and surface area analyses are discussed below.

The variation between individual large particles of coal will be dependent on the homogeneity of the vegetation that was deposited during the coalification process (Falcon, 1989). Therefore, large particles of coal can vary in composition significantly, even when taken from the same bench in a coal seam. As large particles were used in the experimentation, an extensive discussion was conducted with the supervisor of this research around how the analyses should be carried out to ensure data generated was representative of the large particles. To ensure that the coal characterisation was representative of the sample class size, a representative portion was crushed to meet the required size for analysis. Another reason for the decision to conduct analyses on a representative sample was that the analyses used were in many cases destructive of the sample or could only be conducted on a sample with a particle smaller than that used in experimentation.

4.3.1 Petrography

The 22.4 – 16 mm and 9.5 – 6.7 mm size classes were each separately coned and quartered again to obtain a representative samples for further analyses. These samples were crushed down to a passing size of 1 mm in a Retsch ZM 200 rotary mill. This particle size is recommended for petrography and BET analysis. The coal was then set in epoxy resin, and ground and polished to obtain a scratch free surface, following ISO 7404 part 2. This surface is important for the polarised reflected light microscope that is used to analyse the coal. A maceral and mineral count was undertaken on the petrographic blocks, following ISO 7404 part 4. A reflectance analysis was performed to determine the rank of the coal. Vitrinite reflectance is the most accurate determinant of coal rank, as vitrinite is the maceral that changes in the coalification process as the coal increases in rank. Petrography is a highly valuable coal analysis as it provides detailed information about the different organic components and the minerals in the coal. The petrographic analysis was undertaken in the School of Chemical and Metallurgical Engineering at the University of the Witwatersrand, by Professor Wagner, on a Leica DM4500P, magnification X500, with oil immersion.

4.3.2 Surface Area Analysis

A representative sample for surface area analysis for the 22.4 – 16 mm size class coal was crushed to less than 1 mm. The sample for surface area analysis from the 9.5 – 6.7 mm size class coal was not further crushed as the equipment at North West University can take particle sizes up to 10 mm in diameter. Three particles of this size were handpicked from all the particles in the size class, as the particles used in the adsorption experimentation were also handpicked. The option to analyse particles hand selected from the size class existed as the analysis equipment could handle particles of this size.

The particles were selected on the appearance of shiny parts in the particles. The shiny parts are indications of the maceral vitrinite in the coal, and vitrinite has been correlated with good adsorptive capacity of coal.

The analyses were conducted at North West University's Coal laboratory in a micrometrics ASAP 2020 surface area and porosity analyser.

4.3.3 TGA Analysis

A representative sample was taken from both the 22.4 – 16 mm and the 9.5 – 6.7 mm size classes. These samples were further crushed to below 150 µm. A proximate analysis was done in the Perkin Elmer STA 6000 TGA machine housed in the School of Chemical and Metallurgical Engineering, University of the Witwatersrand, Johannesburg.

The sample size used in the analysis was 17.042 mg for the representative sample of the 22.4 – 16 mm size class coal. The sample sized used in the analysis of the representative sample of the 9.5 – 6.7 mm size class coal was 9.990 mg.

The initial and final temperatures in the program were 30 degrees Celsius (^{o}C) and the entire proximate analysis was conducted at atmospheric pressure. The programme that was followed to conduct the analyses is detailed below.

Switch the Gas to Nitrogen at 40.0 ml/min

1) Heat from 30.00°C to 110.00°C at 50.00°C/min
   Switch the Gas to Nitrogen at 40.0 ml/min
2) Hold for 3.0 min at 110.00°C
3) Heat from 110.00°C to 900.00°C at 30.00°C/min
   Switch the Gas to Oxygen at 40.0 ml/min
   ... if the Temperature is >=700.00°C
4) Hold for 1.0 min at 900.00°C
   Switch the Gas to Nitrogen at 40.0 ml/min
   ... if the Time is >= 30.0 min

This programme allows the determination of the moisture content, volatile content, ash content, and the fixed carbon content of the coal.

4.4 Coal Particle Selection for Adsorption Experimentation

The particles in the smaller size class fitted easily in the adsorption equipment. The coal particles in the larger size class were sorted into particles that did and did not fit in the adsorption cell of the high pressure adsorption equipment. Despite screening particles into a size class that was smaller than the adsorption cell, the screening of particles only ensures that at least one side of a coal particle is smaller than the screen mesh. Thus, particles with a width and height smaller than the screen size but with a length larger than the mesh size can be found in classified coal.

Further visual sorting was done to isolate the coal particles that may have high vitrinite content. Vitrinite can be distinguished from the other macerals in coal as it has a brighter appearance. Coal particles that contain vitrinite are desirable for use in experimentation as vitrinite has high CO_2 storage potential due to its microporous nature (Crosdale *et al*., 1998; Dutta *et al*., 2008; Mares *et al*., 2009).

The coal particles in the 9.5 – 6.7 mm size class were also handpicked on the basis of brighter particles. All of these particles were of a size that allowed use in both the larger and smaller high pressure adsorption vessels.

4.5 Coal Degassing and Moisturisation

The particles that were hand selected were degassed before moisture was added and/or adsorption experiments were conducted. The coal was degassed for a minimum period of 12 hours. The conditions that were used to degas the coal were a temperature of 80°C and vacuum pressure. This ensures that the gases are released from the pores and evacuated from the area surrounding the coal. However, the coal remains otherwise unchanged as inherent moisture, volatile matter, carbon, and mineral matter should be unaffected by these conditions. Degassing coal removes previously adsorbed gases and therefore there should not be competition for adsorption sites on the coal.

Moisture was added to the degassed coal particles by submersion in distilled water. The amount of moisture that was added to the particle was determined by the change in mass of the particles before and after the submersion in the distilled water. The surface of the coal particles was allowed to dry before the particle was weighed after removal from the distilled water.

To examine the permanence of moisture that was added to coal by submersion in distilled water, three coal particles from the 9.5 – 6.7 mm size class were submerged in distilled water for a period of more than 24 hours. On removal from the distilled water, the particles were allowed to come to equilibrium with the laboratory environment and the change of mass as a result of the water leaving the particles was recorded. The experiment was repeated with a particle from the 22.4 – 16 mm size class.

The examination of the permanence of the moisture addition was done so that an estimate of the rate of change of the moisture in the particles was available. The adsorption experimentation calculations were performed for an atmosphere of pure CO_2 in the adsorption equipment. However, if the particle of coal was constantly reducing in moisture content during adsorption, then gaseous H_2O would be present in the sample cell as well. Further as water evaporated from the coal particle the mass of the particle would reduce. Thus, for the coal used in adsorption experimentation, the specific adsorption capacity of the coal would change. Therefore, the degree of evaporation of the moisture that was added to the coal should be considered.

4.6 True Volume Measurement

The volume of all coal samples used in the experimentation was determined with the use of a Quantachrome Instruments Helium (He) Stereo Pycnometer. As coal is a porous substance an accurate volume determination is necessary for use in the adsorption calculations. The principle used in the He Stereo Pycnometer is that the He is of such small molecular size that it will have access to the pores in the coal. Therefore the volume of the coal excluding the pores that are accessible to the He can be determined by the pressure of He in a closed system of known volume. The assumption is made that the He does not adsorb to the coal which is commonly made in research, but some doubt exists (Belmabkhout *et al*., 2004).

The Stereo Pycnometer has two internal chambers of which the volume of each is accurately known. In the sample chamber, the He is allowed to come to equilibrium with the particle. This means that all diffusion of He into the pores of the coal has stopped. When this occurs, a pressure reading for the closed chamber is recorded. Then a valve is opened, which allows the He to move freely between both chambers which reduces the pressure and a new equilibrium is obtained. The pressure reading after this second equilibrium is also recorded. Finally the accurate volumes of the system and the pressures that were recorded for the sample are used to calculate the true volume of the sample in the Stereo Pycnometer.

The equation that was used to find the volume of the particle was derived with the assumption that He behaves as an ideal gas. This is reasonable as the equipment does not operate at high pressures where most deviation from ideal gas conditions occurs.

Further, He has a low molecular weight and therefore agrees well with ideal gas assumptions which include: the molecules of an ideal gas have no individual weight, there are no forces of attraction or repulsion between the molecules of an ideal gas, all collisions between the molecules of an ideal gas are perfectly elastic, and the gas molecules are constantly in motion. The derivation for this equation, below, can be found in Appendix B.

$$\boldsymbol{V_P = V_C + \frac{V_A}{\left(1-\frac{P_2}{P_3}\right)}} \qquad 6$$

Where

V_P is the volume of the particle placed in the Pycnomter (cm^3)

V_C is the volume of the sample cell of the Pycnometer (cm^3)

V_A is the added volume available for the expansion of the He into the adjoining cell of the Pycnometer (cm^3)

P_2 is the pressure in the sample cell after equilibrium is achieved between the sample and the He subsequent to the initial pressurization with He

P_3 is the pressure in the sample cell after the addition of V_A and the expansion of the He

The true volume of all particles that were used in adsorption experimentation was measured. Knowing the true volume of the particles was important as the volumetric adsorption system is based on accurate knowledge of the volume of the whole system, and subsequently the void space in the system during experimentation. The void space is the difference between the system volume and the sample volume.

Ideally, the true volume of the particles should have been measured immediately before CO_2 adsorption experimentation started. However, due to leaks on the He line, the volume of the particles used in the preliminary experimentation was only analysed after CO_2 adsorption experimentation. The volume of the rest of the particles used in this research was determined in advance of adsorption experimentation.

4.7 Adsorption Experimentation

4.7.1 Adsorption Capacity Testing Equipment

As discussed in Chapter 2, there is limited published data on CO_2 storage potential in moist coal (Viljoen *et al*., 2010). There is even less research using South African coals, dry or moist. The experimental procedure adopted was based on the best assessment at the time, and the available equipment. This decision was made through consultation of the literature -mentioned above- and options available to the students in the coal

laboratory of the University of the Witwatersrand, in terms of equipment and academic staff's expertise.

The equipment that was available for CO_2 adoption experimentation in this research project was a volumetric adsorption system commissioned by Maphada (2012). Adsorption capacity is tested via two different concepts: a volumetric system where pressure changes are measured as an indicator of adsorption, and a gravimetric system where changes in weight of the sample are used as an indication of the CO_2 adsorbed to the sample. Belmabkhout *et al*., (2004) found that gravimetric adsorption equipment is more accurate due to the direct measurement of adsorption through change in mass. However, when strict experimental procedures are followed, the differences between the systems are not significant (Belmabkhout *et al*., 2004). Volumetric systems are currently the most widely used (Sabir and Chalaturnyk, 2009), due to a far lower cost of construction.

The premise of the volumetric adsorption system is that it is a completely sealed system and therefore experimentation occurs at a constant volume. The CO_2 that is absorbed on the coal can be measured through the change in pressure in the constant volume system using an appropriate gas equation. Belmabkhout *et al*. (2004) discuss the difficulty of keeping adsorption equipment leak proof and the impact of leakage on data inaccuracy. However, the leakage rate is difficult to determine without knowing the adsorption capacity of the sample that is being tested. Nonetheless Belmabkhout *et al*. (2004) have estimated that a leakage rate of the order of 10^{-4}mol/hr leads to an average error of 0.2%.

4.7.2 Equipment Details and Operation

A high pressure volumetric adsorption system was commissioned in 2011 for CO_2 adsorption experiments conducted at the University of the Witwatersrand.

The system consists of:

- a pump to pressurize the system with CO_2
    - the CO_2 used by the system is bottled liquid CO_2 from Afrox. As adsorption isotherms are produced at a constant temperature, but using differing pressures; a pump is necessary to operate above the pressure of the bottled liquid CO_2. The pump can also be used with a good control system to operate below the pressure of the bottled liquid CO_2. The pump used is a Telodyne ISCO pump.
- two pressure vessels/reactors
- a constant temperature oven
- a ventilation system to release system gases to the atmosphere

- a vacuum pump to evacuate the system
- a heating jacket to degas the samples, and
- valves where appropriate to isolate certain areas of the system.

Figure 8 represents the core aspects of the system, and has been included for ease of understanding as Figure 9 does not show the reference and sample cells that are situated in the constant temperature oven.

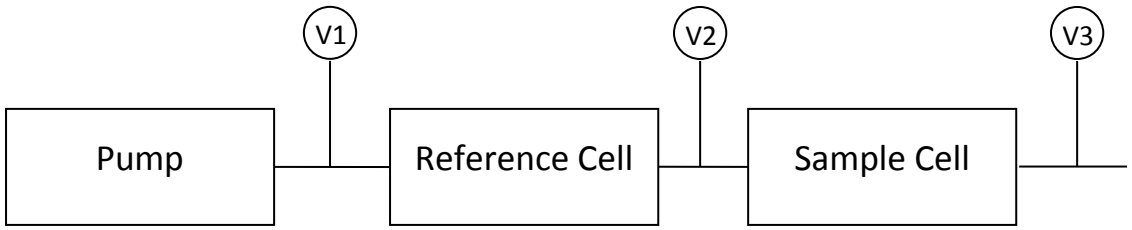

Figure 8: Core aspects of the laboratory CO_2 adsorption equipment

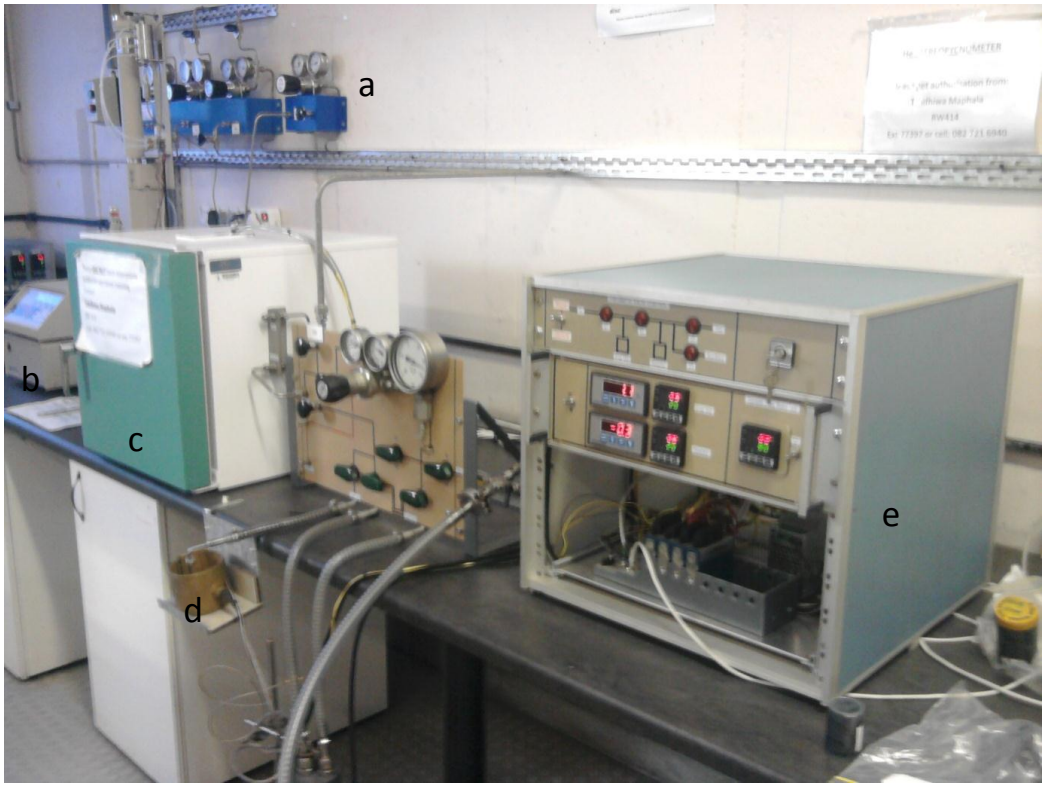

Figure 9: Picture of the laboratory adsorption equipment showing the pump, oven, degassing system, and the data logging system (see text for annotations)

Figure 9 shows the CO_2, Ar and He gas lines that are connected to the equipment (a) to the left of the picture. The equipment in front of the gas lines on the extreme left of the picture is the CO_2 pump (b). The insulated container is the constant temperature oven in which the pressure vessels containing the coal sample and the empty reference cell are placed (c). To the right of the oven is the vent that takes the system gases to the atmosphere and the degassing setup that allows the coal gasses to pass through a volatile trap (used only for high volatile matter coal) and then through a vacuum pump (d). Lastly, on the right of the picture is the control equipment that can be used to manually open and close the valves in the system, the tubing and the valves that connect the system to a vacuum pump (below the picture), the switch for the heating jacket used in coal degassing and the data logging equipment that records the temperatures and pressures in the sample and reference cells (e).

Images of one of the pressure vessels/reactors that was designed for this equipment are in Figure 10 and Figure 11. The pressure vessel is held together with 8 large bolts that have to be tightened adequately to prevent leakage from the system. However, tightening the bolts too much reduced the lifetime of the seals used in the pressure vessels. These seals are only guaranteed to be leak free for a single use.

The seal of the pressure vessel is denoted by “f” in Figure 11. The seals are placed in grooves in the pressure vessels concentric to the internal cavity used for the coal samples. Helicoflex seals were imported for this equipment up to the end of September 2012. There were numerous procurement problems and the seals were costly. From October 2012, cheaper locally produced seals were manufactured in South Africa. These seals were prototypes and their material of construction will be modified with further research at the University of the Witwatersrand. The South African made seals were used in the 22.4 – 16 mm particle adsorption experimentation conducted for this research. The imported Helicoflex seals were used in the 9.5 – 6.7 mm particle adsorption experimentation.

There is a single connection point to link the pressure vessels to the adsorption system. This can be seen clearly in Figure 10.

Figure 10: Top View of Pressure Vessel/Reactor B used in the adsorption capacity testing

Figure 11: Internal view of the pressure vessel/reactor used to hold the coal samples

The procedure for operation of the equipment is:

1. The degassed or degassed and moisturised sample was placed in the pressure vessel. An additional pressure vessel was available for use and allowed for example: a sample to be degassed as well as a sample tested for CO_2 adsorption capacity. The pressure vessel containing the sample was secured in the constant temperature oven and the system was reduced to vacuum pressure. This was an important step as all gases in the system need to be removed for an accurate determination of the adsorption of CO_2 and not other gases on coal. While the system was reduced to vacuum pressure, all valves were opened except valve one between the pump and the system. The gas in the pump should be pure CO_2 as the pump is dedicated to the adsorption system and has never been used with any gases other than CO_2.
2. When the system was evacuated the leakage testing was started. The leakage testing was done by pressurizing the system and confirming that the pressure

did not drop appreciably. It is important to know that the system is not leaking as the method that is used to determine the adsorption of CO_2 onto the coal is the slow reduction of pressure as adsorption occurs.

3. Finally the adsorption experiment was started. The equipment is controlled by a desktop computer that has LabView software installed. The inputs that are used are the start and end pressures for the experiment, the pressure increments that should be used to move from the start to the end pressure, and the time that the system should be given to come to equilibrium before the pressure is increased in the next step towards the final pressure.
4. For each pressure step the pump pressurises the CO_2 to the programmed value. During this step valves V1, V2, and V3 as labelled in Figure 8 are all closed. When the programmed pressure is reached valve V1 is opened and the CO_2 expands into the reference cell. Valve V1 is then closed again. Valve V2 is then opened and the CO_2 expands into the cell containing the coal sample. Valve V2 is closed after 5 seconds. This procedure is repeated until the final pressure step. When the equilibrium time allowed for the sample is complete valve V3 is opened and the pressurised CO_2 is vented to the atmosphere.
5. The sample was removed from the adsorption equipment after the gas in the system was vented to the atmosphere. The coal sample was then placed in distilled water. Thus, the same coal sample was used for the generation of the adsorption isotherm, and particles were not changed for each pressure step.
6. The adsorption tests were conducted isothermally at $40^{o}C$ in the constant temperature oven. This temperature was chosen with reference to the supercritical conditions (Figure 1) of CO_2. The temperature of the system was kept above supercritical temperature to ensure that the CO_2 in the system was either gas or supercritical fluid. All pressure, temperature and time data is continuously logged. The data is retrieved from the equipment with the aid of the file handling programme FileZilla.

The starting pressure for all samples was 10 bar and the pressure increments used were 15 bar. The last pressure used in the experiment was 100 bar. These start and end pressures reflect the pressures that the pump attached to the system attains before valve V1 is opened. The pressure in the reference and sample cells is not equal to these exact pressures; for example, the pressure in the reference cell started at 10 bar, resulting in a pressure around 5 bar in both the reference and the sample cells when V2 was opened. After 10 bar, the pressure sequence in the reference cell was 25 bar, 40 bar, 55 bar, 70 bar, 85 bar and 100 bar. After the first step, there is some pressure in the sample cell so the pressure does not halve again as it does in the first pressure step. Thus, the pressures achieved during experimentation in the sample cell are always lower than those in the reference cell.

Differing periods of time were allowed for the system to come to equilibrium in preliminary testing, as this information was not available for the equipment as it is newly commissioned. Further details may be found in the Results Chapter.

4.7.3 Equipment Volume

Before experimentation commences, the volume of the equipment had to be known to allow interpretation of the pressure data. Therefore, the volume of the adsorption cells as well as the piping between the valves in the system was determined. This was done by expansion of He from the reference sections to the sample sections of the equipment and recording the pressure changes in both cells. The expansion of the He is then repeated with an item of known volume in the sample cell. The calculations of the volumes of the system parts were done using the ideal gas equation, as He is a noble gas of low molecular weight and thus approximates ideal gas behaviour most appropriately.

Let the volume of the reference cell, as well as the piping from the first valve at the entrance to the system to the valve separating the reference and sample sections of the equipment, be V_R. Similarly, let the volume of the sample cell and the piping from the second valve separating the reference and sample sections of the equipment to the valve at the exit of the system, be V_S. Further, the initial state of the system before the expansion shall be denoted by the subscript i and the state after the expansion of the gas with subscript j. Therefore, in line with the ideal gas laws this constant temperature process can be described by:

$$\mathbf{P_i V_R = P_j (V_R + V_S)} \qquad 7$$

Where

P_i is the initial pressure in the system before the expansion of the He (bar)

V_R is the volume of the reference cell and all tubing from the valve after the pump to the valve before the sample cell (mL)

P_j is the pressure in the entire system when the He can move freely between the reference and sample cells (bar)

V_S is the volume of the sample cell and all tubing from the after the valve before the sample cell valve after at the system exit (mL)

Equation 7 can be rearranged to get:

$$\frac{\mathbf{V_S}}{\mathbf{V_R}} = \frac{\mathbf{P_i}}{\mathbf{P_j}} - \mathbf{1} \qquad 8$$

The ratio of sample volume and reference volume, for all pressure vessels used in experimentation, should be determined with a number of experimental runs. This data should be recorded and an average of at least 3 data points should be used to find an average ratio.

This process is then repeated with the sample of known volume (V_K) the equation describing this expansion is:

$$\mathbf{P_k V_R = P_l(V_R + V_S + V_K)} \qquad 9$$

Where:

V_K is a sample of known volume (mL)

P_k is the initial pressure in the system when a sample of known volume is in the sample cell before the expansion of the He out of the reference cell and into the whole system (bar)

P_l is the pressure in the entire system when the He can move freely between the reference cell and sample cell containing the sample of known volume (bar)

Equation 9 can be rearranged to get:

$$\mathbf{V_R = \frac{V_K}{\frac{P_k}{P_l} - 1 - \frac{V_S}{V_R}}} \qquad 10$$

Equation 10 can be solved using the average ratio of the sample and reference volumes determined in the He expansions in the empty system. The volume of the sample cell can then be found using the volume ratio and the calculated reference volume:

$$\mathbf{V_S = \frac{V_S}{V_R} * V_R} \qquad 11$$

The results of the equipment volume determination can be found in the Results Chapter.

4.7.4 Correcting for Leakage in the System

Due to the problems experienced with keeping the system leak free and the need to generate further data for the research, a method for correcting for leakage in the system was devised. After experimental runs the same sample cell was emptied and re-placed in the equipment. The experiment was then run for the same equilibration times and the data on the pressure loss in the sample cell was logged using Labview and FileZilla. This blank run was then used to correct the experimental data to cater for the leakage in the system.

The correction was done by the calculation of a leakage rate at each pressure step and then the addition of the pressure that would have leaked from the system in the time taken to complete the pressure step to the final pressure that was recorded in the runs with a sample in the sample cell.

The potential issues with this approach are as follows:

- The 8 bolts that close the reactor could be tightened differently in the run with the sample and the run without the sample. While all efforts were made to avoid this, this may potentially add error to the results.
- The seals that are used in the experiments are only guaranteed to hold pressure the first time that the pressure vessels are closed. Thus, the leaking from the pressure vessel in the blank run may exceed that of the sample run should the seal be damaged or compromised in the first run in any way. Damage to the seals often cannot be seen with the naked eye. Further, a new seal should not be used in the blank run either as if there were any leaks from the original seal these could not be corrected in the data should a new seal be used.
- The control of the system and the pump through Labview is not precise enough to reach exactly the same pressure on each pressure step. As leaking is driven by the pressure gradient between the system and the atmosphere (the constant temperature oven in which the reference and sample cell are housed is at atmospheric pressure) should the blank run reach a higher pressure than the sample the leakage rate may be higher than it was in the sample run. The same is true for the converse.

The error due to leakage from Belmabkhout et al. (2004) was estimated at an average error of 0.2% from a leakage rate of the order of 10^{-4}mol/hr. The leakage rate of the equipment at the University of the Witwatersrand is unfortunately far greater. An attempt at the quantification of the error in the results can be found in the Discussion Chapter.

4.7.5 Adsorption calculations

The amount of CO_2 that has adsorbed onto the coal shall be determined through the change in the number of moles of the gas in the void space in the sample cell. The void space is the difference between the total volume of the sample cell and the piping that was determined above and the volume of the sample that was determined in the He pycnometer. The change in the moles in the void space due to adsorption shall be determined with the ideal gas equation with the compressibility factor to cater for non-ideal behaviour of the gas. The pressure shall reduce in the void space with the adsorption of the CO_2 onto the coal. The equation showing the number of moles adsorbed in a pressure step is below:

$$\mathbf{N_{ads} = N_{Final} - N_{Initial}} \qquad \mathbf{12}$$

Where:

N_{ads} is the number of moles of CO_2 that have adsorbed on the coal (mol)

N_{Final} is the number of moles of CO_2 that are present in the void space in the sample cell at the end of the current pressure step (mol)

$N_{Initial}$ is the number of moles of CO_2 that are present in the void space in the sample cell at the start of the current pressure step (mol)

$$\mathbf{N_{ads}} = \frac{\mathbf{P_{Final}V}}{\mathbf{Z_{Final}RT_{Final}}} - \frac{\mathbf{P_{Initial}V}}{\mathbf{Z_{Initial}RT_{Initial}}} \quad \textbf{13}$$

Where:

P_{Final} is the pressure in the void space of the sample cell at the end of the pressure step (bar)

V is the volume of the sample cell and all tubing between V2 and V3, less the volume of the coal sample used for experimentation (mL)

Z_{Final} is the compressibility factor used to cater for the non ideality of the system for the pressure and temperature in the sample cell at the end of the pressure step

R is the ideal gas constant (0.08314472 L bar/K mol)

T_{Final} is the temperature in the void space of the sample cell at the end of the pressure step (K)

$P_{Initial}$ is the pressure in the void space of the sample cell at the start of the pressure step (bar)

$Z_{Initial}$ is the compressibility factor used to cater for the non ideality of the system for the pressure and temperature in the sample cell at the start of the pressure step

$T_{Initial}$ is the temperature in the void space of the sample cell at the start of the pressure step (K)

The table of compressibility factors that were used as source data for the CO_2 compressibility factors is in Table 4 (Perry *et al*., 1997). This table does not cater for the temperature of the sample cell or the exact pressure at the start and end of each step. Therefore these values were interpolated, where there was data on either side of the value that was desired, or extrapolated when only a single data point that was close to the desired value existed. The compressibility factors that were found in the interpolation and extrapolation were appreciably different from those in Table 4. The green values in Table 5 are the interpolated and extrapolated values for the temperature in the sample cell at the start and end of each pressure step for experimental data generated in this research. The exact temperature at the start and end of every pressure step was used to interpolate the data, despite the experimentation being conducted in a constant temperature oven. This was done as it was found that the compressibility factor for CO_2 is a strong function of temperature. The red values in Table 5 are the pressures at the start and end of a pressure step and the compressibility factors that were interpolated for these conditions. Where possible the original values in Perry et al. (1997) were used in the calculation of the red values.

The compressibility factors that were interpolated for the other temperature and pressure conditions during all the experimental runs can be found in Appendix A.

Table 4: CO_2 Compressibility factors at different pressures and temperatures (Perry *et al*., 1997[9])

Temp (^oC)	Pressure (bar)									
	1	5	10	20	40	60	80	100	200	300
0	0.9933	0.9658	0.9294	0.8496						
50	0.9964	0.9805	0.9607	0.9195	0.8300	0.7264	0.5981	0.4239		
100	0.9977	0.9883	0.9764	0.9524	0.9034	0.8533	0.8022	0.7514	0.5891	0.6420
150	0.9985	0.9927	0.9853	0.9705	0.9416	0.9131	0.8854	0.8590	0.7651	0.7623
200	0.9991	0.9953	0.9908	0.9818	0.9640	0.9473	0.9313	0.9170	0.8649	0.8619
250	0.9994	0.9971	0.9943	0.9886	0.9783	0.9684	0.9593	0.9511	0.9253	0.9294
300	0.9996	0.9982	0.9967	0.9936	0.9875	0.9822	0.9733	0.9733	0.9640	0.9746
350	0.9998	0.9991	0.9983	0.9964	0.9938	0.9914	0.9896	0.9882	0.9895	1.0053
400	0.9999	0.9997	0.9994	0.9989	0.9982	0.9979	0.9979	0.9984	1.0073	1.0266
450	1.0000	1.0000	1.0003	1.0005	1.0013	1.0023	1.0038	1.0056	1.0070	1.0412
500	1.0000	1.0004	1.0008	1.0015	1.0035	1.0056	1.0079	1.0107	1.0282	1.0522
600	1.0000	1.0007	1.0013	1.0030	1.0062	1.0093	1.0129	1.0168	1.0386	1.0648
700	1.0003	1.0010	1.0017	1.0036	1.0073	1.0161	1.0155	1.0198	1.0436	1.0707
800	1.0002	1.0009	1.0019	1.0040	1.0082	1.0122	1.0168	1.0212	1.0458	1.0731
900	1.0002	1.0009	1.0020	1.0041	1.0083	1.0128	1.0171	1.0221	1.0463	1.0726
1000	1.0002	1.0009	1.0021	1.0042	1.0084	1.0128	1.0172	1.0218	1.046	1.0725

[9]Calculated from density-pressure-temperature data in Vukalovitch and Altunin, *Thermophysical Properties of Carbon Dioxide*, Atomizdat, Moscow, 1965, and Collet's London, 1968, translation.

Table 5: Compressibility factors for CO_2 that were used in the calculation of the results of this research

Temp (° C)	Pressure (bar)										
	1	5	6.798	*6.908*	10	18.935	19.188	20	33.620	33.994	40
0	0.9933	0.9658			0.9294			0.8496			-
37.95					*0.9532*	*0.9080*		*0.9026*			
38.01			*0.9684*		-			*0.9027*	0.8412		0.8124
38.04											0.8124
38.11											
38.17											
38.21											
38.01	0.9961	0.9786			0.9569			0.9116	0.8441	0.8422	0.8124
38.16				*0.9729*							
38.31					*0.9534*		*0.9072*	*0.9032*			
38.35								*0.9032*		0.8400	0.8129
38.67											
38.79								*0.9038*			0.8135
39.00											
39.18											
50	0.9964	0.9805			0.9607			0.9195			0.8300
100	0.9977	0.9883			0.9764			0.9524			0.9034
Temp (° C)	**Pressure (bar)**										
	46.981	47.615	60	62.839	63.616	74.681	75.145	79.505	80	80.696	100
0			-						-		-
37.95											
38.01											
38.04	0.7718		0.6960								
38.11			0.6962			0.5876			0.5482		
38.17			0.6964					0.5534	0.5498		
38.21			0.6965	0.6757					0.5500		
38.16											
38.31											
38.35											
38.67			0.6976		0.6713				0.5518		
38.79		0.7695	0.6979								
39.00			0.6985				0.5885		0.5532		
39.18									0.5539	0.5469	0.3530
50			0.7264						0.5981		0.4239
100			0.8533						0.8022		0.7514

4.8 Desorption of Added CO_2 into Distilled Water

To test the likelihood of water acidification in the event that CO_2 is stored in underground coal seams, desorption into water of the CO_2 from the adsorbed particles was tested. This was tested by the measurement of pH of the distilled water that the particles were submerged in after CO_2 adsorption experimentation.

The way in which this was done was to place the CO_2 saturated coal, after adsorption experimentation, in distilled water and measure the change in pH, if any, of the water. pH is measured using the concentration of Hydrogen ions(H^+) in solution as shown in the equation below.

$$\mathrm{pH} = -\log[\mathrm{H}^+] \qquad 14$$

The most likely reaction that will occur if CO_2 desorbs and dissolves in the distilled water is:

$$H_2O + CO_2 \rightarrow HCO_3^- + H^+ \qquad 15$$

Therefore the molar concentration of H^+ can be obtained by calculation from the reading obtained from the pH meter and the moles of dissolved CO_2 can be obtained by stoichiometry.

The pH of this water was measured with a Crison GLP 21+ pH meter. This pH meter measures pH by stability and required daily calibration with the 4.01, 7 and 9.21 pH standard solutions that were provided with the meter. The daily calibration of the pH meter before use ensured that readings from the meter were more accurate. pH measurement by stability requires the reading registered by the probe to remain constant for a period of time. If a constant reading cannot be obtained repeat measurements must occur until the reading stabilises. The amount of time for pH reading stabilisation that is allowed is 150 seconds.

The time period required for pH reading stabilisation may be problematic for conditions where pH is changing as the measurement occurs. This may be the case with the measurement of the pH in this research as the coal with adsorbed CO_2 remains in a closed system with the distilled water until the measurement of the pH is conducted. This requires the coal and distilled water container to be open to the atmosphere where a new equilibrium state will be attained. Unfortunately, the time when the system is reaching a new equilibrium with the laboratory environment is also the time when the pH is measured. Therefore, pH readings may be reflective of the equilibrium with the laboratory environment and not that of the pH of the distilled water with any desorbed CO_2 dissolved in it.

4.9 Chapter Summary

Coal preparation, coal analyses, and the experimentation conducted for this research report are discussed in this chapter. Operation of the laboratory equipment and additional equipment used in the completion of this research is also detailed. Analyses were conducted on representative samples from the 22.4 – 16 mm and 9.5 – 6.7 mm size classes. Adsorption experimentation was conducted on both size classes. Results are presented in the following chapter.

5 Results

Results of the analyses and experimentation on the 9.5 – 6.7 mm and 22.4 – 16 mm size class particles are detailed below. The coal analyses were conducted on representative samples of the larger size class, with the exception of the surface area analyses as the equipment could take particles up to 10 mm in diameter. The adsorption experimentation was conducted on numerous samples from the 9.5 – 6.7 mm size class to determine the correct equilibration time to use for the volumetric adsorption equipment. Results are presented for four of these samples. Further testing on the same size class was conducted on five more particles from this size class. Lastly, six particles from the largest size class were tested in the volumetric adsorption equipment. This is summarised in Table 6.

Table 6: Summary of Adsorption Experimentation, Particles, Size Classes and Sample IDs

Experimentation	Number of Particles	Particle Size Class	Sample IDs
Preliminary Experimentation	4	9.5 – 6.7 mm	Sample 1, Sample 2, Sample 3, Sample 4
9.5 – 6.7 mm size class experimentation	5	9.5 – 6.7 mm	S1, S2, S3, S4, S5
22.4 – 16 mm size class experimentation	6	22.4 – 16 mm	L1, L2, L3, L4, L5, L6

The results of the adsorption experimentation are presented below with a comparison between all the results of the preliminary, 9.5 – 6.7 mm size class and 22.4 – 16 mm size class experimentation section at the end of that specific section.

5.1 Coal Analyses

5.1.1 Coal Moisture Determination

The results of the analysis conducted by ALS were that the as received coal had 6.3% total H_2O and 0.8% surface H_2O. The laboratory report for the analysis is in Appendix C.

5.1.2 Petrographic Analyses

The results of the petrographic analysis conducted on the representative sample of the 9.5 – 6.7 mm and 22.4 – 16 mm size class coal are in Table 7. The coal has a maceral

distribution and mineral matter content as one would expect for a Witbank coal. There is a slight difference in the maceral and mineral distribution between the size classes, but this should not really influence the adsorption experiments. The vitrinite reflectance analysis determined that the coal was Medium Rank C.

Figure 12, Figure 13 and Figure 14 show reflected light microscope pictures of the coal that was used in these experiments.

Table 7: Maceral groups and the volume percentages in which they occur in the 9.5 – 6.7 mm and 22.4 – 16 mm size class representative samples

Maceral Group	9.5 – 6.7 mm Sample: Volume %	22.4 – 16 mm Sample: Volume %
Vitrinite	21.0	28.8
Inertinite	45.4	46.8
Liptinite	8.8	5.2
Mineral Matter	24.8	19.2

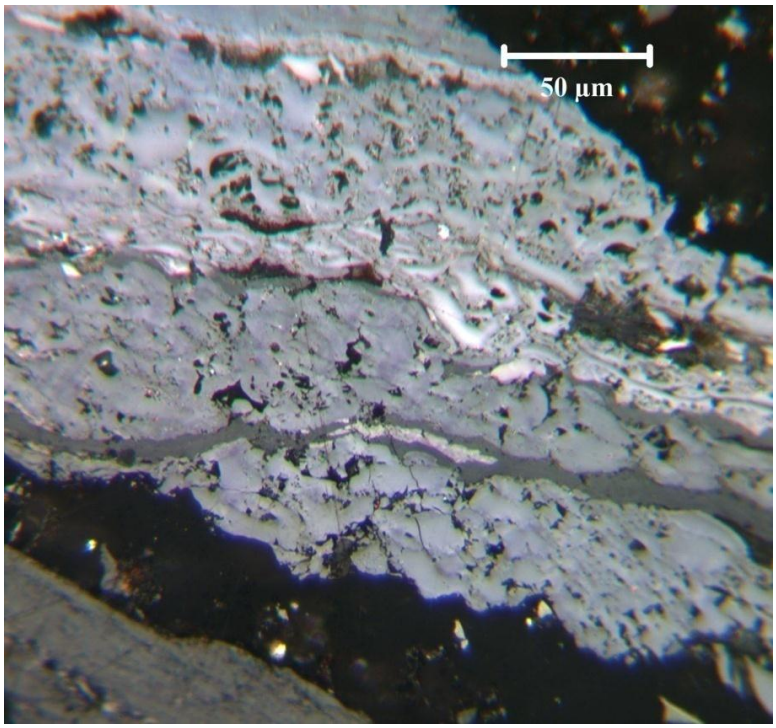

Figure 12: Reactive and inert semifusinite (oil immersion lense, reflected light petrographic image)

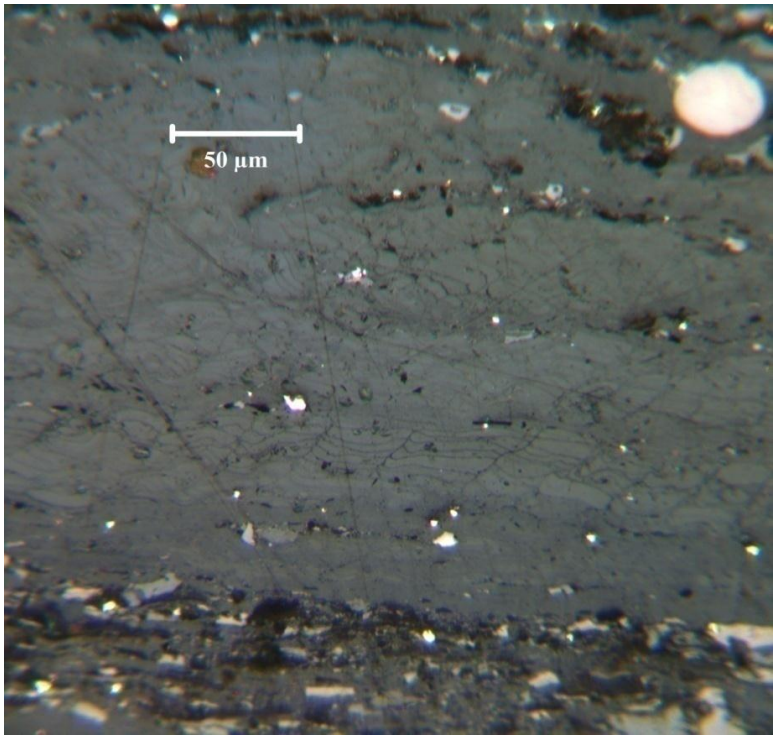

Figure 13: Picture of the vitrinite component in the coal (oil immersion lense, reflected light petrographic image)

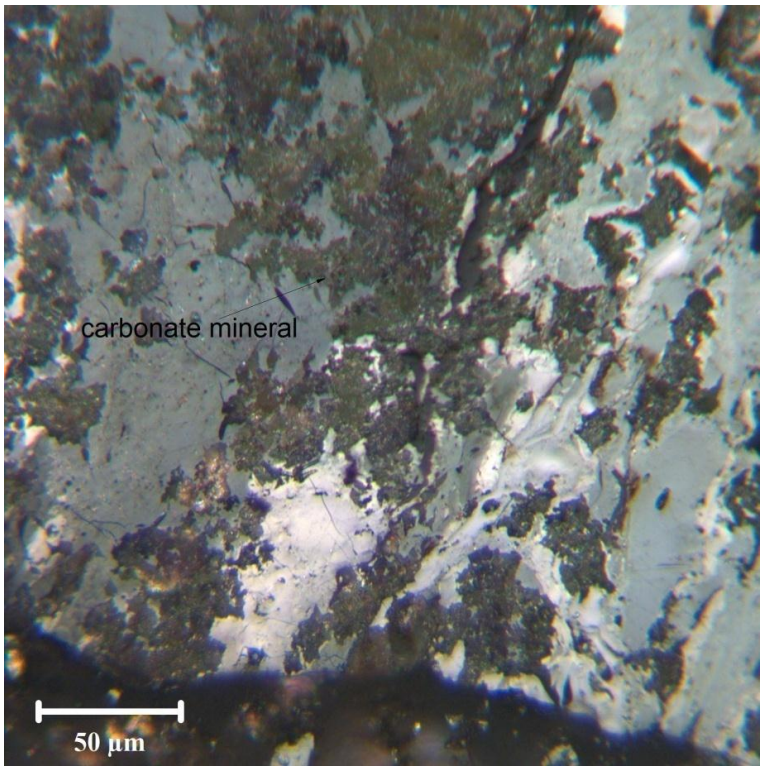

Figure 14: Carbonate minerals (grey/brown) distributed in the coal (Light Grey) [oil immersion lense, reflected light petrographic image]

5.1.3 Surface Area Analyses

The results of the Surface Area Analysis of the 22.4 – 16 mm size class sample (crushed to a passing size of 1 mm) as advised by equipment operator and the two 9.5 - 6.7 mm hand selected particles are in Table 8. The agreement between the results of the two hand selected 9.5 – 6.7 mm particles is good. There is some agreement between the different calculation methods, but differences are clearly observable.

The surface area and adsorption capacity is larger in the 22.4 – 16 mm representative sample when compared to the two 9.5 – 6.7 mm particles. This is as expected as crushing opens pores in coal, and the 22.4 – 16 mm sample was crushed to a passing size of 1 mm as the equipment at North West University could only take particles up to 10 mm in diameter.

Table 8: Surface area analysis results for the 22.4 – 16 mm size class sample and the two 9.5 - 6.7 mm particles

	Analysis Method	Surface Area (m^2/g)	Capacity (cm^3/g)
22.4 - 16 mm size class crushed to 1mm	Dubinin-Radushkevich	118.302839	25.897196
	BET	78.7089 ± 3.1822	17.2298
	Langmuir	86.9349 ± 4.8615	19.0306
First: 9.5 - 6.7 mm particle hand selected for analysis	Dubinin-Radushkevich	77.569033	16.980324
	BET	49.9324±1.5343	10.9305
	Langmuir	54.8208±2.4614	12.0006
Second: 9.5 - 6.7 mm particle hand selected for analysis	Dubinin-Radushkevich	83.792336	18.342642
	BET	54.2648±1.5620	11.8789
	Langmuir	58.8426±2.4626	12.8810

5.1.4 TGA Analyses

As an example, the mass loss of the representative sample of the 9.5 – 6.7 mm size class generated in the Perkin Elmer TGA, as well as the temperature at which the mass loss occurred, is presented below.

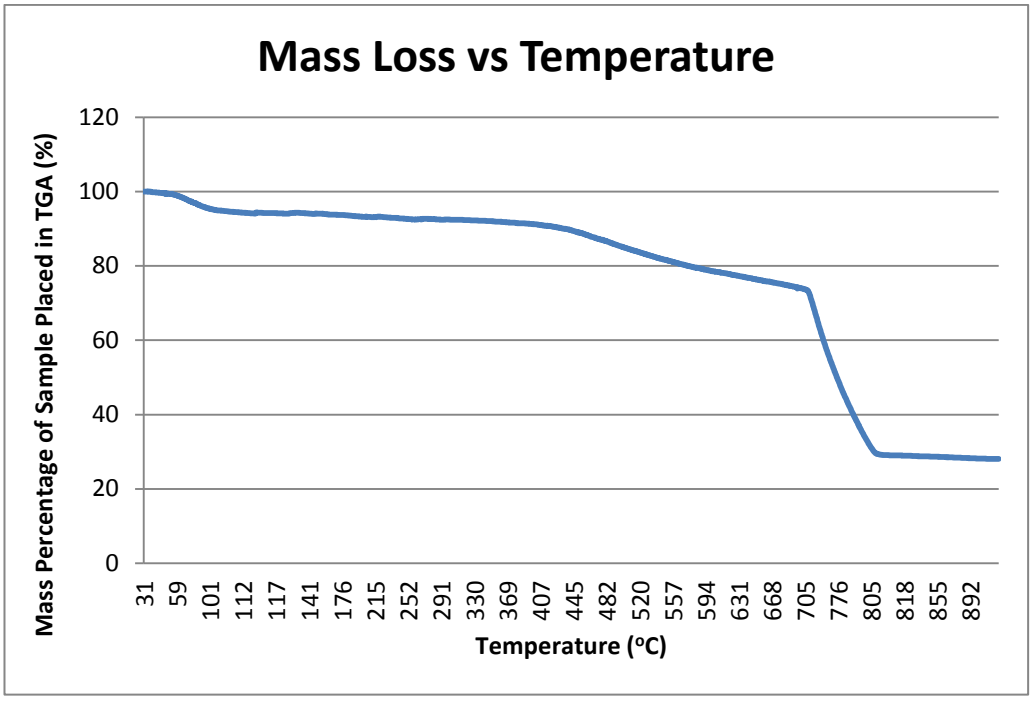

Figure 15: Proximate analysis data - mass loss during heating of the coal sample representing size class 9.5 – 6.7 mm

The points of inflection where the gradient of the graph changed were examined. Then the source data used to draw the graph was consulted to obtain the moisture, volatile and ash content of the sample. The fixed carbon content of the sample was determined by the difference between the total sample mass and the moisture, volatile and ash contents. The proximate analysis of the sample and the 22.4 – 16 mm size class sample was thus completed and is detailed in Table 9. From a proximate perspective, the data is comparable between the size fractions, with a moderate to high ash content as expected from a Witbank coal.

Table 9: Proximate analysis on 9.5 – 6.7 mm and 22.4 – 16 mm size class coal used in experimentation

Coal Constituent	9.5 – 6.7 mm Size Class Content (Mass%)	22.4 – 16 mm Size Class Content (Mass%)
Moisture Content	5.79	3.99
Volatile Carbon	20.37	19.93
Fixed Carbon	45.76	47.82
Ash	28.07	28.26

5.2 Coal Moisturisation

The mass % moisture that was added to the particles submerged in distilled water is tabulated below. All particles were degassed before submersion in distilled water.

Table 10 contains data for the 9.5 – 6.7 mm and 22.4 – 16 mm size classes of coal. While confirming the moisture addition by means of TGA would have been ideal, the TGA at the University of the Witwatersrand is only able to take powdered coal samples and therefore this was not possible. Crushing the moisturised samples would result in the loss of the added moisture as coal would be exposed to the atmosphere during crushing.

Table 10: Moisture addition to particles in the 9.5 – 6.7 mm size class

Sample ID	Dry Mass (g)	Mass after Moisture Addition (g)	Mass % Moisture Added
Sample 2	0.529	0.571	7.94%
Sample 3	0.595	0.681	14.45%
Sample 4	0.369	0.412	11.65%
S2	0.346	0.369	6.65%
S5	0.316	0.322	1.90%
L3	6.565	6.895	3.59%
L5	4.463	4.597	3.00%

The results of the mass change with evaporation following moisturisation of the three 9.5 – 6.7 mm particles are included in Table 11. The mass change of the particles with evaporation slows after 15 minutes of exposure of the particles to the laboratory environment. This confirms the time that was allowed for the surface of the moisturised particles to appear visually dry before adsorption experimentation was conducted. This is an important result as it means the atmosphere in the sample cell will be mostly CO_2 and thus adequately described by the ideal gas equation with the compressibility factor to cater for non ideal behaviour. Further, the mass used to quantify the CO_2 adsorption per ton of coal (specific adsorption capacity) should be more reliable when the mass of coal after the surface has dried is used in the quantification. However, the percentage of moisture loss of all the particles does not seem to plateau at any value. This is unfortunate as it infers that moisture is released from the coal particles throughout adsorption experimentation.

The Johannesburg atmospheric conditions on the day that this evaporation experiment was conducted, at 17h00, were 28.4^{o}C and 37% humidity (South African Weather Service, 2011). These conditions would be the same as those in the laboratory as it is open to the atmosphere.

Table 11: Change in mass of particles from the 9.5 – 6.7 mm size class with evaporation of adsorbed water

	Largest Particle- dry mass 0.779g		Long Thin Particle- dry mass 0.315g		Square Particle- dry mass 0.301g	
Time	**Mass (g)**	**% Moisture Addition**	**Mass (g)**	**% Moisture Addition**	**Mass (g)**	**% Moisture Addition**
19/01/11, 11:46AM	0.825	5.91	0.336	6.67	0.330	9.63
19/01/11, 11:48AM	0.817	4.88	0.333	5.71	0.326	8.31
19/01/11, 11:50AM	0.815	4.62	0.332	5.40	0.324	7.64
19/01/11, 11:53AM	0.812	4.24	0.33	4.76	0.321	6.64
19/01/11, 11:55AM	0.811	4.11	0.328	4.13	0.32	6.31
19/01/11, 12:00PM	0.809	3.85	0.326	3.49	0.319	5.98
19/01/11, 12:09PM	0.807	3.59	0.325	3.17	0.318	5.65
19/01/11, 12:20PM	0.806	3.47	0.325	3.17	0.317	5.32
19/01/11, 12:30PM	0.806	3.47	0.324	2.86	0.317	5.32
19/01/11, 13:04PM	0.803	3.08	0.323	2.54	0.316	4.98
19/01/11, 13:56PM	0.801	2.82	0.321	1.90	0.315	4.65
19/01/11, 15:01PM	0.799	2.57	0.320	1.59	0.314	4.32
19/01/11, 16:08PM	0.798	2.44	0.320	1.59	0.313	3.99
19/01/11, 17:15PM	0.796	2.18	0.319	1.27	0.312	3.65

The results of the mass change with evaporation following moisturisation of a 22.4 –16 mm particle are included in Table 12. The Johannesburg atmospheric conditions on the day that this evaporation experiment was conducted, at 17h00, were 30^{o}C and 32% humidity (World Weather Online, 2012). These conditions would be the same as those in the laboratory as it is open to the atmosphere.

Table 12: Change in mass of particle L7 from the 22.4 – 16 mm size class with evaporation of adsorbed water

	Large Particle 7 - dry mass 2.660g				
Time Particle was Weighed	**Mass (g)**	**% Moisture Addition**	**Time Particle was Weighed**	**Mass (g)**	**% Moisture Addition**
17/09/2012 14:37 PM	2.880	8.27%	17/09/2012 15:06 PM	2.728	2.56%
17/09/2012 14:38 PM	2.792	4.96%	17/09/2012 15:08 PM	2.727	2.52%
17/09/2012 14:39 PM	2.777	4.40%	17/09/2012 15:10 PM	2.725	2.44%
17/09/2012 14:40 PM	2.772	4.21%	17/09/2012 15:14 PM	2.723	2.37%
17/09/2012 14:41 PM	2.768	4.06%	17/09/2012 15:18 PM	2.722	2.33%
17/09/2012 14:42 PM	2.763	3.87%	17/09/2012 15:20 PM	2.721	2.29%
17/09/2012 14:43 PM	2.761	3.80%	17/09/2012 15:25 PM	2.719	2.22%
17/09/2012 14:44 PM	2.758	3.68%	17/09/2012 15:30 PM	2.718	2.18%
17/09/2012 14:45 PM	2.754	3.53%	17/09/2012 15:35 PM	2.716	2.11%
17/09/2012 14:46 PM	2.751	3.42%	17/09/2012 15:41 PM	2.714	2.03%
17/09/2012 14:47 PM	2.748	3.31%	17/09/2012 15:45 PM	2.713	1.99%
17/09/2012 14:48 PM	2.745	3.20%	17/09/2012 15:55 PM	2.711	1.92%
17/09/2012 14:49 PM	2.744	3.16%	17/09/2012 16:02 PM	2.709	1.84%
17/09/2012 14:50 PM	2.743	3.12%	17/09/2012 16:15 PM	2.706	1.73%
17/09/2012 14:51 PM	2.741	3.05%	17/09/2012 16:32 PM	2.703	1.62%
17/09/2012 14:52 PM	2.740	3.01%	17/09/2012 16:46 PM	2.701	1.54%
17/09/2012 14:53 PM	2.738	2.93%	17/09/2012 17:00 PM	2.698	1.43%
17/09/2012 14:54 PM	2.737	2.89%	17/09/2012 17:32 PM	2.688	1.05%
17/09/2012 14:56 PM	2.735	2.82%	17/09/2012 18:07 PM	2.684	0.90%
17/09/2012 14:58 PM	2.734	2.78%	17/09/2012 18:43 PM	2.680	0.75%
17/09/2012 15:00 PM	2.732	2.71%	17/09/2012 19:10 PM	2.667	0.26%
17/09/2012 15:02 PM	2.731	2.67%	17/09/2012 23:15 PM	2.661	0.04%
17/09/2012 15:04 PM	2.729	2.59%	17/09/2012 23:17 PM	2.66	0.00%

5.3 True Volume Measurement

A report sheet from the He Pycnometer is in Figure 16. To increase the accuracy of the volume measurement, the volume measurement by He expansion was repeated a minimum of three times and the average of all of these results was taken. However, the measurement procedure often needed to be repeated more than three times and sometimes was done as many times as six. This was done to ensure that the difference between all volumes measured did not deviate widely as it is the same particle that is measured.

In Figure 16 it can be seen that the three volumes measured are in agreement with each other to the third decimal point.

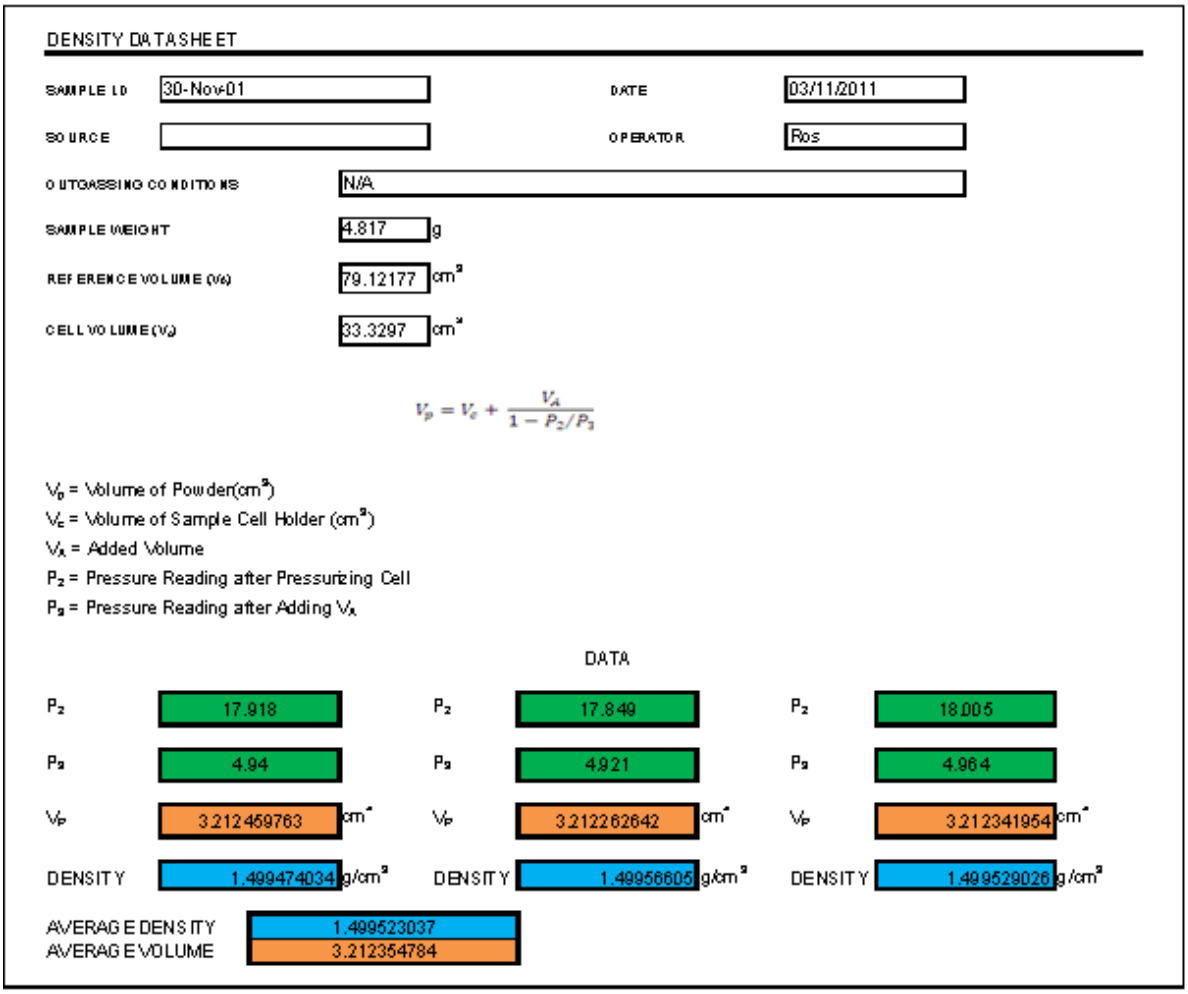

Figure 16: Data sheet from true volume measurement of a coal particle in the He Pycnometer

Table 13 shows the true volume measurements for all particles for which CO_2 adsorption results are presented. The volume of other particles of the 22.4 – 16 mm size class was also measured in the He Stereo Pycnometer as presented above in Figure 16.

Table 13: Volume particles measured in the He Pycnometer

Sample ID	Volume of Particle (cm^3)
Sample 1	0.189
Sample 2	0.175
Sample 3	0.148
Sample 4	0.126
S1	0.222
S2	0.226
S3	0.204
S4	0.193
S5	0.185
L1	4.578
L2	4.060
L3	4.172
L4	2.481
L5	2.954
L6	2.768
L7	1.785

5.4 Calculation of the Equipment Volume

The calculation of the equipment volume was conducted as per the Equipment Volume section in the Methodology Chapter. Equations 7 - 11 should be seen for information on the calculations performed for Table 14. The results of the He expansion in the system with the sample cell empty and then containing a sample of known volume are below. It can be seen that the pressure in the system decreases through the course of the experimental runs. This is most likely a result of the leaking on the He gas line, however the sample volume determination result will be unaffected by the reduced starting pressure.

The sample of known volume used in the sample cell volume determination was a coal particle in the size class 22.4 – 16 mm. The mass of the particle was 2.660 g and the volume as determined on the He Stereo Pycnometer was 1.785 mL.

Table 14: Determination of the Volume of the Sample Cell through Helium Expansion in the constant volume system

	Sample Cell is empty				Sample of known volume in Sample Cell				
	Pressure (P_i)	Pressure (P_j)	Temp (T_i,T_j)	V_s/ V_r	Pressure (P_k)	Pressure (P_l)	Temp (T_k,T_l)	V_r (mL)	V_s (mL)
Run 1	5.50	3.13	36.4	0.76	3.71	2.01	36.7	31.60	23.954
Run 2	4.97	2.79	36.4	0.78	3.35	1.80	36.7	24.78	19.390
Run 3	4.54	2.48	36.4	0.83	3.07	1.62	36.7	16.81	13.981
Average				0.79				24.395	19.108

The equipment volume determination has been performed by Maphada (2012) and Maphala (2012) for the volume of the sample cell and all tubing that the gas has access to between valves V2 and V3. The volume calculated by Maphada (2012) was 29.0370 mL and the volume calculated by Maphala (2012) was 49.225 mL. Due to the large discrepancy between these values, the volume of the sample cell was recalculated. The volume of the sample cell was calculated to be 19.108 mL.

5.5 Adsorption

5.5.1 Preliminary Experimentation to Determine the Correct Equilibration Time for Samples

Experimentation was conducted after the commissioning of the equipment to determine the correct equilibration times for the samples. Four samples from the 9.5 – 6.7 mm size class were run in the equipment to determine the correct equilibration time for samples. Equilibration times of 1, 2 and 3 hours between subsequent pressure steps were allowed. The experimentation on the four samples is detailed further below.

Figure 17 is a plot of the pressure in the sample cell during experimentation on a coal particle in the 9.5 – 6.7 mm size range. The same pressure steps, as discussed in the methodology section above, were used and the equilibrium time allowed for each step was 60 minutes. The small decrease in pressure from the time that the pressure is reached after expansion of the CO_2 into the sample cell to the point before the next pressurisation step can be seen. This small pressure decrease is due to adsorption of the CO_2 onto the coal sample.

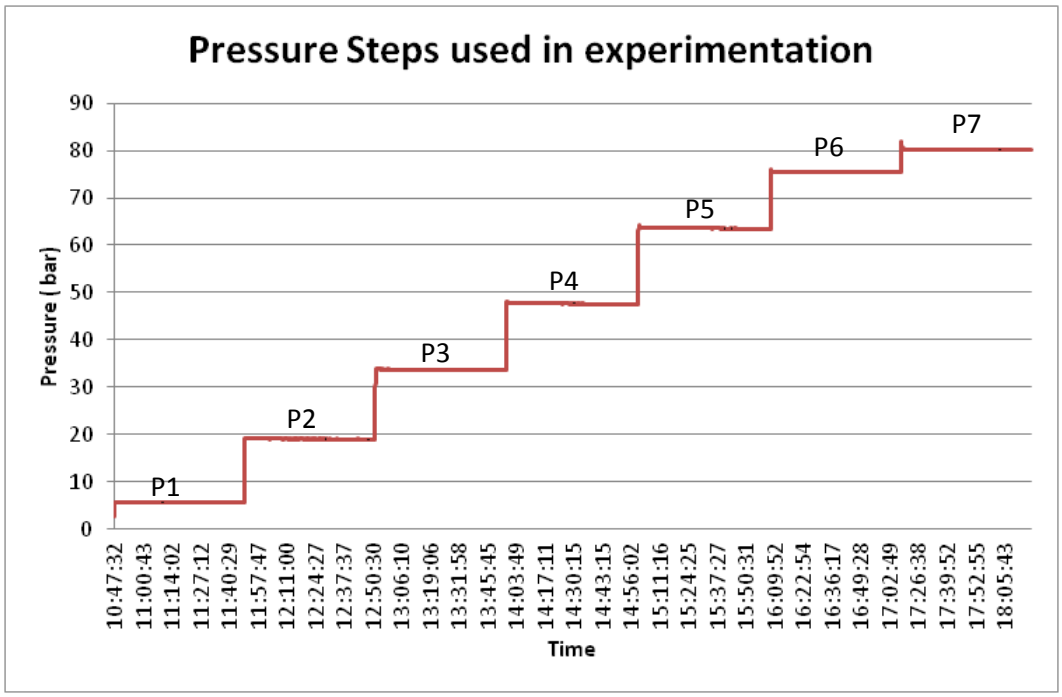

Figure 17: Plot of the pressure steps used in experimentation on the CO_2 adsorptive capacity of coal used in this research

A single pressure step is shown in Figure 18. This was included to allow the reader to see the change in pressure within a pressure step. This change in pressure represents the CO_2 molecules that have left the gas phase and adsorbed onto the coal. There is noise in the measurement, and therefore in the calculations all data is analysed. The ideal gas equation with the CO_2 compressibility factor correction was used in conjunction with the decrease in pressure for each pressure step to calculate the number of moles of CO_2 that had adsorbed onto the coal sample.

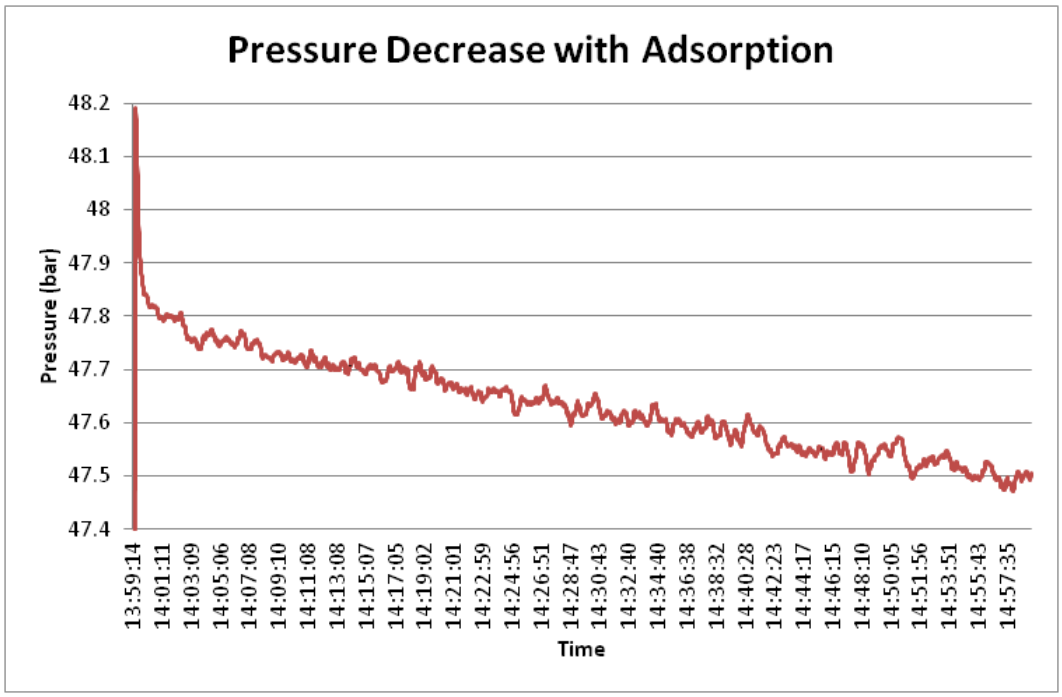

Figure 18: Gradual pressure decrease for a single pressure step as adsorption occurs in the sample cell

Results from the experimental runs are presented further below. Some of the results presented appear incomplete as the equipment had problems with the automation and stopped experimentation. The exact reason for this problem was determined during the further testing. This is detailed below.

5.5.1.1 Sample 1 Adsorption Experiment

Table 15 contains the results of adsorption experiments that were conducted on 9 November 2011 on a particle from the 9.5 – 6.7 mm size class, Sample 1. No moisture was added to this particle before experimentation. The time allowed for equilibrium in each pressure step was one hour.

Table 15: Recorded pressures and temperatures and calculated CO_2 adsorption for Sample 1

	Initial			Final				
	Pressure (bar)	Temp (^oC)	Moles CO_2 (mol)	Pressure (bar)	Temp (^oC)	Moles CO_2 (mol)	Moles Adsorbed	Cumulative Moles CO_2 Adsorbed
P Step 1	6.908	38.160	0.005	6.798	38.013	0.005	5.67E-05	5.67E-05
P Step 2	19.188	38.309	0.015	18.935	37.947	0.015	2.00E-04	2.56E-04
P Step 3	33.994	38.347	0.030	33.620	38.005	0.029	3.35E-04	5.91E-04
P Step 4	47.615	38.790	0.045	46.981	38.036	0.045	6.24E-04	1.22E-03
P Step 5	63.616	38.668	0.069	62.839	38.209	0.068	1.19E-03	2.40E-03
P Step 6	75.145	38.996	0.093	74.681	38.113	0.093	1.75E-04	2.58E-03
P Step 7	80.696	39.182	0.107	79.505	38.172	0.105	2.49E-03	5.07E-03

The mass of the particle was 0.339 g and the results have been further quantified in terms of this in Table 16.

Table 16: CO_2 adsorption quantified in terms of Sample 1 mass

	Moles Adsorbed/g Coal	m^3 CO_2 adsorbed	m^3 CO_2 Adsorbed/t Dry Sample Weight
P Step 1	1.67E-04	2.09E-07	0.617
P Step 2	7.56E-04	4.57E-07	1.347
P Step 3	1.74E-03	6.73E-07	1.986
P Step 4	3.59E-03	9.39E-07	2.769
P Step 5	7.09E-03	1.27E-06	3.745
P Step 6	7.61E-03	1.31E-06	3.851
P Step 7	1.50E-02	1.75E-06	5.175

5.5.1.2 Sample 2 Adsorption Experiment

Table 17 contains the results of adsorption experimentation on a 9.5 – 6.7 mm size class particle where 7.94 mass% moisture was added before experimentation (Table 10). Similarly the time allowed for equilibrium at each pressure step was 1 hour.

Table 17: Recorded pressures and temperatures and calculated CO_2 adsorption for Sample 2

	Initial			Final			Moles CO_2 Adsorbed	Cumulative Moles CO_2 Adsorbed
	Pressure (bar)	Temp (^oC)	Moles CO_2 (mol)	Pressure (bar)	Temp (^oC)	Moles CO_2 (mol)		
P Step 1	5.686	37.948	0.004	5.658	37.993	0.004	2.26E-05	2.26E-05
P Step 2	19.193	38.386	0.015	19.021	38.127	0.015	1.34E-04	1.57E-04
P Step 3	33.963	38.585	0.030	33.564	38.176	0.029	3.50E-04	5.07E-04
P Step 4	48.113	38.770	0.046	47.498	38.298	0.045	6.84E-04	1.19E-03
P Step 5	64.241	38.985	0.070	63.454	38.313	0.069	1.11E-03	2.30E-03
P Step 6	75.581	38.493	0.095	75.374	38.411	0.094	4.31E-04	2.73E-03
P Step 7	80.303	38.813	0.107	80.096	38.402	0.106	2.12E-04	2.94E-03

The mass of the particle (Sample 2) was 0.529g before moisture addition, and 0.571g when the particle was placed in the volumetric adsorption equipment. 7.94 mass% moisture was added (Table 10). The CO_2 adsorption capacity is quantified in terms of this in Table 18.

Table 18: CO_2 adsorption quantified in terms of Sample 2 mass

	Moles Adsorbed/g Coal	m^3 CO_2 adsorbed	m^3 CO_2m Adsorbed/t dry sample weight	m^3 CO_2 Adsorbed/t moist sample weight
P Step 1	3.95E-05	1.00E-07	0.190	0.176
P Step 2	2.74E-04	2.66E-07	0.503	0.466
P Step 3	8.88E-04	4.94E-07	0.933	0.864
P Step 4	2.09E-03	7.81E-07	1.476	1.367
P Step 5	4.03E-03	1.08E-06	2.049	1.899
P Step 6	4.78E-03	1.17E-06	2.213	2.050
P Step 7	5.15E-03	1.21E-06	2.284	2.116

5.5.1.3 Sample 3 Adsorption Experiment

The pressure and temperature recordings from the experiment on the moisturized particle from the 9.5 – 6.7 mm size class that was conducted on the 20th December 2011 are tabulated below. The equilibration time used for this sample was 3 hours before the subsequent pressure step. The time was extended as the automation had recently been completed and therefore equilibration times could be made longer. However, the equipment stopped experimentation/recording when the laboratory was empty in the evening. Time did not allow for repetition of this experiment. Therefore only data for three pressure steps is presented below.

Table 19: Recorded pressures and temperatures and calculated CO_2 adsorption for Sample 3

	Initial			Final				
	Pressure (bar)	Temp (^oC)	Moles CO_2 (mol)	Pressure (bar)	Temp (^oC)	Moles CO_2 (mol)	Moles CO_2 Adsorbed	Cumulative Moles CO_2 Adsorbed
P Step 1	5.520	38.374	0.004	5.083	38.888	0.004	3.44E-04	3.44E-04
P Step 2	17.276	39.306	0.014	14.931	38.711	0.012	1.98E-03	2.33E-03
P Step 3	32.375	39.642	0.028	28.487	38.768	0.024	3.73E-03	6.06E-03

The dry sample mass was 0.595g and 14.45 mass % moisture was added to get an experimental sample mass of 0.681g. The mass of the particle when it was removed from the adsorption equipment was 0.628g. The CO_2 adsorption of the particle is quantified in terms of the particle mass in Table 20.

Table 20: CO_2 adsorption quantified in terms of Sample 3 mass

	Moles Adsorbed/g Coal	m^3 CO_2 adsorbed	m^3 CO_2Adsorbed/t dry sample weight	m^3 CO_2 Adsorbed/t moist sample weight
P Step 1	5.78E-04	1.71E-06	2.880	2.516
P Step 2	3.91E-03	4.91E-06	8.256	7.214
P Step 3	1.02E-02	7.85E-06	13.197	11.531

5.5.1.4 Sample 4 Adsorption Experiment

A 9.5 – 6.7 mm size class particle was used in adsorption experimentation with equilibration times of 2 hours for each pressure step. Unfortunately only five pressure steps were completed due to the unexplained problem with the system automation mentioned above. The pressure and temperature data logging and the calculated CO_2 adsorption for this experiment are in Table 21. The fifth pressure step is incomplete and only lasted 45 minutes.

Table 21: Recorded pressures and temperatures and calculated CO_2 adsorption for Sample 4

	Initial			Final				
	Pressure (bar)	Temp (^oC)	Moles CO_2 (mol)	Pressure (bar)	Temp (^oC)	Moles CO_2 (mol)	Moles CO_2 Adsorbed	Cumulative Moles CO_2 Adsorbed
P Step 1	5.411	38.112	0.004	5.182	38.085	0.004	1.76E-04	1.76E-04
P Step 2	17.276	38.534	0.014	15.837	38.245	0.013	1.23E-03	1.41E-03
P Step 3	33.601	39.165	0.029	30.044	38.151	0.026	3.27E-03	4.68E-03
P Step 4	45.626	38.798	0.043	41.384	38.082	0.038	5.02E-03	9.70E-03
P Step 5	61.695	38.826	0.066	59.670	38.109	0.063	3.15E-03	1.28E-02

The specific adsorption capacity of this coal sample is in Table 22. The dry and moist sample weights were 0.369g and 0.412g respectively with addition of 11.65% moisture.

Table 22: CO_2 adsorption quantified in terms of Sample 4 mass

	Moles Adsorbed/g Coal	m^3 CO_2 adsorbed	m^3 CO_2Adsorbed/t dry sample weight	m^3 CO_2 Adsorbed/t moist sample weight
P Step 1	4.77E-04	8.58E-07	2.326	2.083
P Step 2	3.81E-03	1.86E-06	7.367	6.598
P Step 3	1.27E-02	2.40E-06	13.873	12.425
P Step 4	2.63E-02	2.52E-06	20.713	18.551
P Step 5	3.48E-02	9.54E-07	23.298	20.866

The m^3 CO_2 Adsorbed/t dry and moist sample weight for Pressure Step 5 is contrary to the increasing trend shown with all other values in this table and all other samples in this research. Pressure Step 5 was the pressure step that was not as long as the others in the Sample 4 experimental run. Thus the system had less time to come to equilibrium than in the other pressure steps.

5.5.1.5 Comparison between the 9.5 – 6.7 mm Particle Size Adsorption Experiments

For ease of comparison between the experimental results the sample IDs have been changed as per Table 23. The samples now reflect the additional moisture that was added to the sample by submersion in distilled water and the time allowed for equilibrium to be reached between all successive pressure steps in the volumetric adsorption equipment.

Table 23: New sample identifications for ease of comparison of results

Sample ID	New Sample ID: (Mass % Moisture Added, Equilibration time)
Sample 1	0%, 1hr
Sample 2	7.94%, 1 hr
Sample 3	14.45%, 3 hrs
Sample 4	11.65%, 2 hrs

Figure 19 shows the cumulative moles of CO_2 that were adsorbed on each sample. It can clearly be seen that the gradient for the samples that were given longer equilibrium times for each pressure step is higher. Further, when looking at the samples that were both given an hour equilibration between subsequent pressure steps, the samples that moisture was added to have a lower number of moles of CO_2 that were adsorbed.

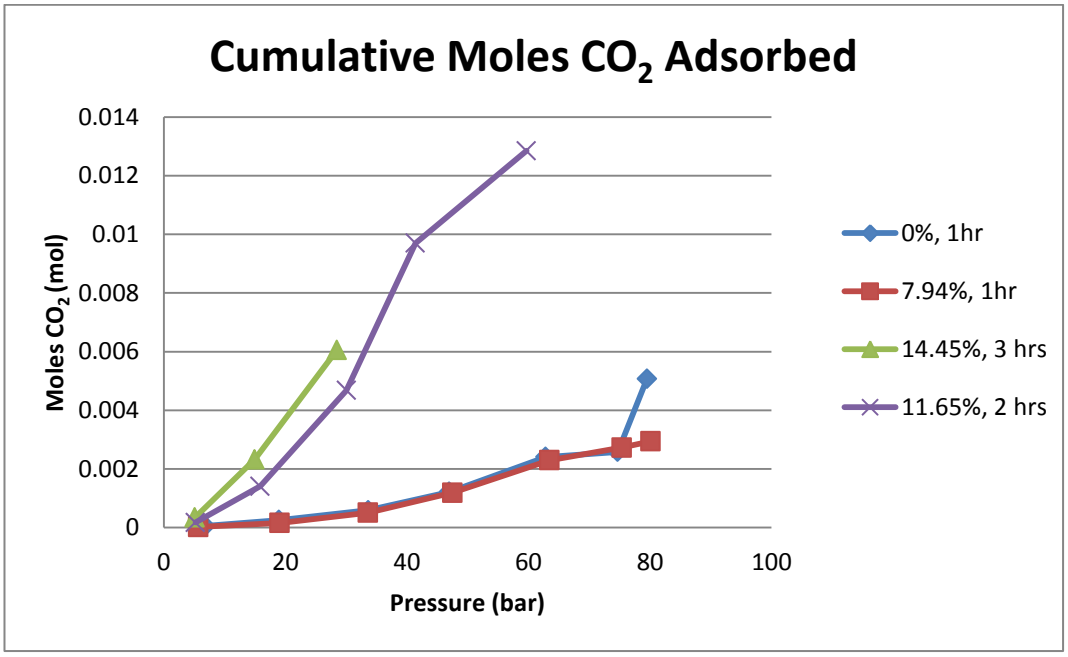

Figure 19: Cumulative moles of CO_2 adsorbed for preliminary testing of 9.5 -6.7 mm samples in the Volumetric Adsorption Equipment

Figure 20 shows the volume of CO_2 adsorbed per ton of sample that was placed in the adsorption testing equipment. The mass used to quantify the results is the moist mass for all samples where moisture was added. The 'dry' mass of 0%, 1hr sample was used as this was the 9.5- 6.7 mm size class particle where moisture was not added before adsorption testing. The use of dry in this context excludes the as received moisture content of the coal and only refers to additional moisture addition conducted in this

research. The trends as described above in Figure 19 are mirrored in Figure 20. The gradient of samples that were left in the equipment for the longest times between pressure steps is higher reflecting greater adsorption. 7.94%, 1hr (Sample 2) lies below 0%, 1 hr (Sample 1) in this Figure indicating reduced adsorption despite the same equilibrium time in a sample with additional moisture content.

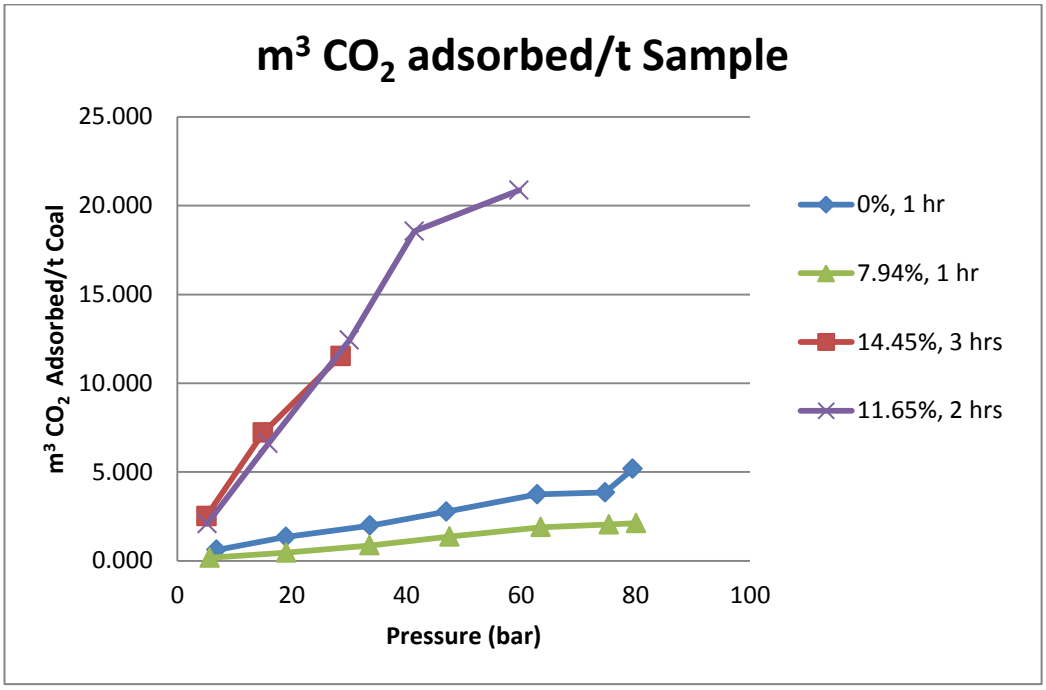

Figure 20: Volume of CO_2 adsorbed per ton for preliminary testing of the 9.5 -6.7 mm samples that were placed in the Volumetric Adsorption Equipment

These graphs were indicative of the largest CO_2 adsorption occurring with equilibration times of 2 to 3 hours. However caution should be exercised with this judgement as it may be just an indication of leakage of the equipment. However, longer equilibration times were used in further experimentation.

5.5.2 Adsorption Experimentation Results with 9.5 – 6.7 mm Size Class Particles

Five particles from the 9.5 – 6.7 mm size class were tested in the volumetric adsorption equipment. These particles shall be named S1 – S5 to indicate they are from the smaller size class used in this research. The results of the experimentation are below.

5.5.2.1 S1 Experimentation

The adsorption experiment using particle S1 was conducted on the 31st July 2012. The equilibration time used for the particle was two hours, as this allowed the equipment to be operated with someone in the laboratory for most of the pressure steps. This was done as the reason for the premature stoppage of the equipment was not know. As, the equipment was leaking at this time; a blank run was used to correct for the leakage rate.

The adsorption experimentation stopped in the fourth pressure step, 30 minutes ahead of the time the pressure step should have been completed. Thus data is not available for an entire experimental run.

A contingency plan was put in place from this point onwards to deal with the experimental runs stopping ahead of scheduled completion times. This plan was to restart the experiment from the point at which it had stopped as soon as the stop was noticed. This contingency plan generated more data points for each experimental run; however the equilibration time for some of the data points was longer due to the equipment stoppage. This can be seen in the results of the other 9.5 – 6.7 mm size class particles.

The pressure, that has been corrected for leakage, and the temperature at the start and end of each pressure step as well as the calculated moles of CO_2 adsorbed can be found in Table 24. The data from the blank run to determine the leakage can be found in Appendix D.

The data from the experimental run and the calculated moles of CO_2 adsorbed can be found below.

Table 24: Recorded pressures and temperatures and calculated CO_2 adsorption for S1

	Initial			Final				
	Pressure (bar)	**Temp (°C)**	**Moles CO_2 (mol)**	**Pressure (bar)**	**Temp (°C)**	**Moles CO_2 (mol)**	**Moles CO_2 Adsorbed**	**Cumulative Moles CO_2 Adsorbed**
P Step 1	5.397	36.347	0.004	5.355	36.583	0.004	3.61E-05	3.61E-05
P Step 2	17.112	36.949	0.014	16.128	36.858	0.013	7.81E-04	8.18E-04
P Step 3	30.134	37.321	0.026	28.424	36.917	0.024	1.63E-03	2.45E-03
P Step 4	44.200	37.496	0.041	42.647	36.855	0.039	1.76E-03	4.21E-03

The specific adsorption capacity of this coal sample is in Table 25. S1 was not moisturised and the mass of the particle was 0.395g after degassing the particle.

Table 25: CO_2 adsorption quantified in terms of Sample S1 mass

	Moles Adsorbed/g Coal	m^3 CO_2 adsorbed	m^3 CO_2 Adsorbed/t Dry Sample Weight
P Step 1	9.15E-05	1.69E-07	0.429
P Step 2	2.07E-03	1.31E-06	3.325
P Step 3	6.20E-03	2.59E-06	6.558
P Step 4	1.07E-02	3.44E-06	8.702

5.5.2.2 S2 Experimentation

The adsorption experiment using particle S2 was conducted from the 15th to the 16th September 2012. The first and second pressure steps ran to completion and the third pressure step was started by Labview. However during the third pressure step Labview stopped running and data was no longer logged. The fourth pressure step was started after resetting the equipment and running Labview again. The fourth pressure step did not run to completion either. The equipment was discovered 15 hours[10] after the pressure step had started. At this time the equipment was reset again and Labview closed and run again. The fifth and sixth pressure steps were then completed without a problem. During the seventh pressure step, the data logging stopped after only 1 hour 40 minutes.

The leakage from the equipment was minimal as determined by a leakage test conducted in advance. The leakage rate was found to be 0.3 bar over 24 hours at a pressure around 50 bar. The results of the leakage test can be found in Appendix D.

The pressure data has been corrected with the leakage rate determined prior to experimentation. Nonetheless a clear spike in the data can be seen in the fourth pressure step where the equipment remained at that pressure for 15 hours. The pressure despite correction for leakage still seems too low. As no data is logged when the equipment stops running correcting the experiment with the predetermined leakage rate is the best option to quantify leakage.

The data from the experimental run and the calculated moles of CO_2 adsorbed can be found below.

[10] This is the time the laboratory was unoccupied and the equilibration time of 3 hours.

Table 26: Recorded pressures and temperatures and calculated CO_2 adsorption for S2

	Initial			Final			Moles CO_2 Adsorbed	Cumulative Moles CO_2 Adsorbed
	Pressure (bar)	Temp (^oC)	Moles CO_2 (mol)	Pressure (bar)	Temp (^oC)	Moles CO_2 (mol)		
P Step 1	6.357	35.831	0.005	6.383	36.471	0.005	7.88E-07	7.88E-07
P Step 2	17.599	36.785	0.014	17.238	36.286	0.014	2.86E-04	2.87E-04
P Step 3	31.293	36.767	0.027	29.825	36.117	0.026	1.38E-03	1.67E-03
P Step 4	47.948	36.709	0.046	43.596	35.640	0.041	5.30E-03	6.97E-03
P Step 5	66.086	36.494	0.075	65.281	35.921	0.074	1.27E-03	8.25E-03
P Step 6	74.555	36.856	0.093	74.202	36.100	0.093	1.95E-04	8.44E-03
P Step 7	80.324	37.286	0.108	78.959	36.169	0.106	2.73E-03	1.12E-02

The specific adsorption capacity of this coal sample is in Table 27. S2 was moisturised before experimentation. The mass of the particle was 0.346g and after moisturisation the mass of the particle was 0.369g. Thus 6.65% moisture was added.

Table 27: CO_2 adsorption quantified in terms of Sample S2 mass

	Moles Adsorbed/g Coal	m^3 CO_2 adsorbed	m^3 CO_2Adsorbed/t dry sample weight	m^3 CO_2 Adsorbed/t moist sample weight
P Step 1	2.28E-06	3.08E-09	0.009	0.008
P Step 2	8.29E-04	3.93E-07	1.137	1.066
P Step 3	4.83E-03	1.41E-06	4.086	3.831
P Step 4	2.02E-02	3.87E-06	11.195	10.498
P Step 5	2.38E-02	4.20E-06	12.139	11.383
P Step 6	2.44E-02	4.24E-06	12.254	11.490
P Step 7	3.23E-02	4.73E-06	13.666	12.814

5.5.2.3 S3 Experimentation

The adsorption experiment using particle S3 was conducted from the 16th to the 18th September 2012. The first pressure step and second pressure step ran to completion and the third pressure step started but stopped after an hour and twenty minutes. The fourth and fifth pressure steps ran to completion. The sixth pressure step stopped after two hours and 20 minutes. The seventh, and final, pressure step ran to completion without problems.

The data has not been corrected for leakage using the pressure drop in the results of the leakage test that can be found in Appendix D.

The data from the experimental run and the calculated moles of CO_2 adsorbed can be found below.

Table 28: Recorded pressures and temperatures and calculated CO_2 adsorption for S3

	Initial			Final			Moles CO_2 Adsorbed	Cumulative Moles CO_2 Adsorbed
	Pressure (bar)	Temp (^oC)	Moles CO_2 (mol)	Pressure (bar)	Temp (^oC)	Moles CO_2 (mol)		
P Step 1	7.994	36.674	0.006	7.787	36.240	0.006	1.54E-04	1.54E-04
P Step 2	18.147	36.615	0.015	18.032	36.049	0.015	7.29E-05	2.27E-04
P Step 3	31.415	36.483	0.027	31.234	36.549	0.027	1.91E-04	4.18E-04
P Step 4	46.662	37.136	0.044	46.281	36.340	0.044	2.95E-04	7.13E-04
P Step 5	62.129	37.009	0.067	61.795	36.361	0.067	2.95E-04	1.01E-03
P Step 6	73.735	37.164	0.091	73.642	36.906	0.091	4.20E-06	1.01E-03
P Step 7	80.314	38.570	0.107	78.545	36.958	0.104	3.21E-03	4.22E-03

The specific adsorption capacity of this coal sample is in Table 29. S3 was not moisturised and the mass of the particle was 0.335g.

Table 29: CO_2 adsorption quantified in terms of Sample S3 mass

	Moles Adsorbed/g Coal	m^3 CO_2 adsorbed	m^3 CO_2 Adsorbed/t Dry Sample Weight
P Step 1	4.60E-04	4.90E-07	1.464
P Step 2	6.78E-04	5.85E-07	1.747
P Step 3	1.25E-03	7.20E-07	2.149
P Step 4	2.13E-03	8.47E-07	2.528
P Step 5	3.01E-03	9.30E-07	2.777
P Step 6	3.02E-03	9.31E-07	2.780
P Step 7	1.26E-02	1.52E-06	4.527

5.5.2.4 S4 Experimentation

The adsorption experiment using particle S4 was conducted from the 18th to the 20th September 2012. The first pressure step and second pressure step were completed. The third pressure step only lasted an hour and twenty minutes and the equipment stopped running. The equipment was found 11 hours after the start of the third pressure step and was restarted from the fourth pressure step. The fourth and fifth pressure step then ran to completion. The sixth pressure step stopped after an hour.

The seventh pressure step was unfortunately not completed as the equipment vented to atmosphere and data was not logged. The experimental data has been corrected for leakage using the pressure test data that can be found in Appendix D.

The data from the experimental run and the calculated moles of CO_2 adsorbed can be found below.

Table 30: Recorded pressures and temperatures and calculated CO_2 adsorption for S4

	Initial			Final				
	Pressure (bar)	Temp (^oC)	Moles CO_2 (mol)	Pressure (bar)	Temp (^oC)	Moles CO_2 (mol)	Moles CO_2 Adsorbed	Cumulative Moles CO_2 Adsorbed
P Step 1	7.660	37.510	0.006	7.597	37.323	0.006	4.59E-05	4.59E-05
P Step 2	17.874	37.716	0.014	17.792	37.170	0.014	3.71E-05	8.30E-05
P Step 3	31.438	37.653	0.027	31.098	37.207	0.027	2.82E-04	3.65E-04
P Step 4	59.572	37.682	0.062	58.838	37.345	0.061	1.01E-03	1.37E-03
P Step 5	73.611	37.929	0.090	73.401	37.382	0.090	3.71E-05	1.41E-03
P Step 6	80.199	38.705	0.106	78.674	37.352	0.104	2.65E-03	4.06E-03

The specific adsorption capacity of this coal sample is in Table 31. Particle S4 was not moisturised and the mass of the particle was 0.321g.

Table 31: CO_2 adsorption quantified in terms of Sample S4 mass

	Moles Adsorbed/g Coal	m^3 CO_2 adsorbed	m^3 CO_2 Adsorbed/t Dry Sample Weight
P Step 1	1.43E-04	1.50E-07	0.469
P Step 2	2.59E-04	2.00E-07	0.622
P Step 3	1.14E-03	3.99E-07	1.243
P Step 4	4.28E-03	7.09E-07	2.209
P Step 5	4.39E-03	7.17E-07	2.233
P Step 6	1.26E-02	1.20E-06	3.738

5.5.2.5 S5 Experimentation

The adsorption experiment using particle S5 was conducted from the 20th to the 21st September 2012. The equipment was leaking badly and thus a blank run was completed to correct the data. The results of the blank run can be found in Appendix D. The first and second pressure steps completed without any stoppage in the equipment. The

third pressure step stopped after an hour and fifty minutes. The equipment was restarted and the fourth and fifth pressure steps were completed. The sixth pressure step stopped after an hour and a half. A seventh pressure step was not completed for the equipment as the leakage was so severe that when the equipment was found after stopping during the sixth pressure step the pressure was less than half the pressure at the start of the sixth pressure step.

The data from the experimental run, that has been corrected for leakage, and the calculated moles of CO_2 adsorbed can be found below.

Table 32: Recorded pressures and temperatures and calculated CO_2 adsorption for S5

	Initial			Final				
	Pressure (bar)	Temp (^oC)	Moles CO_2 (mol)	Pressure (bar)	Temp (^oC)	Moles CO_2 (mol)	Moles CO_2 Adsorbed	Cumulative Moles CO_2 Adsorbed
P Step 1	5.277	37.816	0.004	5.202	37.834	0.004	5.73E-05	5.73E-05
P Step 2	16.985	38.192	0.014	16.948	37.911	0.014	1.28E-05	7.01E-05
P Step 3	29.643	38.597	0.025	29.387	37.864	0.025	1.61E-04	2.32E-04
P Step 4	43.743	38.457	0.040	43.563	37.593	0.040	3.48E-05	2.66E-04
P Step 5	59.238	37.972	0.062	59.098	37.462	0.062	2.40E-05	2.90E-04
P Step 6	70.798	36.451	0.085	70.742	37.365	0.084	8.01E-04	1.09E-03

The specific adsorption capacity of this coal sample is in Table 33. S5 was moisturised before experimentation. The mass of the particle was 0.316g and after moisturisation the mass of the particle was 0.322g. Thus 1.90% moisture was added.

Table 33: CO_2 adsorption quantified in terms of Sample S5 mass

	Moles Adsorbed/g Coal	m^3 CO_2 adsorbed	m^3 CO_2 Adsorbed/t Dry Sample Weight	m^3 CO_2 Adsorbed/t Moist Sample Weight
P Step 1	1.81E-04	2.78E-07	0.880	0.864
P Step 2	2.22E-04	3.76E-07	1.191	1.169
P Step 3	7.33E-04	5.52E-07	1.746	1.713
P Step 4	8.43E-04	6.77E-07	2.141	2.101
P Step 5	9.19E-04	7.65E-07	2.422	2.377
P Step 6	3.45E-03	1.01E-06	3.198	3.138

5.5.2.5 Combined Results of the 9.5 – 6.7 mm Adsorption Experimentation Results

Figure 21 shows the cumulative moles of CO_2 that were adsorbed during experimentation with the 9.5 – 6.7 mm size class particles. It can be seen that the data points for particles S1 and S2 are far higher than the three other particles. It can also be seen that the last data point for particles S2, S3, S4 and S5 is substantially higher than the previous data point.

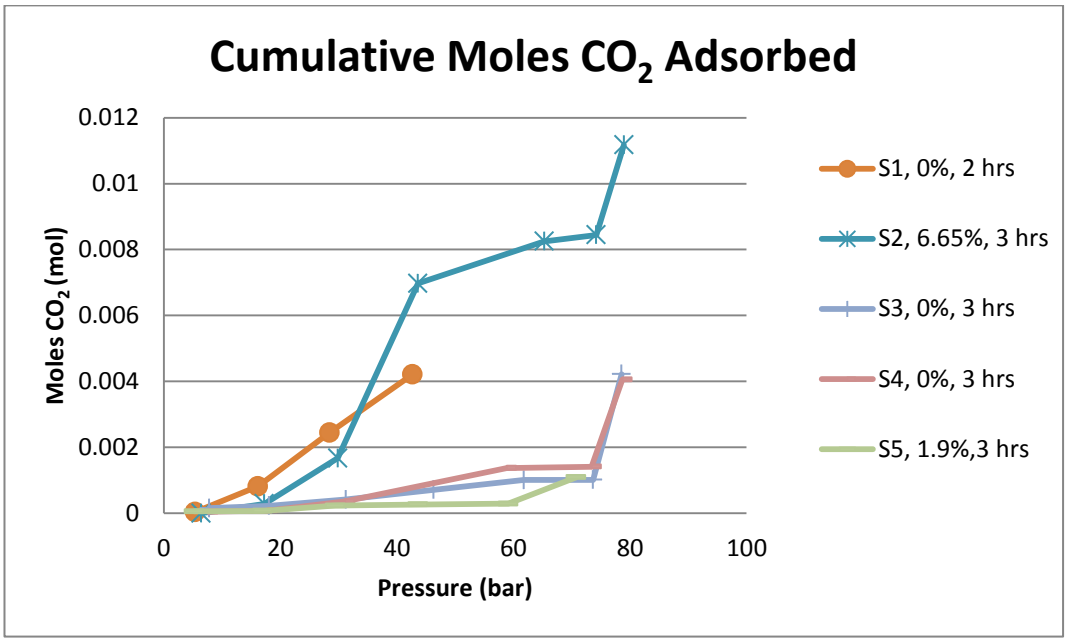

Figure 21: Cumulative moles of CO_2 adsorbed by 9.5 – 6.7 mm size class particles

Figure 22 shows the specific adsorption capacity of the 9.5 – 6.7 mm size class particles. As was the case in the cumulative moles of CO_2 adsorbed, the data points for particles S1 and S2 are far higher than the other particles. Further the last point of particles S2, S3, S4 and S5 are much higher than the previous data point from the lower pressure.

Despite the 2 hour equilibration time for the pressure steps used in experimentation with particle S1 the data points are higher for this particle in two out of the four data points. The fourth pressure step in experimentation with S1 terminated 30 minutes in advance of the two hour equilibration time. Thus, should the pressure step have been completed the fourth point may have also been higher than any of the other data.

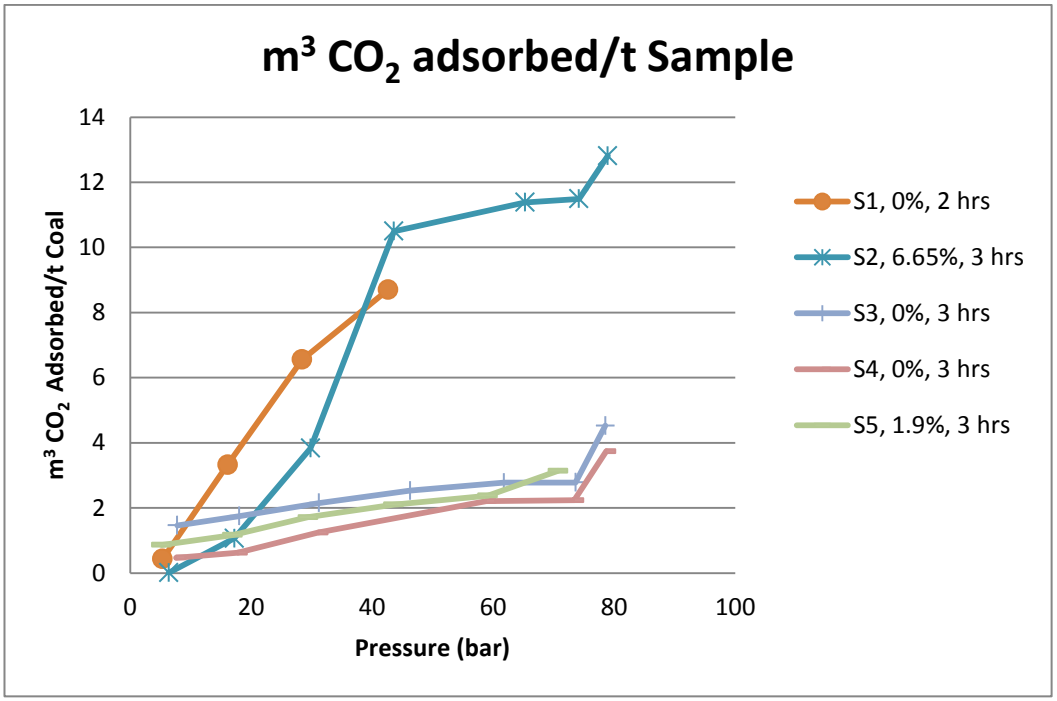

Figure 22: Specific Adsorption Capacity of the 9.5 – 6.7 mm size class particles

5.5.3 Adsorption Experimentation Results with 22.4 – 16 mm Size Class Particles and 3 hr Equilibration Times

Six particles from the 22.4 – 16 mm size class were tested in the volumetric adsorption equipment. These particles shall be named L1 – L6 to indicate they are from the larger size class used in this research. The equilibration time used for each pressure step was 3 hours for all of the large particles of coal. The results of the experimentation are below.

5.5.3.1 L1 Experimentation

The adsorption experiment using particle L1 was conducted from the 20th September 2012. The first pressure step and second pressure step completed without any problems. The third pressure step stopped prematurely after 2 hours. The third pressure step was completed and the fourth pressure step stopped after only a few minutes. The equipment was leaking heavily and the data has been corrected using a blank run conducted on the 21st September 2012. The results of the blank run can be found in Appendix D. A clear spike in the data on the fourth pressure step of this experimental run can be seen. This is believed to be the result of equipment leakage and is still noticeable despite data correction with the results of the blank run.

Table 34: Recorded pressures and temperatures and calculated CO_2 adsorption for L1

	Initial			Final				
	Pressure (bar)	Temp (^oC)	Moles CO_2 (mol)	Pressure (bar)	Temp (^oC)	Moles CO_2 (mol)	Moles CO_2 Adsorbed	Cumulative Moles CO_2 Adsorbed
P Step 1	5.528	37.424	0.003	4.471	37.854	0.003	6.28E-04	6.28E-04
P Step 2	16.985	38.214	0.010	16.906	37.214	0.010	1.82E-06	6.30E-04
P Step 3	30.201	37.836	0.020	30.104	37.206	0.020	1.25E-05	6.42E-04
P Step 4	43.733	37.410	0.031	43.510	37.229	0.031	1.79E-04	8.21E-04

The specific adsorption capacity of L1 is in Table 35. Particle L1 was not moisturised and had a mass of 6.422 g.

Table 35: CO_2 adsorption quantified in terms of Sample L1 mass

	Moles Adsorbed/g Coal	m^3 CO_2 adsorbed	m^3 CO_2 Adsorbed/t Dry Sample Weight
P Step 1	9.78E-05	3.56E-06	0.554
P Step 2	9.81E-05	3.56E-06	0.555
P Step 3	1.00E-04	3.57E-06	0.556
P Step 4	1.28E-04	3.65E-06	0.569

5.5.3.2 L2 Experimentation

The adsorption experiment using particle L2 was conducted from the 22nd to the 23rd September 2012. The first pressure step and second pressure step completed without any problems. The third pressure step stopped after 57 minutes. This pressure step was thus restarted and this is evident through the starting pressure in the third step in this experimental run being higher than the other experimental runs. Restarting the pressure step was in line with the contingency planning for equipment stoppage to ensure data was generated in this research. After restarting the equipment the third and fourth pressure steps completed without problems. The fifth pressure step however ended after an hour and ten minutes. The results of the experimental run have been corrected for leakage with the use of a blank run. The results of the blank run can be found in Appendix D.

Table 36: Recorded pressures and temperatures and calculated CO_2 adsorption for L2

	Initial			Final			Moles CO_2 Adsorbed	Cumulative Moles CO_2 Adsorbed
	Pressure (bar)	Temp (^oC)	Moles CO_2 (mol)	Pressure (bar)	Temp (^oC)	Moles CO_2 (mol)		
P Step 1	6.275	37.266	0.004	5.077	37.051	0.003	7.35E-04	7.35E-04
P Step 2	17.283	37.581	0.011	17.232	37.232	0.011	1.47E-05	7.50E-04
P Step 3	34.954	37.712	0.024	34.176	37.107	0.024	5.72E-04	1.32E-03
P Step 4	45.121	38.150	0.034	43.514	36.914	0.032	1.39E-03	2.71E-03
P Step 5	59.312	37.923	0.049	58.285	36.847	0.048	1.02E-03	3.73E-03

The specific adsorption capacity results for particle L2 can be found in Table 37. The mass of particle L2 was 5.807 g and it was not moisturised prior to experimentation.

Table 37: CO_2 adsorption quantified in terms of Sample L2 mass

	Moles Adsorbed/g Coal	m^3 CO_2 adsorbed	m^3 CO_2 Adsorbed/t Dry Sample Weight
P Step 1	1.27E-04	3.65E-06	0.628
P Step 2	1.29E-04	3.67E-06	0.631
P Step 3	2.28E-04	4.03E-06	0.694
P Step 4	4.66E-04	4.68E-06	0.805
P Step 5	6.43E-04	5.13E-06	0.883

5.5.3.3 L3 Experimentation

The adsorption experiment using particle L3 was conducted from the 22nd to the 23rd September 2012. The first pressure step, second pressure step and third pressure step completed without any problems as the reason for the equipment stoppage in the third step was determined when the pattern was noticed.

The error logs of the volumetric adsorption equipment were consulted and it was found that the equipment did not have enough memory to store all the data for the long equilibration time runs. To avoid this problem the time between the logging of successive data points was increased from the system default of every second to every ten seconds. This assisted greatly with the completion of experimental runs. A screen shot of the error log is in Figure 23.

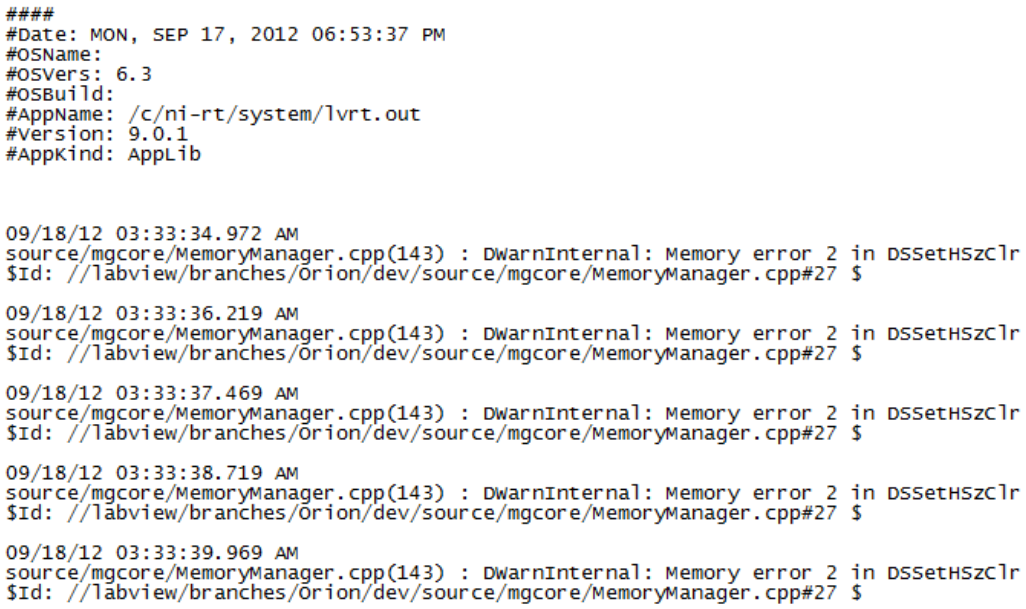

Figure 23: Screenshot of the error logs from the volumetric adsorption equipment

Nevertheless a power failure occurred at the University of the Witwatersrand during the fourth pressure step and thus it was not completed. The equipment was then restarted from the fifth pressure step in line with the contingency planning. The fifth pressure step ran to completion. The sixth pressure step could not be started as there was a problem with pressurising the reference cell. The liquid CO_2 pump was increasing CO_2 to the desired pressure but the gas was not entering the reference cell. The problem is believed to be a result of problems with the valves on the liquid CO_2 pump. The agent was called out and the equipment was fixed.

The results of the five pressure steps completed are below:

Table 38: Recorded pressures and temperatures and calculated CO_2 adsorption for L3

	Initial			Final				
	Pressure (bar)	Temp (°C)	Moles CO_2 (mol)	Pressure (bar)	Temp (°C)	Moles CO_2 (mol)	Moles CO_2 Adsorbed	Cumulative Moles CO_2 Adsorbed
P Step 1	5.978	40.471	0.004	5.608	36.835	0.003	1.81E-04	1.81E-04
P Step 2	17.733	36.918	0.011	17.424	37.140	0.011	2.07E-04	3.88E-04
P Step 3	31.752	37.289	0.022	31.505	37.181	0.021	1.85E-04	5.73E-04
P Step 4	46.484	37.335	0.035	46.292	37.088	0.035	1.51E-04	7.24E-04
P Step 5	72.748	36.692	0.071	72.744	36.689	0.071	5.38E-06	7.29E-04

The specific adsorption capacity of particle L3 is in Table 39. Particle 3 was moisturised and had an original mass of 6.656g and a moisturised mass of 6.895g. 3.59% moisture was added to the particle.

Table 39: CO_2 adsorption quantified in terms of Sample L3 mass

	Moles Adsorbed/g Coal	m^3 CO_2 adsorbed	m^3 CO_2 Adsorbed/t Dry Sample Weight	m^3 CO_2 Adsorbed/t Moist Sample Weight
P Step 1	2.72E-05	8.09E-07	0.122	0.117
P Step 2	5.83E-05	1.09E-06	0.164	0.158
P Step 3	8.61E-05	1.22E-06	0.183	0.177
P Step 4	1.09E-04	1.28E-06	0.193	0.186
P Step 5	1.10E-04	1.29E-06	0.193	0.186

5.5.3.4 L4 Experimentation

The adsorption experimentation using particle L4 was conducted from the 1st to the 2nd November 2012. Seven pressure steps were completed without equipment stoppage due to the longer time of 10 seconds between subsequent data recordings that was implemented with experimentation from the 30th October 2012. The data was not corrected for leakage as the blank run had a higher leakage rate than the pressure drop after each pressure step while particle L4 was in the volumetric adsorption equipment. This may indicate the seal of the pressure vessel was not as effective when the empty pressure vessel was run in the equipment to correct for leakage. Further, this does not mean that the equipment was not leaking during experimentation on particle L4.

The results of the experimental run using particle L4 are below.

Table 40: Recorded pressures and temperatures and calculated CO_2 adsorption for L4

	Initial			Final				
	Pressure (bar)	Temp (^oC)	Moles CO_2 (mol)	Pressure (bar)	Temp (^oC)	Moles CO_2 (mol)	Moles CO_2 Adsorbed	Cumulative Moles CO_2 Adsorbed
P Step 1	6.806	36.229	0.005	6.237	36.641	0.004	3.98E-04	3.98E-04
P Step 2	17.643	36.701	0.012	17.240	36.771	0.012	2.89E-04	6.87E-04
P Step 3	31.439	36.875	0.024	31.129	36.628	0.024	2.46E-04	9.33E-04
P Step 4	46.829	36.765	0.039	46.423	36.378	0.039	4.12E-04	1.34E-03
P Step 5	62.201	36.594	0.059	61.716	36.143	0.059	5.87E-04	1.93E-03
P Step 6	73.758	36.390	0.081	73.550	35.837	0.081	2.45E-05	1.96E-03
P Step 7	78.980	36.433	0.093	78.670	35.751	0.093	9.04E-05	2.05E-03

The specific adsorption capacity of L4 is in Table 41. Particle L4 was not moisturised and the mass of the particle was 3.886 g.

Table 41: CO_2 adsorption quantified in terms of Sample L4 mass

	Moles Adsorbed/g Coal	m^3 CO_2 adsorbed	m^3 CO_2 Adsorbed/t Dry Sample Weight
P Step 1	1.02E-04	1.60E-06	0.411
P Step 2	1.77E-04	1.99E-06	0.512
P Step 3	2.40E-04	2.16E-06	0.556
P Step 4	3.46E-04	2.34E-06	0.602
P Step 5	4.97E-04	2.58E-06	0.665
P Step 6	5.03E-04	2.59E-06	0.667
P Step 7	5.26E-04	2.62E-06	0.675

5.5.3.5 L5 Experimentation

The experimentation using particle L5 was conducted from the 2nd to the 3rd November 2012. The seven pressure steps completed without stoppages. The data has been corrected for leakage, but despite this correction the final pressures when compared to the initial pressures are lower than those for the other samples. Thus the pressure vessel when containing sample L5 may have been leaking at a greater rate than the blank run. The results of the experimentation are below.

Table 42: Recorded pressures and temperatures and calculated CO_2 adsorption for L5

	Initial			Final				
	Pressure (bar)	Temp (°C)	Moles CO_2 (mol)	Pressure (bar)	Temp (°C)	Moles CO_2 (mol)	Moles CO_2 Adsorbed	Cumulative Moles CO_2 Adsorbed
P Step 1	5.527	36.599	0.004	5.470	36.705	0.004	3.92E-05	3.92E-05
P Step 2	17.473	36.798	0.012	14.758	36.390	0.010	1.84E-03	1.88E-03
P Step 3	29.815	36.548	0.022	25.032	36.019	0.018	3.91E-03	5.79E-03
P Step 4	45.878	36.240	0.037	37.826	35.847	0.029	8.27E-03	1.41E-02
P Step 5	60.431	36.001	0.055	52.292	35.784	0.044	1.13E-02	2.53E-02
P Step 6	71.946	35.907	0.075	68.126	35.983	0.068	7.28E-03	3.26E-02
P Step 7	76.592	36.410	0.085	76.157	36.342	0.084	9.02E-04	3.35E-02

The specific adsorption capacity of L5 has been quantified and is in Table 43. Particle L5 was moisturised before adsorption experimentation. The dry weight of L5 was 4.463g and the weight after moisturisation by submersion in distilled water was 4.597g. 3.00% moisture was added to the sample.

Table 43: CO_2 adsorption quantified in terms of Sample L5 mass

	Moles Adsorbed/g Coal	m^3 CO_2 adsorbed	m^3 CO_2Adsorbed/t dry sample weight	m^3 CO_2 Adsorbed/t moist sample weight
P Step 1	8.78E-06	1.80E-07	0.040	0.0391
P Step 2	4.22E-04	3.12E-06	0.698	0.6780
P Step 3	1.30E-03	6.64E-06	1.488	1.4443
P Step 4	3.15E-03	1.13E-05	2.523	2.4497
P Step 5	5.68E-03	1.68E-05	3.764	3.6547
P Step 6	7.31E-03	1.95E-05	4.380	4.2523
P Step 7	7.51E-03	1.99E-05	4.448	4.3186

5.5.3.6 L6 Experimentation

The adsorption experimentation using particle L6 was conducted from the 3rd to the 4th November 2012. Seven pressure steps were completed without equipment stoppage. The data was not corrected for leakage as the blank run had a higher leakage rate than the pressure drop after each pressure step while particle L6 was in the volumetric adsorption equipment. This may indicate the seal of the pressure vessel was not as effective when the empty pressure vessel was run in the equipment to correct for leakage. Further, this does not mean that the equipment was not leaking during experimentation on particle L6.

Data correction was however performed on pressure step 6. This correction was performed as the pressure at the end of the pressure step was larger than the pressure at the start of the pressure step and the temperature was lower than the temperature at the start of the pressure step. In terms of the ideal gas law and the principle of a constant volume system this is not feasible. Thus the pressure at the end of the pressure step was corrected to ensure that a negative amount of moles had not adsorbed to the coal. The moles adsorbed as reflected in the table is very small for this step, approximately equal to zero. The corrected data for the experimental run is below.

Table 44: Recorded pressures and temperatures and calculated CO_2 adsorption for L6

	Initial			Final			Moles CO_2 Adsorbed	Cumulative Moles CO_2 Adsorbed
	Pressure (bar)	Temp (^oC)	Moles CO_2 (mol)	Pressure (bar)	Temp (^oC)	Moles CO_2 (mol)		
P Step 1	5.487	36.491	0.004	4.442	36.907	0.003	7.00E-04	7.00E-04
P Step 2	17.102	37.115	0.012	16.281	36.823	0.011	5.53E-04	1.25E-03
P Step 3	31.041	37.118	0.023	30.568	36.622	0.023	3.53E-04	1.61E-03
P Step 4	47.137	37.018	0.039	46.759	36.592	0.038	3.52E-04	1.96E-03
P Step 5	62.089	37.013	0.058	61.904	36.568	0.058	1.06E-04	2.06E-03
P Step 6	73.794	37.191	0.079	73.557	36.526	0.079	1.14E-08	2.06E-03
P Step 7	79.327	37.246	0.091	79.013	36.576	0.091	1.05E-04	2.17E-03

The specific adsorption capacity of L6 is in Table 45. The mass of Particle L6 was 3.643g and the particle was not moisturised.

Table 45: CO_2 adsorption quantified in terms of Sample L6 mass

	Moles Adsorbed/g Coal	m^3 CO_2 adsorbed	m^3 CO_2 Adsorbed/t Dry Sample Weight
P Step 1	1.92E-04	3.98E-06	1.092
P Step 2	3.44E-04	4.78E-06	1.312
P Step 3	4.41E-04	5.04E-06	1.382
P Step 4	5.37E-04	5.18E-06	1.423
P Step 5	5.67E-04	5.23E-06	1.435
P Step 6	5.67E-04	5.23E-06	1.435
P Step 7	5.95E-04	5.26E-06	1.445

5.5.3.7 Combined Results of the 22.4 - 16 mm Adsorption Experimentation Results

Figure 24 shows the cumulative moles of CO_2 that were adsorbed during experimentation with the 22.4 – 16 mm size class particles. The equilibration time for each sample has not been included in the heading for each set of data points. The reason for this is that all the 22.4 – 166 mm size class particles were given 3 hour equilibration times between pressure steps.

It can be seen that the data points for particles L5 are far higher than those of the other particles. This is the run where a large amount of leakage above the leakage during the blank run was suspected due to the large pressure drops in each pressure step.

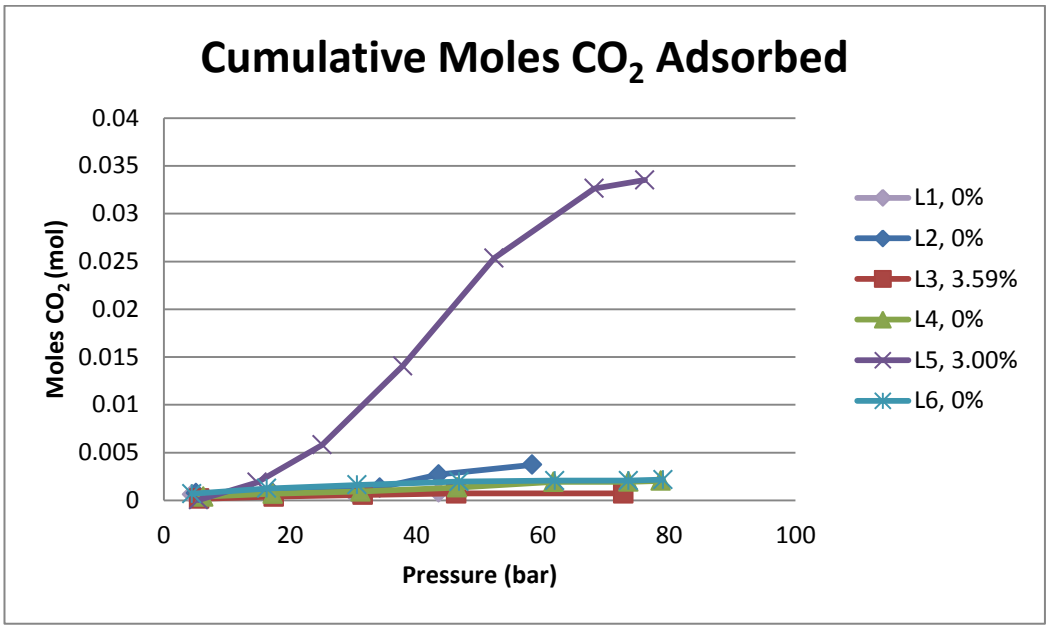

Figure 24: Cumulative moles of CO_2 adsorbed by 22.4 - 16 mm size class particles

Figure 25 shows the specific adsorption capacity of the 22.4 - 16 mm size class particles. As was the case in the cumulative moles of CO_2 adsorbed, the data points for particle L5 are far higher than the other particles.

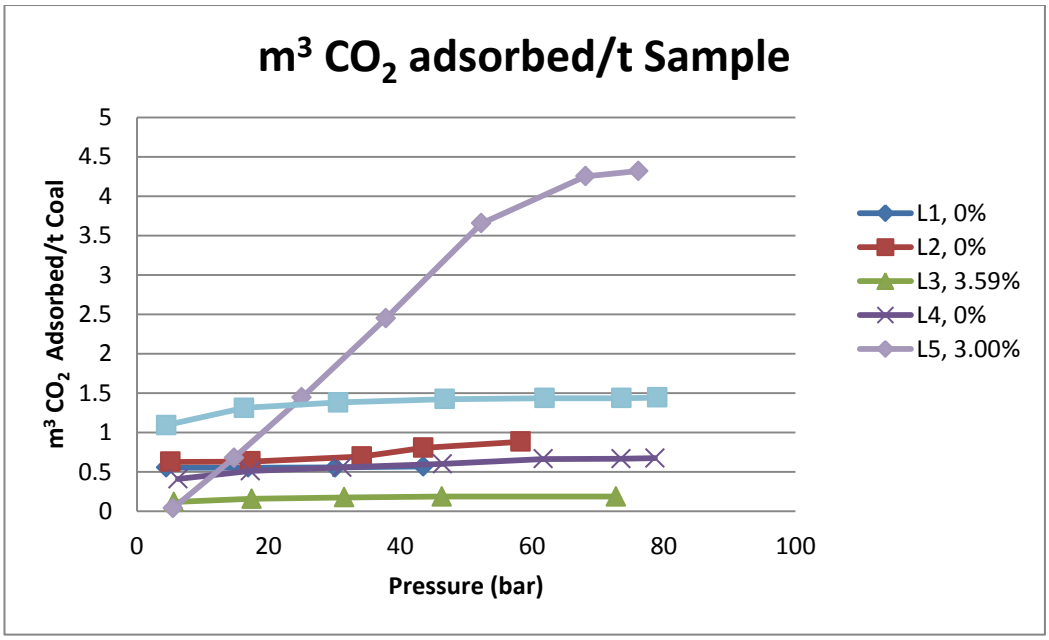

Figure 25: Specific Adsorption Capacity of the 22.4 to 16 mm size class particles

5.6 Desorption

The pH of the distilled water in which the particles were placed after experimentation was tested. Results for the preliminary work conducted on the 9.5 – 6.7 mm size class particles to determine the correct equilibration time between pressure steps are available for the 0%, 1hr, 7.94%, 1hr and 11.65%, 2 hrs samples. The 14.45%, 3 hrs sample was not tested as the experimental run terminated early and it was expected that the experiment could be repeated at a later stage. Unfortunately the adsorption equipment was out of operation from December 2011 to September 2012 and completing the 14.45%, 3hrs run was not possible. Table 46 contains the desorption results. The pH of the distilled water in which the samples were placed was 7.11.

Table 46: pH readings of distilled water in which the samples used for preliminary experimentation were placed after adsorption experimentation

Sample ID	Stable pH Reading	First pH Reading
0%, 1hr	8.08	no data
7.94%, 1hr	8.29	no data
11.65%, 2 hrs	7.46	6.57

The pH of the distilled water in which the 5 particles from the 9.5 – 6.7 mm size class were placed after adsorption experimentation was measured. This can be found in Table 47. The pH of the distilled water in which the coal samples were placed was 6.38.

Table 47: pH readings of distilled water in which the samples from the 9.5 – 6.7 mm size class were placed after adsorption experimentation

Sample ID	Stable pH Reading	First pH Reading
S1, 0%, 2 hrs	7.89	7.02
S2, 6.65%, 3 hrs	7.23	7.37
S3, 0%, 3 hrs	7.82	7.63
S4, 0%, 3 hrs	7.74	7.72
S5, 1.9%, 3 hrs	7.65	7.64

Further, the pH of the water in which the 6 large particles from the 22.4 – 16 mm size class were placed after adsorption experimentation was also measured. This is in Table 48. The pH of the distilled water in which the coal samples were placed was 6.38.

Table 48: pH readings of distilled water in which the samples from the 22.4 - 16 mm size class were placed after adsorption experimentation

Sample ID	Stable pH Reading	First pH Reading
L1, 0%	7.04	7.13
L2, 0%	7.65	7.51
L3, 3.59%	8.09	8.07
L4, 0%	5.83	5.97
L5, 3.00%	6.10	6.01
L6, 0%	5.79	5.82

Figure 26 shows the adsorbed CO_2 forming bubbles on the surface of the coal particle after the coal was removed from the adsorption experiment. Despite the fact that the coal had been at atmospheric pressure for 5 to 15 minutes, an estimate of the time takes to remove the eight bolts from the reactor in which the coal was placed in the volumetric adsorption equipment, numerous bubbles formed on the surface of the coal.

Figure 26: 22.4 – 16 mm particle placed in distilled water after removal from the Volumetric Adsorption Equipment

As stated in the methodology section the pH meter takes readings based on stability. When taking the readings for all the particles it was noticed that the first pH reading was usually lower than the stable pH reading. As the Crison pH meter is designed to test based on stability, the accuracy of the first reading results in not known. It is however interesting that ten out of fourteen pH readings started lower than the final reading and over 5 minutes, which was the time taken in some cases for a stable reading to be obtained, increased. 5 minutes is large in comparison to the 150 second stability time used by the Crison pH meter.

Blank runs were conducted with coal particles that had not been used for CO_2 adsorption experimentation. These particles were placed in distilled water and the pH

was measured before submersion of particles and after removal of the particles from water. The results indicated that the pH of the distilled water increased when coal particles were placed in it. For example, when coal particles were removed from distilled water that had a pH of 7.58, the pH had increased to 7.92. The increase in pH of the distilled water in which particles S2, S5, L3 and L5 can be found, below. The pH of the water into which the particles were placed for moisturisation was 6.38. The trend of increasing pH with submersion of blank samples in distilled water draws further attention to the low pH of the distilled water on removal of particles with added CO_2.

Table 49: pH of distilled water used to moisturise coal particles after removal of the particle

Sample ID	pH Reading
S2, 6.65%, 3 hrs	6.82
S5, 1.9%, 3 hrs	6.94
L3, 3.59%	7.84
L5, 3.00%	7.11

The H+ ion molar concentration was not calculated to obtain an indication of the degree of dissolution of CO_2 from the coal into the distilled water as the data was too erratic. When more repeatable pH/dissolution of adsorbed CO_2 from coal data is available, further quantification of this would be recommended. Hence these results can only be considered exploratory and require extensive reworking.

5.7 Chapter Summary

Results for the analyses and experimental work conducted for this research were presented in this chapter. Congruency, outlying points and disparities between the results were pointed out. These will be discussed further in the next chapter.

6 Discussion

6.1 Coal Analyses

6.1.1. Coal Moisture Determination

The moisture content analysis will not reflect the as received moisture content of the coal. The coal was stored in large open plastic bags before use for experimentation. The coal at the top of the bag was exposed to the atmosphere and therefore would contain less surface moisture than the rest of the coal. While coning and quartering and other techniques were used to ensure the samples taken were representative of the bulk; the surface moisture of the particles in the sample will vary greatly from particle to particle depending on the proximity of the particle to the open top end of the plastic bag.

The total moisture content as determined by ALS laboratory group agrees with the TGA analysis that was conducted on the sample prepared from the 9.5 – 6.7 mm size class coal used in experimentation. The total moisture content determined by ALS laboratories does not agree with the moisture content determined by TGA for the larger size class 22.4 – 16 mm.

In all other respects, the proximate analyses of the representative samples of both coal size classes agree well with each. A possible reason for the moisture content discrepancy was that the preparation of the larger size class took a longer period of time and therefore the coal was exposed to the atmosphere for a longer time. In contrast the preparation of the analysis sample for the 9.5 – 6.7 mm coal was quickly done as the quantity of coal that was handled was less than an eighth of the original sample size. Thus even though both representative samples were crushed to the same small particle size for the TGA at the University of the Witwatersrand, the one that has the moisture content closer to that reflected in the moisture content analysis done by the independent laboratory was exposed to the atmosphere for a shorter period of time. This is presumed to be the reason for the difference in moisture content.

6.1.2 Surface Area Analysis

The surface area analysis was conducted by measuring CO_2 adsorption of samples at low pressures and fitting this data with accepted adsorption models. The results for the Langmuir, BET and D-R models are presented in Table 8. This method of surface area analysis has proved fortunate as some adsorption data has been generated, albeit at low pressures, on samples with differing particle sizes.

The results of the analyses have shown that more CO_2 is adsorbed when particle sizes are smaller. The CO_2 adsorption capacity of the two particles from the 9.5 – 6.7 mm size range is smaller than that of the 1 mm passing size sample for all three mathematical analyses methods. As a complement to this the surface area of the 1 mm passing size sample is larger than that of the two 9.5 – 6.7 mm particles. The reason for the increased surface area is that crushing opens pores of coal that may be inaccessible to the gas in a whole particle (Busch *et al*., 2004).

6.1.3 TGA Analysis and Petrographic Analysis

The TGA results were as expected for a Witbank coal and the 9.5 - 6.7 mm representative sample TGA results agree with the moisture content determination that was conducted at ALS laboratory. They are thus believed to be a true reflection of the coal properties of the 9.5 – 6.7 mm size class.

The volatile carbon content of the sample prepared from the 9.5 – 6.7 mm size class is lower than that of the 22.4 – 16 mm size class. This is as was expected as the volatility of coal is generally attributed to the maceral vitrinite. Vitrinite has a lower relative density than inertinite which is the less volatile carbon form. Therefore vitrinite is more friable and is expected to report to the smaller size classes during crushing and coal preparation. Therefore the higher volatile content of the smaller size class coal agrees with accepted and published coal data.

The results of the Petrographic Analysis were as expected. There were however some anomalies between the analyses of the different size class samples. These are discussed briefly but detail on the reasons for this is beyond the scope of this research. Higher vitrinite content was expected in the smaller size class sample when compared to that of the larger size class sample. The reason for this is that vitrinite is the least dense component of coal and therefore is the most likely to break in crushing and sample preparation. However petrography found that the vitrinite content of the 22.4 – 16 mm is on average higher than the 9.5 – 6.7 mm particles. Also the mineral matter content of the smaller particles was expected to be lower on average than that of the large particles. The reason for this is that the mineral matter in coal is often the most dense portion and therefore is expected to be concentrated in the larger size fraction due to inability to break the mineral matter. This was also contrary to the petrographic results as the 9.5 – 6.7 mm size class sample showed a larger mineral matter content than the 22.4 – 16 mm sample.

The petrographic analysis was also as expected for a Witbank coal, being low in vitrinite and high in mineral matter (Table 7). Ash is the product that remains after combustion and provides an indication of the mineral matter of the coal (Falcon 2011; Johns, 2011). There is good agreement between the TGA and petrographic analyses for this

component. Care must be exercised in comparison as the percentages are volume percent in Petrography but mass percent in TGA; therefore some disparity is expected. However, this is not large and the analyses complement each other with the properties of the representative sample.

6.2 Coal Particle Selection

Visual selection of particles in terms of brightness as an indicator of the vitrinite content of the particle is problematic. However, it was deemed to be the best way to obtain a sample higher in vitrinite compared to other particles. The less preferable options for determining a sample high in vitrinite are to break the particles and use density separation techniques or to use expensive equipment such as QEMSCAN which will identify the exact composition of a coal particle. QEMSCAN is however also limited by particle size and does not analyse beyond the surface of the particle. As large particles were desired for the experimentation crushing and density separation was not an option.

The problem with visual sorting is that the presence of vitrinite on the surface of the coal particle is not a definite indication that the inside of the particle is vitrinite rich. Selection of coal particles in this manner will become more inaccurate in terms of desired high vitrinite content as coal particle diameter increases. When coal particle diameter decreases to the point where visual identification of different parts of the particle is not possible as it is too small, visual sorting will also not be possible. However, it remains an inexpensive manner of coal particle selection that will ensure that some vitrinite is present in the particle used in experimentation.

The results of the research are not believed to be widely influenced by the visual sorting of particles for experimentation and analyses were conducted to determine average coal properties of each size class. The results generated in each size class are comparable with each other and thus the visual selection method is not believed to have influenced the results.

6.3 Coal Moisturisation

When the coal was moisturised by submersion in distilled water often particles would break and therefore reduce the size of the original particle that was placed in the distilled water. This is problematic as moisture addition was determined by the change in mass of the particle. As the coal particles were breaking in the water, this added inaccuracy. The largest particle that separated from the original particle in water was 1 mm in diameter. This particle was not used in experimentation to avoid inaccuracy.

However, some separation of coal dust/small particles occurred from all particles moisturised in distilled water.

Another problem that occurred was that moisture evaporates from the moisturised particle in appreciable amounts as the experimental times are in the order of 8 to 21 hours depending on the time chosen for equilibration in each pressure step. When there were automation difficulties with the equipment the experimental times could be over 48 hours. The mass loss due to moisture can clearly be seen in Table 11 and Table 12. The constant temperature oven was operated at 40^{o}C. When moisturised particles are left in an environment with a different temperature and humidity, they will come to equilibrium with the environment. Therefore the particles will lose moisture should the conditions of the environment allow drying of the particle. This phenomenon would occur in the volumetric adsorption equipment as well. The temperature in the constant temperature oven of 40^{o}C will promote loss of moisture from the sample, further the atmosphere will be mostly CO_2 and thus there should not be much humidity in the system. Thus diffusion of moisture from the particle into the less humid surrounding area in the adsorption equipment will occur. Therefore the moisture content of the sample will decrease as the coal particle dries in the 40^{o}C temperature. During operation the moisture content of the sample cell and then the reference cell would increase when V2 was opened to allow pressure into the sample cell, and CO_2 flows through the system between V1 and V3 for subsequent pressure steps. Further, when V1 is opened to start the new pressure step and increase the pressure in the system the moisture should remain in the reference cell as pressurised CO_2 will be flowing into the reference cell. Thus diffusion of water vapour out of the reference cell would be against the direction of CO_2 flow. However, some diffusion of water vapour between the pump and the entrance to the reference cell (V1) may occur. Finally, when the system is vented at the end of the experimental run the moisture that has left the particle and is in the CO_2 environment of the equipment shall be vented to the atmosphere. Therefore, the moisture content of the particle that is placed in the sample cell at the start of the experiment will differ from the moisture content of the particle that is removed from the cell and placed in distilled water after experimentation.

Moisturisation of the coal in distilled water was effective for short periods of time. However, to ensure that the moisture content of the experimental sample remains constant for the entire time of experimentation, it is recommended that high moisture content coals are used in experimentation and the practice of moisturising the coal is avoided. This is in line with the work of Mares *et al*. (2009). This however creates its own problems as there are few naturally high moisture content coals in South Africa.

6.4 True Volume Measurement

The determination of the volume of the coal particles in the He Pycnometer was difficult as one could not tell when equilibrium was obtained. Equilibrium, as it is used in this paragraph, is the diffusion of He into all the accessible pores in the particle and thus reaching a state of equilibrium where no further diffusion will occur. However in the operation of the equipment it was noticed that the pressure reading continued to decrease and a steady value was not reached even over 3 hour equilibration time periods. Longer equilibration times were not possible due to demand for equipment.

Therefore, the P_2 value was taken when the pressure readings only changed in the third decimal place every ten seconds. The P_3 reading was taken after expansion into V_A when the pressure reading stopped changing significantly and changes in the third decimal place started to happen. As an error check for this, the density of the coal particle was calculated as the mass could be accurately determined on a scale and the volume of the particle was calculated as an average of three Stereo Pycnometer runs. The density of coal is determined by the component parts: as mineral matter is more dense than the maceral forms of carbon. However the density should be around a sg of 1.3 – 1.5 (this is highly dependent on the coal being analysed). With the density checking of the true volume measurement it is believed that the results of the true volume measurement in the He Stereo Pycnometer are correct. Therefore the estimation of the void volume that was used in the calculation of the CO_2 adsorption of the coal should not have unreasonable errors.

6.5 Equipment Volume

Due to the large differences between the volumes of the sample cell that were determined in this research and in the research of Maphada (2012) and Maphala (2012), the volume of the cavity in the pressure vessel (sample cell) was measured. The volume available in the pressure vessel was filled with distilled water. The cavity in the pressure vessel held approximately 15 mL, when filled to the point where it would overflow should more water be added. The system volume determined through experimentation and calculation was 19.108 mL. The tubes connecting the pressure vessel to valves V2 and V3 would also have some volume in the system. This volume is not expected to be large as the diameter of the tubes is not large and the tubes have thick walls as a result of the high pressures that the equipment operates at. Thus the volume of 19.108 mL measured and calculated for the sample cell is expected to be correct.

6.6 Adsorption Testing

6.6.1 Volumetric Adsorption Equipment

There were many difficulties encountered in the operation of the volumetric adsorption system. As the equipment was newly commissioned, this is to be expected. However, the progress of the project was significantly affected by these problems. The problems included:

- leaking from the system,
- incompatibility of local component parts when international components were delayed or unavailable,
- automation challenges,
- problems with communication between the equipment and software,
- equipment failure,
- unavailability of resources such as compressed air from the School of Chemical and Metallurgical Engineering compressor that was used for the pump valves, and
- differences between pressures displayed on the equipment and on the automation software.

The high pressure CO_2 environment caused fatigue of the bolts that were sealing the reactors. Bolts sheared or snapped when tightened. This can be seen in Figure 27. Leakage from the equipment is controlled by the tightening of the bolts and failure of the bolts often resulted in poor and unusable experimental data.

Figure 27: Sheared and snapped bolt from the pressure vessels/reactors

Many of these difficulties have been resolved in conjunction with other students who are also completing degrees at the University of the Witwatersrand. However, the leaking of the system will continue to be a problem as the pressures at which it is operated are high (above supercritical pressure of CO_2 [73 atm]) and the material and equipment is quickly fatigued.

Operation procedures are currently being put in place to ensure fewer failures and less downtime on the equipment. The time spent working on the equipment to produce the data and understand the operation of the volumetric adsorption equipment has been valuable to overcoming many of these difficulties. This is believed to be a part of the results of this project as future students will generate data and conduct research more easily and efficiently.

6.6.2 Experiment Design

The use of large particles in this project was to approximate underground storage conditions as closely as possible. The dry masses of the particles used in adsorption experimentation are in Table 50. The particles in the 9.5 – 6.7 mm size class can be clearly distinguished from the particles in the 22.4 – 16 mm size class due to the large difference in particle masses.

Table 50: Dry Masses of all Particles used in Adsorption Experimentation

Paricle ID	Dry Mass of Particles (g)
Sample 1	0.339
Sample 2	0.529
Sample 3	0.595
Sample 4	0.369
S1	0.404
S2	0.346
S3	0.335
S4	0.312
S5	0.316
L1	6.422
L2	5.819
L3	6.656
L4	3.886
L5	4.463
L6	3.892
L7	2.66

These particle size classes are larger than the coal used for the majority of coal CO_2 adsorption capacity research discussed in Chapter 2. Gamson *et al*. (1993) however used a coal particle size similar to the 9.6 – 6.7 mm size class of roughly 1 cm^3.

A disadvantage in the use of large coal particles is that the composition of the different particles may vary greatly due to the natural heterogeneity of coal. The analyses conducted on the particles were done on a representative sample of the size class that was reduced to appropriate analyses sizes. Therefore, the average coal composition of the entire size class is known, but the actual composition of the individual particles is not. An advantage in the use of large particles in experimentation is that the surface area that is available for adsorption is smaller than that of powdered sample. Therefore the results for adsorption capacity that one gets from the larger particles is lower than that of the small particle size samples as crushing opens inaccessible pores in the coal for CO_2 storage (Busch *et al*., 2004). In large scale operation the coal used for storage will be fractured, but will not be of the same size as small particle sizes used in the majority of CO_2 adsorption research. Thus, it is believed that these results are less of an overestimate of the adsorption capacity that one may expect in the pilot scale testing of CO_2 storage in unmineable coal seams. As the particles of coal shall be larger than those used in this experiment, in pilot scale testing; a lower adsorption capacity than is reflected in these results should be expected.

The procedure of degassing the coal before use in the equipment was necessary as there was no means of analysis of gases in the reaction vessel, and therefore may have altered the results of this research. The results may be slightly inaccurate as the atmosphere in the vessels was assumed to be pure CO_2. Any gases that may remain in the system or coal despite the degassing of the coal or the evacuation of the system before experimentation would affect the assumption of the single gas atmosphere.

The degassing of the coal was thus necessary to determine the coal CO_2 adsorption potential using our equipment. However, underground coal is not totally gas free and many seams contain large amounts of CH_4 and other gases. Therefore the use of degassed coal in the research of the coal adsorption capacity may cause difficulties when extending the results from laboratory scale to implementation. It is well known that CH_4 desorbs when CO_2 adsorbs on to coal (Krooss *et al*., 2002; Saghafi *et al*., 2007; Mares *et al*., 2009) but the presence of other gases in the coal seam maybe have different adsorption and desorption characteristics. Therefore the use of degassed coal in experimentation may result in an overestimation of the coal CO_2 storage capacity.

6.6.3 Impact of Equilibration Time on Adsorption Capacity

Preliminary experimentation was conducted to determine the correct time for equilibration for the large particles used in this research. Before equipment automation,

to complete an experiment only an hour was possible between pressure steps as the operator needed to remain in the laboratory, and this was discouraged after hours. When automation was complete longer periods of time could be used.

Longer equilibration times were used and a time of up to 3 hours was allowed for each pressure step. The results generated for Sample 2 (7.94%, 1 hr), Sample 3 (14.45%, 3 hrs) and Sample 4 (11.65%, 2 hrs) are presented below. As all particles were moisturized, the differences between the adsorption curves generated can be attributed to the differing periods of time before the subsequent pressure steps. Nonetheless some difference may be due to differing moisture contents or differing mineral and maceral composition of the particles. Moisture content of a particle has been found by Ozdemir and Schroeder (2009) to negatively affect adsorption capacity. Crosdale *et al*. (1998) found that vitrinite rich coals had higher adsorption capacities than inertinite rich coals. As large particles have been used in experimentation there may be differences between the maceral and mineral matter content of the individual particles.

However, the magnitude of the difference between the curves is large and thus it is believed to be as a result of differing equilibrium times, or system leakage, as small differences in moisture or particle composition should not cause differences as large as those observed. The time used for equilibration before each of the successive pressure step was 1 hour for Sample 2, 3 hours for Sample 3, and 2 hours for Sample 4.

Figure 28 clearly shows the difference between the 1 hour time duration of each pressure step and the 2 and 3 hour time durations. The particles that were left in the adsorption equipment for longer time periods showed greater CO_2 adsorption capacities which lead to the belief that equilibrium and all adsorption that was possible did not occur when times less than three hours were used between pressure steps. Day *et al*. (2008b) in experiments conducted on coal of a smaller particle size, 0.5 – 1.0 mm diameter, used 4 hours as an equilibration time between pressure steps. Other authors have used longer equilibration times.

The orientation of the fifth point in the Sample 4 (11.65%, 2 hrs) adsorption isotherm is believed to be caused by the premature termination of the pressure step. Thus all possible adsorption may not have occurred. Two hours were allowed for each pressure step in this experiment however the experiment terminated after only 45 minutes at this pressure step. The reason for the premature termination of the experimentation was determined to be a lack of memory in the volumetric adsorption equipment. The frequency at which data was logged was then changed to avoid the repeat of this problem from particle L3 onwards. Difficulties such as these were a result of working on newly commissioned equipment where operations procedures were being determined through this work and that of other master's students.

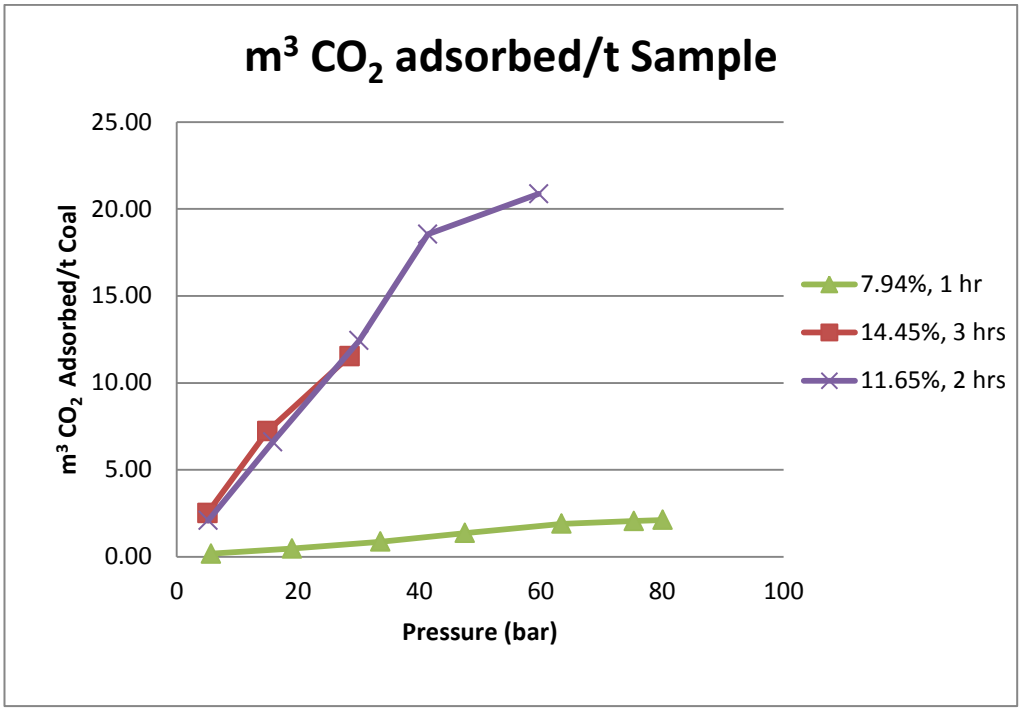

Figure 28: Difference in specific adsorption capacities with 9.5 – 6.7 mm size class particles where different adsorption equilibration times were used

Another possible explanation for the perceived greater adsorption capacity at longer equilibration times is leakage of the equipment. This shall be examined in Figure 29. Particle S1 is the only other particle in this research that was run with a 2 hours equilibration time instead of 3 hours. The results for particle S1 were corrected for leakage with a blank run, and so the above mentioned challenges with regard to corrected experimental work for leakage with a blank run must be kept in mind. However, the specific adsorption capacity of particle S1 is far below that of Sample 4 (11.65%, 2 hrs). Further the results of Ozdemir and Schroeder (2009) indicate that particles with increased moisture content should have reduced adsorption capacities. Thus, it is believed that the equipment was leaking during the determination of the correct equilibration time. It is very difficult to keep an adsorption system airtight (Belmabkhout *et al*., 2004). Leaking during experimentation was tested by the application of soapy water that showed small leaks readily in the form of bubble formation. Should the leakage from the system be great, it was experienced that no bubbles were formed as the CO_2 moved from the system to the larger constant temperature oven so quickly the bubble formation was not possible.

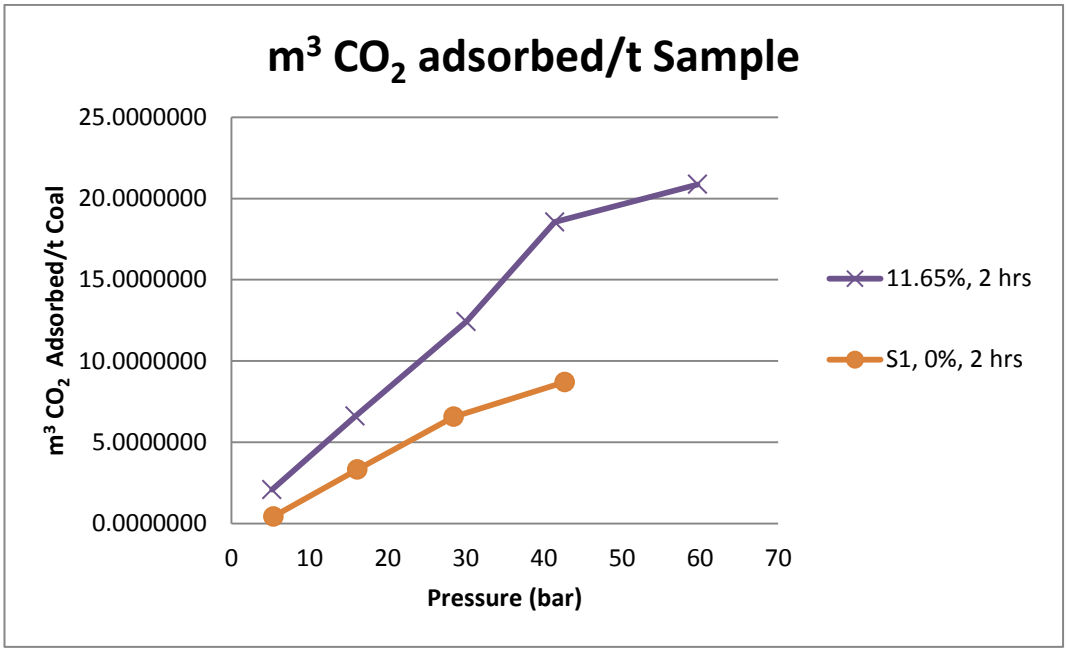

Figure 29: Comparison of 9.5 – 6.7 mm particles to determine whether the equipment was leaking during preliminary testing to determine the correct equilibration time

Additionally, it was expected that once all the CO_2 that could be adsorbed on a coal particle had done so, the pressure decrease would stop. This will be true for a closed system with no leaks. This trend was not noticed in any of the individual results presented above and therefore the coal may have additional adsorption capacity or all adsorption that may have happened at that pressure has already occurred and further pressure decreases are due to leakage. Figure 30 shows pressure data from the second three hour pressure step in the Sample 3 (14.45%, 3 hrs) experiment. It can be seen that the gradient of the line is reducing as the time increases, but a horizontal point is never achieved. This may be a sign that further adsorption could take place on the particle. Alternatively, this may just indicate there is leakage in the system.

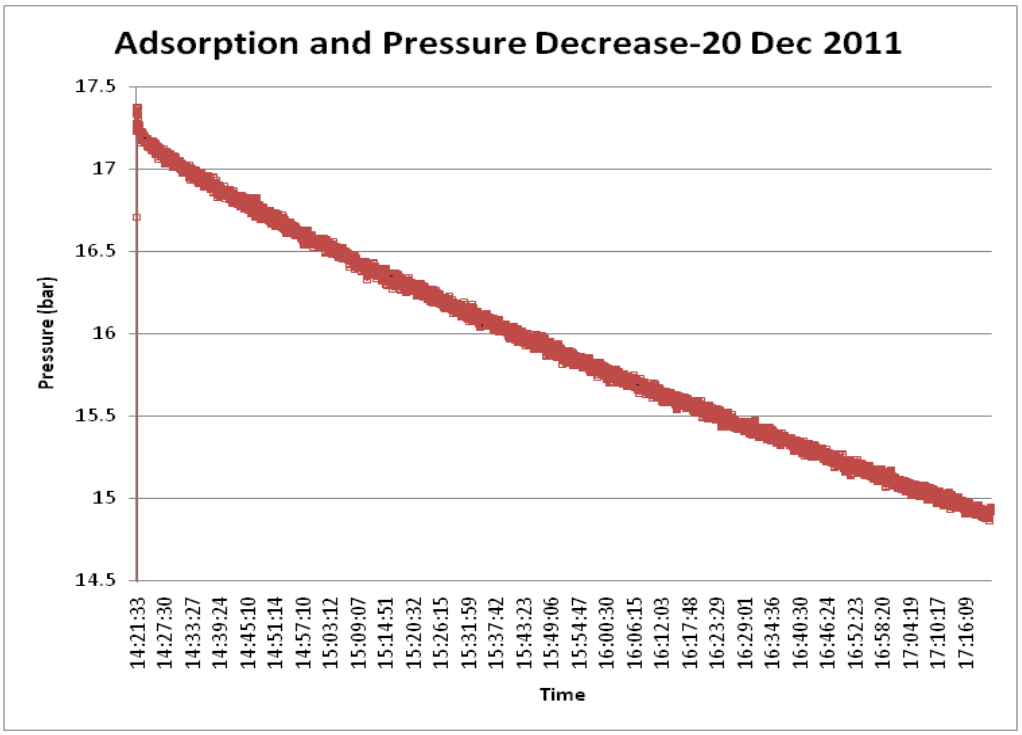

Figure 30: Pressure decrease with adsorption on Sample 3 (14.45%, 3hrs) in the second pressure step

6.6.4 Adsorption Experimentation Results with 9.5 – 6.7 mm Size Class Particles

Figure 22 contains the specific adsorption capacity of particles S1 to S5 from the 9.5 – 6.7 mm size class. Particles S1 and S2 have data points far above those of the other three particles. The discrepancy is so large it is believed to be a result of equipment leakage and not greater adsorption capacity of these particles. The data for both particles was corrected for leakage but it is believed to be inadequate. Thus the data generated for these particles is excluded from further discussion.

Figure 31 contains the results for the particles S3 to S5. Data for Sample S4 and Sample S5 has been corrected for leakage. Data for particle S3 could not be corrected for leakage as the blank run conducted to correct the data showed greater leakage than the experimental run.

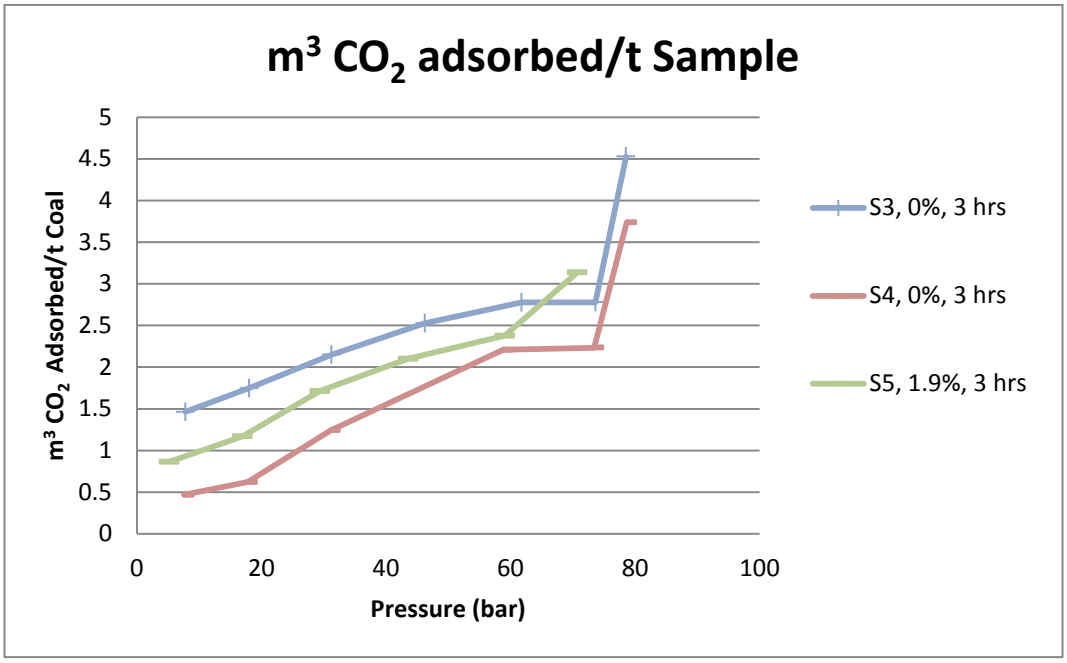

Figure 31: Specific Adsorption Capacity of particles S3 to S5 from the 9.5 – 6.7 mm size class particles

The impact of moisture on the adsorption capacity of coal cannot be seen clearly in these results. As the specific adsorption capacity is used for comparison, the different masses of the particles should not affect the results.

The last data point for each experimental run is higher than the previous despite correction for leakage.

The correction for leakage may be the reason for the unclear results, however without this correction data would not be able to be generated on the equipment at the University of the Witwatersrand.

6.6.5 Adsorption Experimentation Results with 22.4 – 16 mm Size Class Particles

Figure 25 contains the results of the specific adsorption capacity of particles L1 to L6. The data points for particle L5 are far higher than those of the other experimental runs. The data generated for particle L5 was corrected for leakage, but the large discrepancy between the data points leads to the belief that this correction did not account for enough leakage in the experimental run. Reasons for the differing leakage could include the status of the seal used on the pressure vessel during experimentation, the tightness of any of the 8 bolts on the pressure vessel or leakage from any of the connection points

in the system, of which there are numerous. Thus the data from sample L5 is excluded from further discussion.

Figure 32 contains the results of adsorption experimentation with particles L1, L2, L3, L4 and L6. Particle L6 is the experimental run where data correction for leakage could not be performed and the blank run to quantify the leakage in the system had a higher leakage than the experimental run. Thus, the reason for the situation of the data points for particle L6 above all the other experimental data may be the inability to correct for leakage.

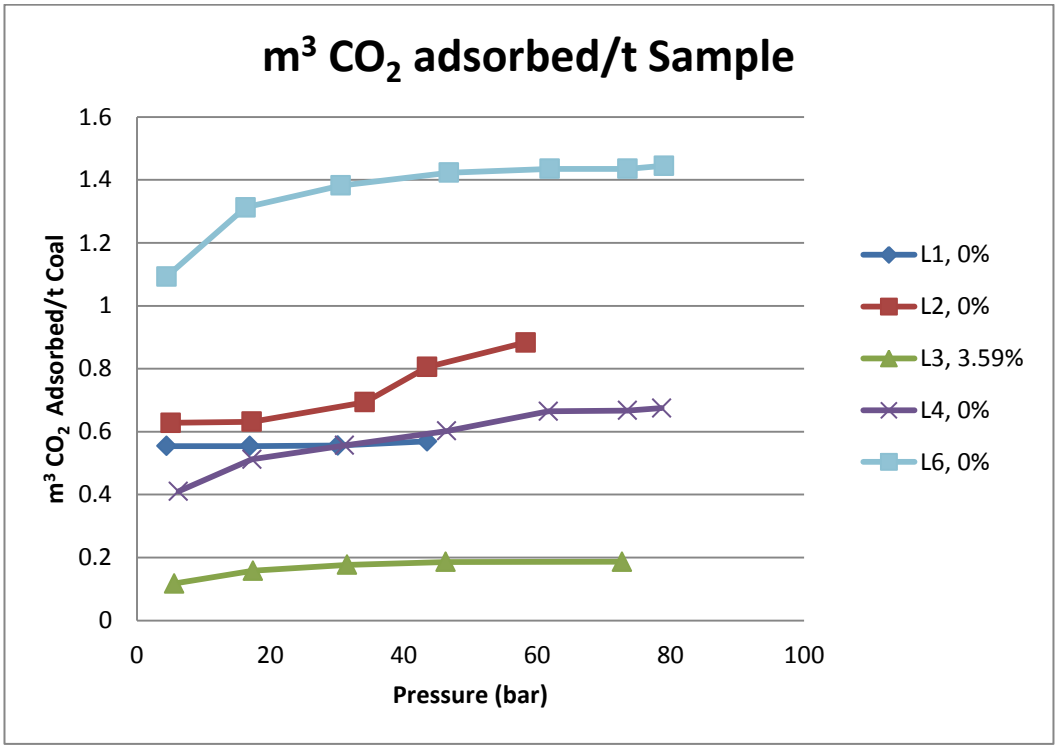

Figure 32: Specific Adsorption Capacity of particles L1, L2, L3, L4 and L6 from the 22.4 – 16 mm size class particles

6.6.6 Impact of Moisture on Adsorption Capacity

6.6.6.1 Preliminary Experimentation

The results generated on Sample 1 (0%, 1hr) and Sample 2 (7.94%, 1 hr) shall be used for the comparison of the difference that moisture content of coal has on adsorption capacity.

Sample 1 was not moisturised. After degassing the particle was placed in the adsorption equipment and the pressure and temperature results were used in calculation of the

adsorption capacity of the coal at different pressures. Sample 2 was placed in distilled water for moisturisation for 30 minutes before use in the adsorption equipment. The mass percentage of water that was added to the particle after removal from the distilled water and allowing the surface of the particle to visually dry was 7.94%. Despite this short period of submersion in the distilled water the difference in the adsorption capacity of the two particles can be clearly seen in Figure 33. One should be careful in attributing the entire difference to the difference in moisture content of the coal as the composition of the particles could vary and therefore the difference may lie in maceral composition of the particles. This is not believed to be the case as the agreement in the surface area analyses of two particles from this size class was good (Table 8) and therefore similar particle composition is assumed.

The last point on the graph for the 0%, 1hr sample is higher than the previous due to increased adsorption calculated from the pressure and temperature data generated in the adsorption equipment. The calculations have been checked and it is not believed that there is an error. It may be a result of increased equipment leakage at the last and higher pressure. The higher last data point has been found in other experimental data as well. The last point on the 7.94%, 1hr sample run is also higher than the previous recorded point but not to the same degree as the 0%, 1hr sample. This is not believed to be as a result of the use of the ideal gas equation in calculation as the compressibility factor correction should account for deviation from ideal gas behaviour even under these conditions.

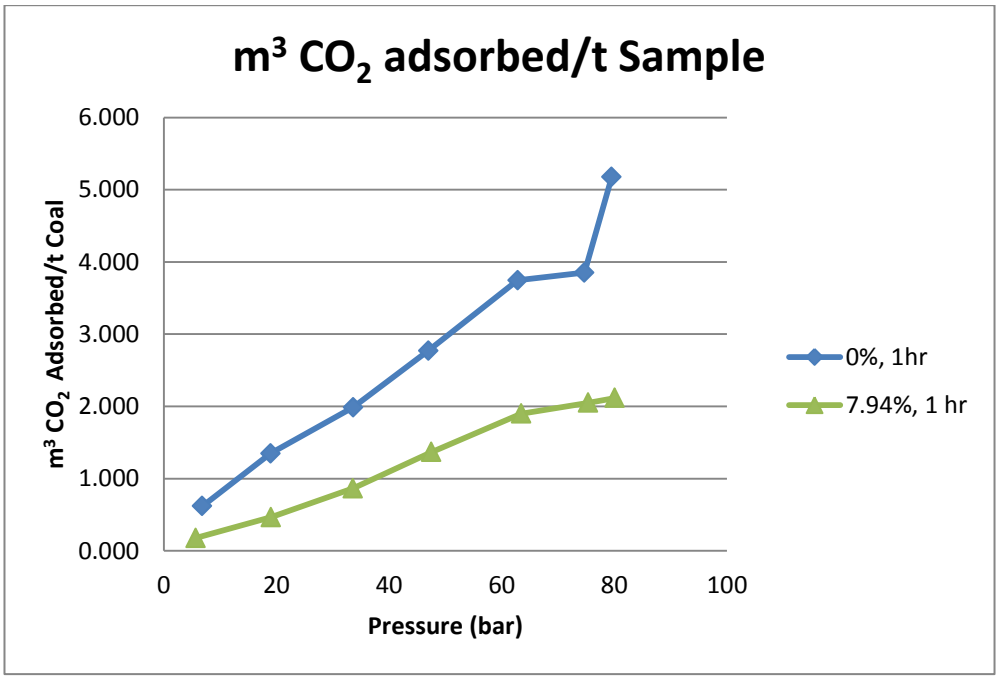

Figure 33: Differing adsorption capacities between dry and moisturized 9.5 – 6.7 mm size class samples

6.6.6.2 Further 9.5 – 6.7 mm Sample Experimentation

The results from the further experimentation on the 9.5 – 6.7 mm size class are inconclusive with regards to moisture content. The particle with increased moisture content is sitting between the results of two particles with no added moisture. Further experimentation is recommended.

6.6.6.3 Further 22.4 – 16 mm Sample Experimentation

The results of the 22.4 – 16 mm sample experimentation show the particle with increased moisture content has the lowest specific adsorption capacity. Unfortunately the results from the other moisturised particle in this size class have been excluded from discussion as significant leakage of the equipment is believed to have occurred.

Thus despite the fact that the results for the larger size class confirm the hypothesis that moisture in coal negatively affects adsorption capacity, further experimentation is recommended. This is due to the persistent equipment problems and the need to correct for leakage. The premise of a constant volume system is compromised with equipment leakage and thus results must be interpreted with care.

6.6.6.4 Summary of Moisture effect on Adsorption

Moisture in coal was found to negatively affect the adsorption capacity of the coal for two out of three instances at pressures up to 80 bar. In the experimentation with the 9.5 – 6.7 mm size class particles the particle with increased moisture content was found to sit between two particles with no added moisture. Thus, the hypothesis is neither proved nor disproved in this case. Further experimentation is advisable as coal seams at greater depths will be at greater pressures than 80 bar (Day *et al*., 2008b). However, coals at depths of 300 – 600 m are likely to have better permeability and less cost implications than storage in deeper coals (Vijoen *et al*., 2010).

The repeatability of these results is not good due to the aforementioned equipment issues. However, the results are in line with what was expected from peer reviewed literature that was consulted during this research work. Further, because large coal particles were used in experimentation; the composition of the samples could be variable. This is another reason to repeat the experimentation as the effect of particle composition cannot be fully excluded from the reduced adsorption capacity of the moisturised coal particle as opposed to the as received particle. The effect of particle

composition could be fully explored in a long term project where particles are crushed and analysed after adsorption experimentation.

6.6.7 Impact of Particle Size on Adsorption

The impact of particle size on adsorption can clearly be seen in Figure 34. The smaller particles have higher adsorption capacities than the larger particles. This is in line with the work of Busch *et al*. (2004) who found that adsorption increases with decreasing particle size as crushing opens further pores.

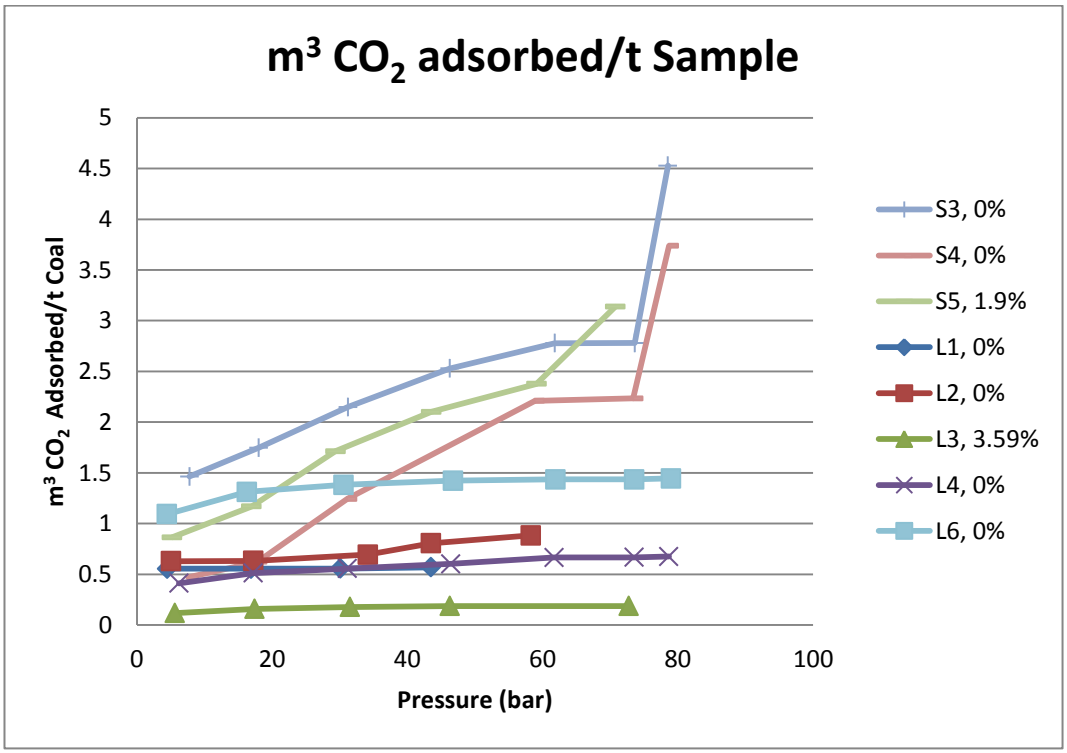

Figure 34: Specific Adsorption capacity of different size class particles (S3, S4, S5, L1, L2, L3, L4, L6)

Figure 35 shows the same data with particle L6 removed from the plot. This was the particle where data correction for leakage was not possible as the blank run had a higher leakage rate than the experimental run. In this Figure the difference between the specific adsorption capacities of the different size class particles can be seen with even greater clarity.

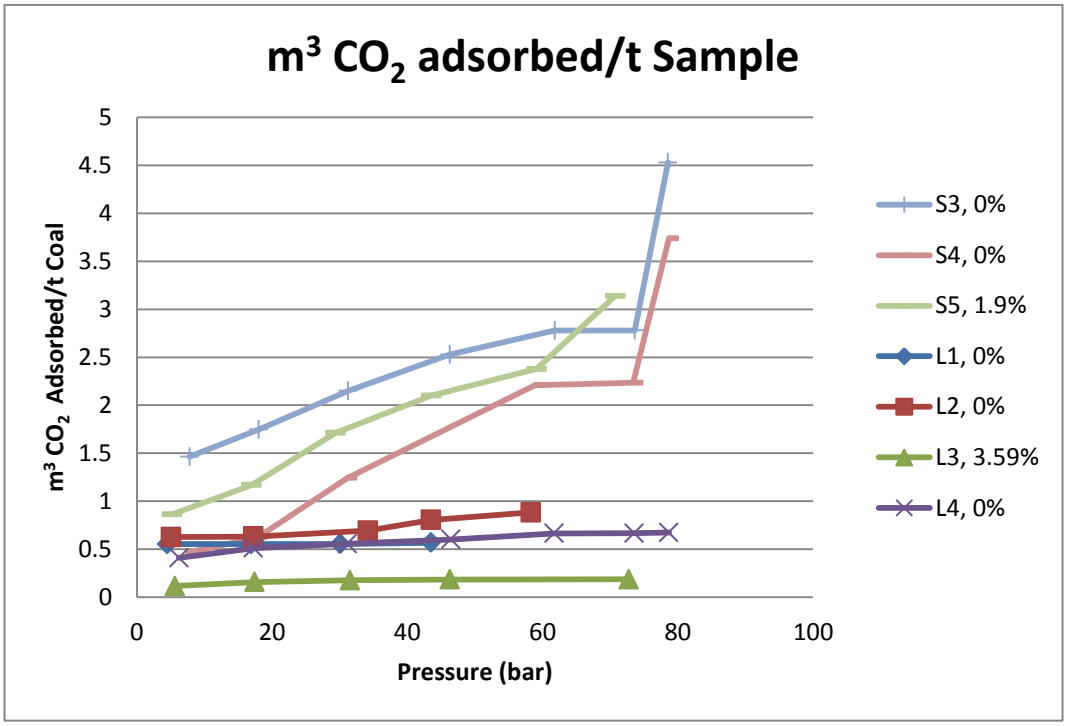

Figure 35: Specific Adsorption capacity of different size class particles (S3, S4, S5, L1, L2, L3, L4)

The average difference between the graphs for the small and large particles has been calculated. The average distance between the points in the moisturised small and large particles (S5/L3) is 9.7. The same calculation was performed for the particles with no additional moisture and the average distance between these curves is 1.8 for S4/L2, 2.9 for both S3/L2 and S4/L4, and 4.3 for S3/L4. In an attempt to find a correlation between these values and the particle size the ratio of the top size classes (22.4/9.5) and bottom size classes (16/6.7) were calculated, i.e. 2.4 for both ratios.

The average values for the distance between the adsorption capacities is in range with the ratio of the size classes, however the individual ratios tend to start from lower values and increase with the pressure. Thus, more work is needed to adjust adsorption data for larger particle sizes.

6.6.8 Comparison with Published Results

The results generated in the research for this project were compared with Saghafi *et al*. (2008) who also worked on South African coal. Their study was on the enhancement of adsorption potential due to igneous intrusions and therefore their coal samples were heat affected. Saghafi *et al*. (2008) samples used for comparison with the results generated in this project are 'MDT2' and 'MDT15'. These samples were chosen as they

are the ones that are represented graphically in Saghafi *et al*. (2008). These samples were taken from 4.6m and 57m from the dyke respectively. Proximate Analyses were conducted on both samples (Table 51).

Table 51: Proximate analyses of samples from Saghafi *et al*. (2008)

Sample ID	Distance from Dyke (m)	Moisture (%)	Volatile Matter (%)	Fixed Carbon (%)	Ash Yield (%)	Volatile Matter, daf(%)	Density (g/cm^3)
MDT 2	4.6	3.1	11.9	60.4	24.6	16.5	1.73
MDT 15	57.0	5.4	20.2	54.6	19.8	27.0	1.65

The moisture content of MDT15 is close to the as received moisture content of the Witbank coal used in this research. Considering the moisture contents of the two Saghafi *et al*. (2008) samples, it can be seen that the coal with higher moisture content has the lower adsorption capacity (Figure 36).

Petrography was conducted only on MDT2. The results of this analysis were that coal sample MDT2 contained 2% vitrinite, 0% liptinite, 86.83% inertinite and 11.17% mineral matter (Saghafi *et al*., 2008). The petrography of these samples differs from the petrography of the coal used in this research. The petrographic result of the representative sample of the 9.5 – 6.7 mm size class had 21% vitrinite, 8.8% liptinite, 45.4% inertinite and 24.8% mineral matter. The petrographic result of the representative sample of the 22.4 – 16 mm size class had 28.8% vitrinite, 5.2% liptinite, 46.8% inertinite and 19.2% mineral matter. Therefore, the coals used by Saghafi *et al*. (2008) are different to those used in this research, but the limited amount of data on CO_2 adsorption capacity of South African coal has necessitated this comparison.

Literature leads us to expect that, in terms of composition, the coal used in this research should have a higher CO_2 adsorption capacity than lower grade coals, due to the greater vitrinite content (Crosdale *et al*., 1998; Dutta *et al*., 2008; Mares *et al*., 2009). However another important factor that should be considered is the particle size of the samples. Saghafi *et al*. (2008) used a size range of 90 to 150 µm. This is vastly smaller than the coal used in this research. As noted by Busch *et al*. (2004), adsorption increases with decreasing particle size as crushing opens further pores. Thus in terms of particle size the results of Saghafi *et al*. (2008) are expected to exceed those produced in this experimentation using larger particles. This is the case.

Nevertheless the results of Saghafi *et al*. (2008) that have shown that heat affected coal can have a storage capacity a factor of 2 larger, should be kept in mind. This is due to enhanced porosity and gas diffusivity as a result of dolerite intrusions (Saghafi *et al*., 2008). The cubic meters of CO_2 that were adsorbed per ton of the coal, that was not heat affected and of a far larger particle size, is lower than that of Saghafi *et al*. (2008).

Only the top two curves in Figure 36 are compared to results generated in this project as no CH_4 adsorption capacity was tested as part of this research.

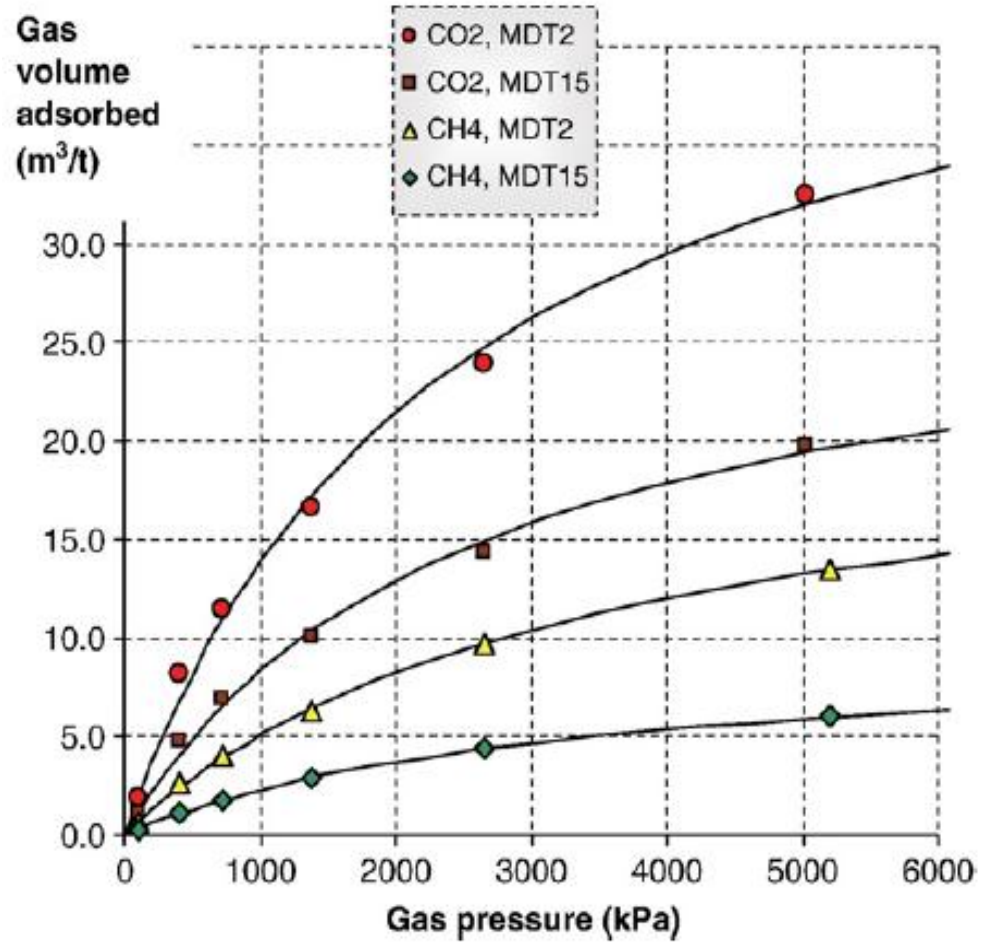

Figure 36: Adsorption curves generated in research on South African coal by Saghafi *et al*. (2008)

The results of Viljoen *et al*. (2010) have been included for comparison with these results. Vijoen *et al*. (2010) used the results of Billenkamp (1988) and Saghafi *et al*. (2008) to determine the CO_2 adsorption in m^3/ton for South African coal. Billenkamp (1988) constructed CH_4 sorption isotherms for temperatures of 10, 20 and 30°C and pressures of 0.5, 1.0, 2.0, 3.0, 4.0, 6.0, 8.0, and 10.0[11] MPa.

Viljoen *et al*. (2010) adapted the CH_4 sorption results of Billenkamp (1988) using CO_2:CH_4 adsorption ratios, for a category of low rank coals and a category of high rank coals. The category of low rank coals has been used for comparison with the results of this study as

[11] The range of these pressures in bar is 5 bar to 100 bar

the petrography conducted on the Witbank coal used in this research found that it is a medium rank C coal. Further the results of Viljoen *et al*. (2010) show that higher rank coals have a higher CO_2 adsorption capacity while low rank coals have one that is lower. Unfortunately no vitrinite reflectance is provided by Viljoen *et al*. (2010) for their separation of the coals into low and high rank. However, the low rank coals are described as unaffected while their high rank coals are described as metamorphosed. Thus, the data generated for low rank coals has been used in the comparison of these results.

Figure 37 shows the results from Viljoen *et al*. (2010). The adsorption capacities far exceed those found in this research as is the case for the results of Saghafi *et al*. (2008). Unfortunately the coal used in the research of Billenkamp (1988) was not classified in terms of size class. 200 to 300g of the coal was however run through a disc mill for 2 minutes in the sample preparation (Billenkamp, 1988) and thus the particle size would be fine and far smaller than the coal used in this research.

Therefore, as with the results of Saghafi *et al*. (2008), the reduced specific adsorption capacity of coals tested in tested in this research when compared to the results of Viljoen *et al*. (2010)[12] is expected to be a result of difference in the particle size.

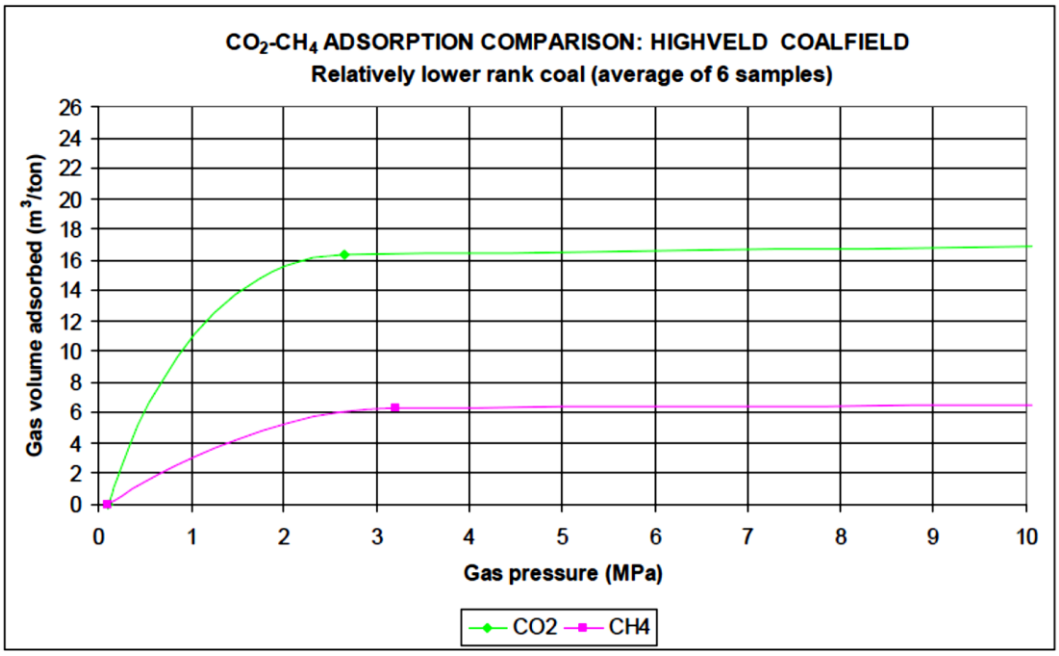

Figure 37: CO_2 and CH_4 adsorption capacities of low rank South African Coal

[12] Adapted from the work of Billenkamp (1988)

The adsorption experimentation in this research was conducted in a constant temperature oven as temperature also has a role in adsorption capacity, namely: the greater the temperature; the lower the adsorption capacity (Viljoen *et al*., 2010). However small fluctuations did occur in the temperature and while the number of moles in the system was accounted for through use of the ideal gas equation with the compressibility factor, a correction factor for reduced adsorption capacity with small temperature changes was not available.

Finally, the maximum error in the Results has been quantified in line with Belmabkhout *et al*. (2004) who found that a leak rate of 10^{-4} mol/hr leads to an average error of 0.2% in the high pressure measurements. Again high pressure is not quantified, but Belmabkhout et al. (2004) worked up to pressures of 10000 kPa (100 bar). As difficulty would exist with the separation of moles leaked versus moles adsorbed, the quantification has been performed on the blank run data. Thus this is the maximum leakage from the system[13]. The error in the blank run data used to correct the results for S1 ranges from 4.4 to 20.9%. The error in the blank run data from the 21st to the 22nd September is in the range of 0.8 to 37.7%. Lastly the error in the blank run data used to correction the experimentation in November 2012 ranges between 0.5 and 12.5%. It should be noted that the error in the results shall be lower than these values as the data has been corrected for leakage.

6.7 Desorption

Further research should be conducted on desorption of adsorbed CO_2 on coal into water. The design of this experiment did not allow for optimal testing of this concept. The majority of the CO_2 is likely to desorb from the coal sample after the last pressure step when the high pressure volumetric adsorption equipment vented all gas in the system to the atmosphere. This would occur as the amount of adsorbed CO_2 that can remain on the coal is different at different pressures, but low at low pressures such at atmospheric pressures. Further, all testing on the desorption of the CO_2 into water was conducted at atmospheric pressure which is contrary to the pressure under which the CO_2 on the coal will be stored. As underground coal seams will be used, and deep coal seams will probably be more suitable due to the poor economics of mining at that depth, desorption of the CO_2 into water should be carried out at high pressure to determine the likelihood of pH change in the ground/coal bed moisture. This will require the design of a different experimental set up and will be a complex endeavour as the system will need to handle high pressure gas and liquid safely.

[13] Aforementioned problems with correcting data for leakage should remain in mind here.

The data generated with the simple Crison pH meter did indicate that desorption of CO_2 into water may be a concern for storage. Viljoen *et al*. (2010) state that the presence of potable ground water is a concern as CO_2 storage can contaminate groundwater. Therefore water movement through coal seams should be considered carefully in the decision on whether to store CO_2 in a particular unmineable coal seam.

6.8 Chapter Summary

Adsorption was negatively affected by increasing particle size and increasing moisture content. Further work is however recommended due to persistent leakage problems with the equipment.

7 Conclusions

The results of this research have shown that moisture content negatively affects the CO_2 adsorption capacity of coal. This was found for all pressures up to 80 bar. These experiments should however be repeated to confirm results as the results were confirmed in two instances and neither proved or disproved in another. This is in line with the hypothesis for the research. The first research question with regard to the effect of different moisture contents on the CO_2 adsorption of the coal unfortunately cannot be answered as the two of the experimental runs where leakage was so bad the work could not be corrected were moisturised particles. Thus not enough data was generated for comparison of different moisture contents within each size class. The fourth research question on whether adsorption results for dry coal can be adjusted to compensate for wet coal has not been answered for the reasons mentioned above.

The impact of coal particle size on the adsorption capacity of the coal was quantified. Crushing opens the pores of coal and therefore increases surface area for adsorption of CO_2 onto the coal. Coal with a smaller particle size has a higher CO_2 adsorption capacity. This has been proven in all results generated in this research report. Literature also indicates this trend repeatedly. The second research question has been answered; in all cases the size of the particles negatively affected adsorption capacity.

The time required for all CO_2 adsorption that could occur on a coal sample of a certain size was unfortunately not quantified. The reasons for this include the leakage of the equipment. The data shall not plateau at any value while the equipment is leaking and thus equilibrium and maximum adsorption capacity for a coal and a particular particle size shall be difficult to determine.

Adsorption equipment operation procedures were refined during this research.

The method for testing desorption of CO_2 into water was flawed and it is believed that a better method should be developed. The repeated practice of the pH meter starting at a lower pH and then increasing in pH until a stable reading could be obtained indicates that acidification of groundwater is a possibility in the storage of CO_2 in unmineable coal seams. Therefore this should be seriously considered in the decision on whether to store CO_2 in unmineable coal seams. The third question as to whether dissolution into water of adsorbed CO_2 will occur was answered, however further investigation is required as this is a first attempt of the test.

This research project has produced outcomes which have agreed with published literature. Thus, is it believed that the results are feasible and may add to a small but growing body of research on CO_2 adsorption capacity of South African coal. The limits of the research have been pushed further as South African coals with increased moisture content and of a larger particle size than previous experimentation were used.

Storage of CO_2 in coal is a possibility, but caution must be exercised. Further research is necessary before large scale implementation could start. Research should take into account storage experience from other projects around the world that are in the monitoring phases for issues such as water contamination, experience from CBM projects that are currently in operation, and focus on research using conditions closer to those that will occur in CO_2 storage in unmineable coal. When all this is complete a pilot project should be undertaken to confirm all research is correct. Finally a large scale project could be started.

An advantage of CO_2 storage in coal is that the coal fields in South Africa are generally close to the CO_2 emission sources and therefore CO_2 transportation costs will be avoided. A high pressure pipeline for delivery of CO_2 to offshore saline aquifer storage basins may prove prohibitively expensive. Further barriers include the lack of strict GHG legislation in South Africa. Despite the stringent emission reduction targets made by President Zuma at COP17, without a credible national GHG inventory and a GHG reduction plan, these targets may be difficult to meet. These targets are also contingent on funding and technology transfer from the developed world. Therefore it is unlikely that CO_2 storage in unmineable coal seams will happen in South Africa for a long time period, if at all.

8 Recommendations

The following recommendations are presented for any research that could build upon this and confirm the results in the volumetric adsorption equipment at the university:

- The difficulties experienced in this research were largely related to the equipment issues. Therefore the experimentation should be repeated to confirm any results generated. Results generated were however in line with published literature which is positive.
- It is recommended that different coals with high as received moisture contents are used in further research. This will allow the use of the ASTM standards for moisture determination. The moisture content of the as received coal would then be the high moisture content coal in experimentation and a low moisture sample could be produced through the drying of a portion of the sample in a low heat vacuum pressure environment. This approach will also generate data on the specific adsorption potential of coals in the different coal fields in South Africa. This is valuable as coal is highly variable in composition by nature of its formation from plant materials over 280 millions of years ago (Saghafi *et al*., 2008; Falcon, 2011). A consideration for this research will be that the as received coal cannot be degassed as this may reduce the moisture content as well as remove previously adsorbed gases. Further, when the coal is dried to form a low moisture sample previously adsorbed gases may be released. Thus a method for quantification, of the effect of degassing the samples, on the results should be determined.
- A further reason to use coal with high moisture content, other than bringing the project in line with international coal testing standards, is the fluctuation in added moisture contents. Addition of moisture to coal has been difficult as a large amount of the added moisture leaves the coal when it is placed in a dryer environment. Therefore, other research that has been conducted on moist coal suggests starting with a high moisture coal and removal of water to create comparative samples for analysis (Mares *et al*., 2009). This should ensure that the moisture content of the sample that is being used for experimentation will not fluctuate as widely as it is assumed to have done in the volumetric adsorption equipment.
- Gravimetric Adsorption equipment may be better suited to test the adsorption capacity of moisturised coals. This is because if the moisturised particle is losing mass it can be assumed that the moisture is leaving the pores of the coal. If the sample is gaining mass then the CO_2 is adsorbing on the coal or dissolving at high pressure into the moisture in the pores of the coal. The volumetric adsorption equipment with no gas chromatograph or way to analyse the environment in the reaction cell is thus not ideal for experimentation with high moisture content particles.

- Larger particle sizes should be used in further experimentation. While this presents difficulties to the researcher as most analysis techniques or systems are designed for coal with small particle sizes and exact composition of large particles versus average composition may vary; it is important to have this data on hand. This is reflected in literature as well, for example Sabir and Chalaturnyk (2009).
- An equilibration time that is suitable for the majority of CO_2/gas adsorption that will occur on coal in the University of the Witwatersrand Volumetric Adsorption equipment should be determined. This time may be dependent on particle size, moisture content and coal composition amongst other factors but an equilibration time from previous use of the equipment should be able to be used as an indication for future research.
- Further examination of the large increase in CO_2 adsorption capacity, beyond supercritical pressures, of coal tested in the University of the Witwatersrand volumetric adsorption equipment is needed. This increase is a deviation from the trend of other data used. This also deviates from published literature.
- More data should be generated on the dissolution of adsorbed CO_2 from coal into surrounding water. This CO_2 may originate from the surface moisture of the coal in which the CO_2 may already be dissolved after CO_2 adsorption on the coal (Day *et al.*, 2008b) or in the free space in the coal particles (Sakurovs *et al.*, 2007).

References

Alstom, 2009. *CCS Solutions*, Alstom (Switzerland) Ltd, Switzerland, pp. 10 -11.

Airey, E. M., 1968. *Gas emission from broken coal an experimental and theoretical investigation.*International Journal of Rock Mechanics and Mining Sciences &Geomechanics Abstracts, vol. 5, issue 6, pp. 475 – 494.

ASTM D1412-07, *Standard Test Method for Equilibrium Moisture of Coal at 96 to 97 Percent Relative Humidity at 30^{o}C,* ASTM International, United States.

ASTM D3302-74, *Standard Test Method for Total Moisture in Coal*, ASTM International, United States.

Bachu, S., 2007. *Carbon dioxide storage capacity in uneconomic coalbeds in Alberta, Canada: Methodology, potential and site identification*. International Journal of Greenhouse Gas Control, 1, pp. 374–385.

Beck, B., 2011. *CCS Internationally and in South Africa*, Course Notes from Coal Combustion and Power Generation, University of the Witwatersrand

Beck, B., Surridge, T., Liebenberg, J., Gilder, A., 2011. *The current status of CCS development in South Africa*, Energy Procedia, v4, pp. 6157 – 6162.

Belmabkhout, Y., Frère, M., De Weireld, G., 2004. *High-pressure adsorption measurements.A comparative study of the volumetric and gravimetric methods*, Measurement Science and Technology, v 15, pp. 848 – 858.

Bhebhe, S., 2008. *The effect of coal composition on carbon dioxide adsorption*.University of the Witwatersrand, Johannesburg, South Africa.

Bolland, O., 2012. *CO_2 Capture in power plants*, Course Notes from Advanced Course CHMT 7069, University of the Witwatersrand, Johannesburg

Brown, T.L., Le May, Jr, H. E., Bursten, B. E., Burdge, J. R., 2003. *Chemistry The Central Science,* 9th edition, Prentice Hall, United States of America, pp. 557.

Bureau of Economic Geology, 2012. *Gulf Coast Carbon Centre, SACROC Research Project.* INTERNET http://www.beg.utexas.edu/gccc/sacroc.php Cited 29 November 2012.

Busch, A., Gensterblum, Y., Krooss, B. M., Littke, R., 2004. *Methane and carbon dioxide adsorption – diffusion experiments on coal: upscaling and modelling.* International Journal of Coal Geology, vol. 60, pp. 151 – 168.

Charrière, D., Behra, P., 2010. *Water sorption on coals*. Journal of Colloid and Interface Science, vol. 344, pp. 460 – 467.

Changbing, 2011. *Sensitivity of shallow groundwater systems to CO_2; Case studies from the Cranfield and SACROC EOR fields,* Presentation at the 6th Trondheim Conference on CO_2 Capture, Transport and Storage, Norway.

Cloete, M., 2010. *Atlas on geological storage of carbon dioxide in South Africa*, Pretoria, South Africa, Council of Geoscience.

CO_2 Info, 2006.*CO_2 Phase Diagram*, INTERNET http://www.teamonslaught.fsnet.co.uk/co2_info.htm Cited 4 January 2012.

Crosdale, P. J., Beamish, B. B., Valix, M., 1998. *Coalbed methane sorption related to coal composition*, International Journal of Coal Geology, v35, pp. 147 – 158.

Day, S., Sakurovs, R., Weir, S., 2008a. *Supercritical gas sorption on moist coals*, International Journal of Coal Geology, v 74, pp. 203 – 214.

Day, S., Duffy, G., Sakurovs, R., Weir, S., 2008b. *Effect of coal properties on CO_2 sorption capacity under supercritical conditions*, International Journal of Greenhouse Gas Control, pp. 342 – 352.

Department of Energy, *IRP 2010 – 2030 Final Report*, INTERNET http://www.doe-irp.co.za/content/IRP2010_2030_Final_Report_20110325.pdf, Cited 11 October 2011.

Department of Environmental Affairs and Tourism, 2007. *Long Term Mitigation Scenarios: Technical Summary*. INTERNEThttp://www.environment.gov.za/hotissues/2009/LTMS2/LTMSTechnicalSummary.pdf Cited 27 February 2012.

Department of Environmental Affairs and Tourism, 2009. *Greenhouse Gas Inventory South Africa: Report*. INTERNET http://www.pmg.org.za/node/17759, Cited 27 February 2012.

Dutta, P., Harpalani, S., Prusty, B., 2008. *Modeling of CO_2 sorption on coal.* Fuel, vol. 87, pp 2023 – 2036.

Energy Research Centre, 2007. *Long Term Mitigation Scenarios: Technical Summary*, INTERNET http://www.erc.uct.ac.za/Research/publications/07ERC-LTMSTechnical_Summary.pdf Cited 27 November 2012

Engelbrecht, A., Golding A., Hietkamp, S., Scholes, B., 2004. *The potential for sequestration of carbon dioxide in South Africa.* Manufacturing and Materials Technology, CSIR, Pretoria, South Africa. pp 1 -55

Falcon, R. M. S., 2011. *Conventional analyses, their limitations and the true nature of coal*, Coal Sampling, Its Quality and Utilisation course at the University of the Witwatersrand, Johannesburg.

Falcon, R. M. S., 1989. *Macro and micro-factors affecting coal-seam quality and distribution in southern Africa with reference to the No. 2 seam, Witbank coalfield, South Africa*, International Journal of Coal Geology, vol. 12, pp. 681 – 731.

Gamson, P. D., Beamish, B. B., Johnson, D. P., 1993. *Coal microstructure and micropermeability and their effects on natural gas recovery.*Fuel, vol. 72, pp. 88 – 99.

Gibson-Poole, C.M., Edwards, S., Langford, R.P. and Vakarelov, B., 2006. *Review of geological storage opportunities for carbon capture and storage (CCS) in Victoria.* Prepared for the State of Victoria, Department of Primary Industries, Cooperative Research Centre for Greenhouse Gas Technologies, Australian School of Petroleum, University of Adelaide, Adelaide, ICTPL Consultancy Report Number ICTPL-RPT06_0506.

Goodman, A. L., Busch, A., Duffy, G. J., Fitzgerald, J. E., Gasem, K. A. M., Gensterblum, Y., Krooss, B. M., Levy, J., Ozdemir, E., Pan, Z., Robinson Jr., R. L., Schroeder, K., Sudibandriyo, M., White, C. M., 2004. *An Inter-Laboratory Comparison of CO_2 Isotherms Measured on Argonne Premium Coal Samples*. Energy and Fuels.

Johns, A., 2011. *Moisture in Coal – Forms and Analysis*, Coal Sampling, Its Quality and Utilisation course at the University of the Witwatersrand, Johannesburg.

Joubert, J. I., Grein, C. T., Bienstock, D., 1974. *Effect of moisture on the methane capacity of American coals*.Fuel, vol 53, pp. 186 – 191.

Krooss, B. M., van Bergen, F., Gensterblum, Y., Siemons, N., Pagnier, H. J. M., David, P., 2002. *High-pressure methane and carbon dioxide adsorption on dry and moisture-equilibrated Pennsylvanian coals.*International Journal of Coal Geology, vol. 51, pp. 69 – 92.

Letete, T., Guma, N., Marquard, A., 2009. *Information on climate change in South Africa: greenhouse gas emissions and mitigation options*, Energy Research Centre, INTERNET http://www.erc.uct.ac.za/Information/Climate%20change/Climate_change_info-complete.pdf, Cited 26 February 2012.

Maphada, M., 2012. *The automation of a Volumetric Adsorption System*, University of the Witwatersrand, Johannesburg.

Maphala, T., 2012. *Research work conducted at the University of the Witwatersrand,* Johannesburg.

Mares, T. E., Radlinski, A. P., Moore, T. A., Cookson, D., Thiyagarajan, P., Ilavsky, J., Klepp, J., 2009. *Assessing the potential for CO_2 adsorption in a subbituminous coal, Huntly Coalfield, New Zealand, using small angle scattering techniques*, International Journal of Coal Geology, vol. 77, pp. 54 – 68.

Mastalerz, M., Gluskoter, H., Rupp, J., 2004. *Carbon dioxide and methane sorption in high volatile bituminous coals from Indiana, USA*. International Journal of Coal Geology, vol 60, pp. 43 – 55.

McCusker, L. B., Liebau, F., Engelhardt, G., 2001. *Nomenclature of structural and compositional characteristics of ordered microporous and mesoporous materials with inorganic hosts.*Pure Applied Chemistry, vol. 73, no. 2, pp. 381 – 394.

Ozdemir, E., Schroeder, K., 2009. *Effect of Moisture on Adsorption Isotherms and Adsorption Capacities of CO_2 on Coals.*Energy and Fuels, vol 23, pp. 2821 – 2831.

Paton, C., 2010. *Climate Change – SA's carbon footprint Hot air vs action*, Financial Mail, INTERNET http://www.fm.co.za/Article.aspx?id=116438, Cited 30 October 2011.

Perry, R. H., Green, D. W., Maloney, J.O., 1997. *Perry's Chemical Engineers' Handbook*, 7th Edition, McGraw-Hill, New York.

Sabir, A. and Chalaturnyk, R. J., 2009. *Adsorption characteristics of coal in constant pressure tests.*INTERNEThttp://www.thefreelibrary.com/Adsorption+characteristics+of+coal+in+constant-pressure+tests.-a0211365933 Cited 12 January 2011.

SACCCS, 2012. *Roadmap: Carbon capture and storage roadmap,* INTERNET http://www.sacccs.org.za/roadmap/roadmap/, Cited 29 November 2012.

Saghafi, A., Faiz, M., Roberts, D., 2006. *CO_2 storage and gas diffusivity properties of coals from Sydney Basin, Australia.*International Journal of Coal Geology, vol. 70, pp. 240 – 254.

Saghafi, A., Pinetown, K. L., Grobler, P. G., van Heerden, J. H. P., 2008. *CO_2 storage potential of South African coals and gas entrapment enhancement due to igneous intrusions.*International Journal of Coal Geology, vol. 63, pp. 74 – 87.

Sakurovs, R., Day, S., Duffy, G., Weir, S., 2007. *Application of a modified Dubinin–Radushkevich equation to adsorption of gases by coal under supercritical conditions*. Energy Fuels 21, pp. 992–997.

Solomon, S., Carpenter, M. and Flach, T.A., 2008. *Intermediate storage of carbon dioxide in geological formations: A technical perspective*. International Journal of Greenhouse Gas Control, vol 2, pp. 502 – 510.

South Africa Climate Change, 2012. *South African Government's Position on Climate Change.* INTERNET http://www.climateaction.org.za/cop17-cmp7/sa-government-position-on-climate-change

South African Weather Service, 2011.INTERNET http://www.weathersa.co.za/web/home.asp?sp=1&f=&z=Ctry&v=7&g=gT&h=0&m=Str

m&anim=aStr&av=AvWarn&uid=&p=&dbug=&TL=&PC=&mw=w&ht=&ib=1&f=1220, Cited 19 January 2012, 17:30.

Statoil, 2011. *Leading the world in carbon capture and storage*. INTERNET http://www.statoil.com/en/TechnologyInnovation/NewEnergy/Co2Management/pages/carboncapture.aspx, Cited 30 November 2012.

Suuberg, E. M., Otake, Y., Yun, Y., Deevi S. C., 1993. *Role of Moisture in Coal Structure and the Effects of Drying upon the Accessiblity of Coal Structure*. Energy and Fuels, vol 7, pp. 384 - 392

Treybal, R. E., 1981. *Mass-Transfer Operations,* 3rd edition, McGraw-Hill Book Company, pp. 566.

United Nations Framework Convention on Climate Change. *Home, Kyoto Protocol.* INTERNET.http://unfccc.int/kyoto_protocol/items/3145.php Cited 3 September 2010.

Unsworth, J. F., Fowler, C. S., Jones, L. F., 1989. *Moisture in coal 2.Maceral effects on pore structure.* Fuel, vol. 68, pp. 18 – 26.

Viljoen, J. H. A., Stapelberg, F. D. J., Cloete, M., 2010. *Technical Report on the Geological storage of Carbon Dioxide in South Africa*, Council for Geoscience, South Africa, pp. 18 – 236

White, C.M., Strazisar, B.R., Granite, E.J., Hoffman, J.S., Pennline,H.W., 2003. *Separation and capture of CO_2 from large stationary sources and sequestration in geological formations—coalbeds and deep saline aquifers*.Journal of the Air and WasteManagement Association, v53, pp. 645–715, INTERNET http://www.ncbi.nlm.nih.gov/pubmed/12828330, Cited 26 February 2012.

White, C. M., Smith, D. H., Jones, K. L., Goodman, A. L., Jikich, S. A., LaCount, B. L., DuBose, S. B., Ozdemir, E., Morsi, B. I., Schroeder, K. T., 2005. *Sequestration of Carbon Dioxide in Coal with Enhanced Coalbed Methane Recovery - A Review*, Energy and Fuels, v19, p 659 – 724

World Coal Institute, 2007. *Coal Conversion Facts.* INTERNET http://www.google.co.za/url?sa=t&rct=j&q=&esrc=s&frm=1&source=web&cd=1&ved=0CEAQFjAA&url=http%3A%2F%2Fwww.worldcoal.org%2Fbin%2Fpdf%2Foriginal_pdf_file%2Fcoalconversionfacts2007(04_06_2009).pdf&ei=BUu4UJeeKaeH0AXwrIG4DQ&usg=AFQjCNEWKJjXRnDl8vvn7klvmXpjLHIl3A&sig2=y41d-qK0QTsgGlr4f6TM2w, Cited 30 November 2012

World Weather Online, 2012. INTERNET http://www.worldweatheronline.com/v2/weather.aspx?q=Johannesburg,%20South%20Africa&day=21 Cited 30 November 2012

Appendix A – Compressibility Factors used in the Calculation of CO_2 Adsorption

The Tables below contain all the interpolation work that was done for the compressibility factors for each experimental run. The compressibility factors used in the calculation of the results for Sample 1 are in the main body of the report where the use of the compressibility factor in calculations is discussed.

Table 52: Compressibility Factors used in the Calculation of the Results for Sample 2

	Pressure (bar)																					
Temp (deg C)	1	5	5.657747	*5.686043*	10	19.02128	19.19263	20	33.56365	33.96272	40	47.49763	48.11284	60	63.45389	64.24116	75.37378	75.58135	80	80.0959	80.30281	100	200
0	0.9933	0.9658			0.9294			0.8496			-			-					-			-	-
37.95		*0.9770*		*0.9737*	*0.9532*																		
37.99		*0.9770*	*0.9738*		*0.9532*																		
38.13					*0.9533*	*0.9078*		*0.9029*															
38.18								*0.9030*	0.8417		0.8126												
38.30																							
38.31														0.6967	0.6715				0.5504				
38.39					*0.9534*		*0.9073*	*0.9033*			0.8130	0.7695		0.6969									
38.41														0.6970			0.5846		0.5508				
38.49														0.6972				0.5834	0.5511				
38.40	0.9961	0.9787			0.9571			0.9119	0.8448	0.8428	0.8130	0.7695	0.7659	0.6970	0.6717	0.6660	0.5846	0.5831	0.5508	0.5498	0.5477	0.3479	
38.59								*0.90354*		0.8405	0.8132												
38.77											0.8135		0.7666	0.6979									
38.81																			0.5524		0.5494	0.3506	
38.99														0.6984		0.6676			0.5531				
50	0.9964	0.9805			0.9607			0.9195			0.8300			0.7264					0.5981			0.4239	-
100	0.9977	0.9883			0.9764			0.9524			0.9034			0.8533					0.8022			0.7514	0.5891

Table 53: Compressibility Factors used in the Calculation of the Results for Sample 3

	Pressure (bar)														
Temp (deg C)	1	5	5.082536	*5.52013*	10	14.93084	17.27639	20	28.48691	32.37515	40	60	80	100	200
0	0.9933	0.9658			0.9294			0.8496			-	-	-	-	-
38.37		*0.9771*		*0.9746*	*0.9534*										
38.71					*0.9536*	*0.9290*		*0.9037*							
38.89		*0.9772*	*0.9768*		*0.9537*										
38.77	*0.9957*	*0.9772*	*0.9768*	*0.9748*	*0.9537*	*0.9291*	*0.9174*	*0.9038*	0.8655		0.8135				
39.31					*0.9540*		*0.9180*	*0.9046*							
39.64								*0.9050*		0.8492	0.8148				
50	0.9964	0.9805			0.9607			0.9195			0.8300	0.7264	0.5981	0.4239	-
100	0.9977	0.9883			0.9764			0.9524			0.9034	0.8533	0.8022	0.7514	0.5891

Table 54: Compressibility Factors used in the Calculation of the Results for Sample 4

	Pressure (bar)																	
Temp (deg C)	1	5	5.182066	*5.410822*	10	15.83703	17.27555	20	30.04403	33.60106	40	41.38383	45.62637	59.67035	60	61.69473	80	100	200
0	0.9933	0.9658			0.9294			0.8496			-				-		-	-	-
38.08											0.8125	0.8045			0.6962				
38.08		*0.9770*	*0.9761*		*0.9532*														
38.11		*0.9770*		*0.9751*	*0.9533*														
38.15								*0.8914*	0.8518		0.8126								
38.25					*0.9533*	*0.9240*		*0.9031*											
38.11	*0.9961*	*0.9786*			*0.9570*			*0.9117*	0.8619	0.8443	0.8125	0.8045	0.7798	0.6981	0.6962	0.6838	0.5496	0.3460	
38.53					*0.9535*		*0.9171*	*0.9035*											
38.80											0.8136		0.7810		0.6980				
38.83															0.6980	0.6857	0.5525		
39.17								*0.9044*		0.8430	0.8141								
50	0.9964	0.9805			0.9607			0.9195			0.8300				0.7264		0.5981	0.4239	-
100	0.9977	0.9883			0.9764			0.9524			0.9034				0.8533		0.8022	0.7514	0.5891

Table 55: Compressibility Factors used in the Calculation of the Results for S1

	Pressure (bar)																
Temp (deg C)	1	5	5.355112	5.397474	10	16.12784	17.11179	20	28.42448	30.1342	40	42.64702	44.19971	60	80	100	200
0	0.9933	0.9658			0.9294			0.8496			-			-	-	-	-
36.35		0.9765		0.9746	0.9522												
36.58		0.9766	0.9748		0.9523												
36.86	0.9956	0.9766	0.9749	0.9747	0.9525	0.9160	0.9160	0.9011			0.8107	0.7951		0.6930			
37.32								0.9018		0.8560	0.8114						
36.92								0.9012	0.8631		0.8108						
36.95					0.9525		0.9161	0.9013									
37.50											0.8116		0.7871	0.6947			
50	0.9964	0.9805			0.9607			0.9195			0.8300			0.7264	0.5981	0.4239	-
100	0.9977	0.9883			0.9764			0.9524			0.9034			0.8533	0.8022	0.7514	0.5891

Table 56: Compressibility Factors used in the Calculation of the Results for S2

	Pressure (bar)																					
Temp (deg C)	1	5	6.378859	6.356707	10	17.22796	17.59867	20	29.80068	31.29299	40	43.55682	47.94791	60	65.26672	66.08569	74.18047	74.55458	78.95426	80	80.32385	100	200
0	0.9933	0.9658			0.9294			0.8496			-			-						-		-	-
35.64											0.8089	0.7878		0.6900									
35.83		0.9748		0.9677	0.9487																		
35.92														0.6907	0.6512					0.5406			
36.10														0.6911			0.5849			0.5414			
36.12								0.9001	0.8558		0.8096												
36.29					0.9521	0.9147		0.9003															
36.17	0.9960	0.9783			0.9564			0.9104	0.8611	0.8535	0.8097	0.7886	0.7626	0.6913	0.6519	0.6458	0.5852	0.5824	0.5495	0.5416	0.5383	0.3333	
36.47		0.9765	0.9698		0.9522									0.6921		0.6467				0.5429			
36.49																							
36.71											0.8105		0.7637	0.6927									
36.77								0.9010		0.8499	0.8106												
36.79					0.9524		0.9134	0.9010															
36.86														0.6930				0.5849		0.5444			
37.29																				0.5462	0.5429	0.3406	
50	0.9964	0.9805			0.9607			0.9195			0.8300			0.7264						0.5981		0.4239	-
100	0.9977	0.9883			0.9764			0.9524			0.9034			0.8533						0.8022		0.7514	0.5891

Table 57: Compressibility Factors used in the Calculation of the Results for S3

	Pressure (bar)																					
Temp (deg C)	1	5	7.780959	7.993834	10	18.01778	18.14674	20	31.12084	31.41458	40	46.24393	46.6624	60	61.74557	62.12871	73.59368	73.73546	78.48128	80	80.31407	100	200
0	0.9933	0.9658			0.9294			0.8496			-			-						-		-	-
36.05					0.9520	0.9103		0.9000															
36.24		0.9765	0.9629		0.9521																		
36.34											0.8099	0.7730		0.6917									
36.36														0.6918	0.6787					0.5424			
36.48								0.9006		0.8490	0.8102												
36.55								0.9007	0.8504		0.8103												
36.62					0.9493		0.9098	0.9008															
36.67		0.9766		0.9621	0.9524																		
36.91														0.6932			0.5922			0.5447			
37.01														0.6934		0.6776				0.5451			
36.96	0.9956	0.9767	0.9632	0.9622	0.9525	0.9114	0.9108	0.9013															
36.96	0.9961	0.9785			0.9566			0.9109	0.8553	0.8538	0.8109	0.7742	0.7717	0.6933	0.6803	0.6775	0.5924	0.5914	0.5561	0.5449	0.5416	0.3385	
37.14											0.8111		0.7720	0.6938									
37.16														0.6938				0.5921		0.5457			
38.57																				0.5514	0.5483	0.3490	
50	0.9964	0.9805			0.9607			0.9195			0.8300			0.7264						0.5981		0.4239	-
100	0.9977	0.9883			0.9764			0.9524			0.9034			0.8533						0.8022		0.7514	0.5891

Table 58: Compressibility Factors used in the Calculation of the Results for S4

	Pressure (bar)																					
Temp (deg C)	1	5	7.590634	7.659994	10	17.77776	17.87432	20	31.09798	31.43781	40	58.83755	59.57208	60	73.40099	73.61111	78.67381	80.19916	80	100	200	
0	0.9933	0.9658			0.9294			0.8496			-			-					-	-	-	
37.17					0.9527	0.9129		0.9016														
37.21								0.9016	0.8515		0.8112											
37.32		0.9768	0.9643		0.9528																	
37.35											0.8114	0.7011		0.6943								
37.38														0.6944	0.5954				0.5466			
37.51		0.9768		0.9641	0.9529																	
37.35	0.9956	0.9768	0.9643	0.9640	0.9528	0.9131	0.9127	0.9018														
37.35	0.9961	0.9785			0.9567			0.9112	0.8558	0.8541	0.8114	0.7011	0.6968	0.6943	0.5952	0.5937	0.5563	0.5450	0.5465	0.3411		
37.65								0.9022		0.8506	0.8119											
37.68											0.8119		0.6976	0.6951								
38.71														0.6977				0.5505	0.5520			
37.72					0.9530		0.9131	0.9023														
37.93														0.6958		0.5958			0.5488			
50	0.9964	0.9805			0.9607			0.9195			0.8300			0.7264					0.5981	0.4239	-	
100	0.9977	0.9883			0.9764			0.9524			0.9034			0.8533					0.8022	0.7514	0.5891	

Table 59: Compressibility Factors used in the Calculation of the Results for S5

	Pressure (bar)																											
Temp (deg C)	1	5	5.20233	5.27654	5.467375	4.825699	10	16.94775	16.98521	12.86461	17.05332	20	29.38686	29.64258	22.5634	29.64045	40	43.56304	43.74322	27.49444	43.2167	60	59.09797	59.23765	70.7419	70.79846	80	100	200
0	0.9933	0.9658					0.9294					0.8496					-					-					-	-	-
38.07		*0.9770*			*0.9748*		*0.9532*																					
37.88		*0.9769*				*0.9778*	*0.9531*																					
38.30							*0.9534*				*0.9179*	*0.9031*																
37.69							*0.9530*			*0.9385*		*0.9023*																
37.08												*0.9014*			0.8899		0.8110											
36.88																	0.8107			0.8843		0.6931						
38.16												*0.9030*				0.8594	0.8126											
37.67																	0.8119				0.7931	0.6951						
37.82		*0.9769*		*0.9756*			*0.9531*																					
37.46																						0.6946	0.7012			0.5469		
37.59																	0.8118	0.7910				0.6949						
36.45																						0.6920			0.6114	0.5428		
37.37																						0.6943			0.6149		0.5465		
37.83		*0.9769*	*0.9760*				*0.9531*																					
37.91	*0.9957*	*0.9769*	*0.9760*	*0.9756*			*0.9531*	*0.9178*	*0.9178*			*0.9026*					0.8123	0.7915				0.6957						
37.91	0.9961	0.9786					0.9569					0.9115	0.8649	0.8637			0.8123	0.7915	0.7904			0.6957					0.5488	0.3447	
37.97																						0.6959		0.7015			0.5490		
38.60												*0.9036*		0.8600			0.8133												
37.86												*0.9025*	0.8601				0.8122												
38.19							*0.9533*		*0.9182*			*0.9030*																	
38.46																	0.8131		0.7914			0.6971						
50	0.9964	0.9805					0.9607					0.9195					0.8300					0.7264					0.5981	0.4239	-
100	0.9977	0.9883					0.9764					0.9524					0.9034					0.8533					0.8022	0.7514	0.5891

Table 60: Compressibility Factors used in the Calculation of the Results for L1

	Pressure (bar)																							
Temp (deg C)	1	5	4.470658	5.528445	5.467375	4.825699	10	16.90599	16.98499	12.86461	17.05332	20	30.10443	30.20115	20.00205	29.64045	40	43.51048	43.73277	27.49444	43.2167	60	80	100	200
0	0.9933	0.9658					0.9294					0.8496					-					-	-	-	-
38.12		0.9770			0.9748		0.9533																		
37.88		0.9769				0.9778	0.9531																		
38.30							0.9534				0.9179	0.9031													
37.69							0.9530			0.9385		0.9023													
37.08												0.9014			0.9014		0.8110								
36.88																	0.8107			0.8843		0.6931			
38.16												0.9030				0.8594	0.8126								
37.67																	0.8119				0.7931	0.6951			
37.42		0.9768		0.9743			0.9528																		
37.23																	0.8113	0.7907				0.6940			
37.85		0.9769	0.9795				0.9531																		
37.21	0.9956	0.9767	0.9793	0.9742			0.9527	0.9170	0.9170			0.9016					0.8112	0.7906				0.6939			
37.84												0.9025		0.8564			0.8121								
37.21												0.9016	0.8559				0.8112								
38.21							0.9533		0.9182			0.9030													
37.41																	0.8115		0.7897			0.6944			
50	0.9964	0.9805					0.9607					0.9195					0.8300					0.7264	0.5981	0.4239	-
100	0.9977	0.9883					0.9764					0.9524					0.9034					0.8533	0.8022	0.7514	0.5891

Table 61: Compressibility Factors used in the Calculation of the Results for L2

	Pressure (bar)																								
Temp (deg C)	1	5	5.077199	6.275005	5.467375	4.825699	10	17.23239	17.28263	12.86461	17.05332	20	34.17566	34.95417	20.00205	29.64045	40	43.5145	45.12136	27.49444	43.2167	60	58.28546	59.31194	80	100	200
0	0.9933	0.9658					0.9294					0.8496					-					-			-	-	-
38.12		0.9770			0.9748		0.9533																				
37.88		0.9769				0.9778	0.9531																				
38.30							0.9534				0.9179	0.9031															
37.69							0.9530			0.9385		0.9023															
37.08												0.9014			0.9014		0.8110										
36.88																	0.8107			0.8843		0.6931					
38.16												0.9030				0.8594	0.8126										
37.67																	0.8119				0.7931	0.6951					
37.27		0.9768		0.9706			0.9527																				
36.85																						0.6930	0.7058		0.5444		
36.91																	0.8108	0.7901				0.6932					
37.05		0.9767	0.9763				0.9526																				
37.23	0.9956	0.9767	0.9764	0.9706			0.9527	0.9155	0.9155			0.9017					0.8113	0.7907				0.6940					
37.92																						0.6957		0.7008	0.5488		
37.71												0.9023		0.8348			0.8120										
37.11												0.9015	0.8374				0.8111										
37.58							0.9529		0.9159			0.9021															
38.15																	0.8126		0.7828			0.6963					
50	0.9964	0.9805					0.9607					0.9195					0.8300					0.7264			0.5981	0.4239	-
100	0.9977	0.9883					0.9764					0.9524					0.9034					0.8533			0.8022	0.7514	0.5891

Table 62: Compressibility Factors used in the Calculation of the Results for L3

	Pressure (bar)																										
Temp (deg C)	1	5	5.608319	5.978495	6.698511	6.74729	10	17.42366	17.7327	17.63166	17.66348	20	31.50479	31.75173	31.14724	31.34924	40	46.29231	46.48438	46.96963	47.32004	60	72.74439	72.74819	80	100	200
0	0.9933	0.9658					0.9294					0.8496					-					-			-	-	-
35.69		0.9763			0.9680		0.9517																				
35.99		0.9764				0.9678	0.9519																				
36.15							0.9520				0.9123	0.9001															
36.23							0.9521			0.9125		0.9003															
36.28												0.9003			0.8499		0.8099										
36.35																	0.8100			0.7688		0.6918					
36.36												0.9004				0.8491	0.8100										
36.44																	0.8101				0.7669	0.6920					
40.47		0.9777		0.9732			0.9547																				
36.69																						0.6926	0.5978		0.5438		
37.09																	0.8110	0.7741				0.6936					
36.84		0.9766	0.9737				0.9525																				
37.14	0.9956	0.9767	0.9738	0.9720			0.9526	0.9131	0.9131			0.9015					0.8111	0.7742				0.6938					
36.69																						0.6926		0.5977	0.5438		
37.29												0.9017		0.8486			0.8113										
37.18												0.9016	0.8496				0.8112										
36.92							0.9525		0.9128			0.9012															
37.33																	0.8114		0.7734			0.6943					
50	0.9964	0.9805					0.9607					0.9195					0.8300					0.7264			0.5981	0.4239	-
100	0.9977	0.9883					0.9764					0.9524					0.9034					0.8533			0.8022	0.7514	0.5891

Table 63: Compressibility Factors used in the Calculation of the Results for L4

	Pressure (bar)																													
Temp (deg C)	1	5	6.237375	6.806242	6.698511	6.74729	10	17.24035	17.64315	17.63166	17.66348	20	31.1287	31.43889	31.14724	31.34924	40	46.42337	46.82865	46.96963	47.32004	60	61.71555	62.20051	73.55049	73.75844	78.6704	78.97953	80	100	200
0	0.9933	0.9658					0.9294					0.8496					-					-							-	-	-
35.69		0.9763			0.9680		0.9517																							
35.99		0.9764				0.9678	0.9519																							
36.15							0.9520				0.9123	0.9001																		
36.23							0.9521			0.9125		0.9003																		
36.28												0.9003			0.8499		0.8099													
36.35																	0.8100			0.7688		0.6918								
36.36												0.9004				0.8491	0.8100													
36.44																	0.8101				0.7669	0.6920								
36.23		0.9765		0.9676			0.9521																							
36.14																						0.6912	0.6784						0.5415		
36.38																	0.8100	0.7720				0.6918								
36.39																						0.6919				0.5891			0.5425		
35.84																						0.6905			0.5887				0.5403		
35.75																						0.6902					0.5499		0.5399		
36.43																						0.6920						0.5503	0.5427		
36.64		0.9766	0.9706				0.9523																							
36.77	0.9956	0.9766	0.9706	0.9679			0.9524	0.9131	0.9131			0.9010					0.8106	0.7728				0.6928								
36.59																						0.6924		0.6760					0.5434		
36.88												0.9012		0.8494			0.8107													
36.63												0.9008	0.8505				0.8104													
36.70							0.9524		0.9130			0.9009																		
36.77																	0.8106		0.7704			0.6928								
50	0.9964	0.9805					0.9607					0.9195					0.8300					0.7264							0.5981	0.4239	-
100	0.9977	0.9883					0.9764					0.9524					0.9034					0.8533							0.8022	0.7514	0.5891

Table 64: Compressibility Factors used in the Calculation of the Results for L5

	Pressure (bar)																													
Temp (deg C)	1	5	5.469675	5.526911	6.698511	6.74729	10	14.75781	17.47322	17.63166	17.66348	20	25.0318	29.8154	31.14724	31.34924	40	37.82556	45.87822	46.96963	47.32004	60	52.29202	60.43095	68.12595	71.94558	76.15718	76.59187	80	100	200
0	0.9933	0.9658					0.9294					0.8496					-					-							-	-	-
35.69		0.9763			0.9680		0.9517																							
35.99		0.9764				0.9678	0.9519																							
36.15							0.9520				0.9123	0.9001																		
36.23							0.9521			0.9125		0.9003																		
36.28												0.9003			0.8499		0.8099													
36.35																	0.8100			0.7688		0.6918								
36.36												0.9004				0.8491	0.8100													
36.44																	0.8101				0.7669	0.6920								
36.60		0.9766		0.9740			0.9523																							
35.78																						0.6903	0.7482						0.5401		
35.85																	0.8092	0.8221				0.6905								
35.91																						0.6906				0.6010			0.5406		
35.98																						0.6908			0.6299				0.5409		
36.34																						0.6917					0.5711		0.5423		
36.41																						0.6919						0.5681	0.5426		
36.70		0.9766	0.9743				0.9524																							
36.39	0.9956	0.9765	0.9742	0.9739			0.9522	0.9135	0.9135			0.9005					0.8100	0.8229				0.6919								
36.00																						0.6909		0.6876					0.5410		
36.55												0.9007		0.8563			0.8103													
36.02												0.9000	0.8772				0.8095													
36.80							0.9524		0.9140			0.9010																		
36.24																	0.8098		0.7750			0.6915								
50	0.9964	0.9805					0.9607					0.9195					0.8300					0.7264							0.5981	0.4239	-
100	0.9977	0.9883					0.9764					0.9524					0.9034					0.8533							0.8022	0.7514	0.5891

Table 65: Compressibility Factors used in the Calculation of the Results for L6

	Pressure (bar)																						
Temp (deg C)	1	5	4.441909	5.487159	10	16.28133	17.10231	20	30.56797	31.04063	40	46.75859	47.13666	60	61.90384	62.08946	73.55727	73.79399	79.01271	79.32664	80	100	200
0	0.9933	0.9658			0.9294			0.8496			-			-							-	-	-
36.49		0.9765		0.9742	0.9522																		
36.53														0.6922			0.5911				0.5431		
36.57														0.6923	0.6781						0.5433		
36.58														0.6923					0.5507		0.5433		
36.59											0.8103	0.7705		0.6924									
36.91		0.9767	0.9793		0.9525																		
36.82	0.9956	0.9766	0.9793	0.9743	0.9525	0.9160	0.9160	0.9011			0.8107	0.7709		0.6930									
37.01														0.6934		0.6779					0.5451		
37.12								0.9015		0.8516	0.8111												
36.62								0.9008	0.8530		0.8104												
37.11					0.9526		0.9163	0.9015															
37.02											0.8109		0.7690	0.6935									
37.19														0.6939				0.5918			0.5458		
37.25														0.6940						0.5510	0.5460		
50	0.9964	0.9805			0.9607			0.9195			0.8300			0.7264							0.5981	0.4239	-
100	0.9977	0.9883			0.9764			0.9524			0.9034			0.8533							0.8022	0.7514	0.5891

Appendix B– Derivation of He Stereo Pycnometer Equation

Assume ideal gas behaviour and let the initial state be denoted by 2 and the final state be denoted by 3. Therefore:

$$\frac{P_2V_2}{n_2RT_2} = \frac{P_3V_3}{n_3RT_3} \quad \text{B1}$$

Where:

P is the pressure in the system
V is the volume of the system
n is the number of moles of gas in the system
R is the ideal gas constant
T is the temperature of the system

As it is a closed system the number of moles in the initial state will equal the number of moles in the final state. The temperature in the initial and final state will be equal as the system is allowed to come to equilibrium in both states and there is no reaction or external source or drain of energy. Therefore equation A1 simplifies to:

$$P_2V_2 = P_3V_3 \quad \text{B2}$$

When a sample is placed in the sample cell of the Pycnometer then:

$$V_2 = V_C - V_P \quad \text{B3}$$

After the expansion of the He into the additional volume in the Pycnometer then:

$$V_3 = V_C - V_P + V_A \quad \text{B4}$$

Where:

V_P is the volume of the particle placed in the Pycnometer (cm^3)
V_C is the volume of the sample cell of the Pycnometer (cm^3)
V_A is the added volume available for the expansion of the He into the adjoining cell of the Pycnometer (cm^3)

Substituting A3 and A4 into A2 yields:

$$P_2V_C - P_2V_P = P_3V_C - P_3V_P + P_3V_A \quad \text{B5}$$

Solving for V_P yields:

$$V_P = \frac{P_3V_C + P_3V_A - P_2V_C}{(P_3 - P_2)} \quad \text{B6}$$

Dividing the numerator and denominator by P_3:

$$V_P = \frac{V_C + V_A - \frac{P_2}{P_3}V_C}{\left(1 - \frac{P_2}{P_3}\right)} \quad \text{B7}$$

Finally V_C can be taken out of two terms in the numerator and then the equation simplifies to:

$$V_P = V_c + \frac{V_A}{\left(1 - \frac{P_2}{P_3}\right)} \quad \text{B8}$$

Appendix C– Coal Analyses Results

The full results of the analyses that were not presented in the main body of the report are below.

Coal Moisture Determination

ALS Laboratory group

ALS Witbank - Coal division
Registration No. 2003 / 009138 / 07

TO WITS UNIVERSITY

Analyses Report

Coal and Mineral Analysts
P.O.Box 1569, Witbank 1035
Tel : 013 692 8000
Fax : 013 692 5609
e-mail : laboratory@witlab.co.za

Date 2011/05/06
Job No. 438/11-1

			Analysis on an Air Dry Basis							
Lab.no.	Sample name	Description	Inherent Moisture %	Ash %	Volatile Matter %	Fixed carbon %	Calorific Value MJ/kg	Total sulphur %	Surface H2O %	Total H2O %
			ISO 11722: 1995	ISO 1171: 1997	ISO 562 1998	By Difference	ISO 1928 2009	ASTM D4239-05	ISO589 2008	ISO589 2008
519230	WITS UNIVERSITY JOB NO:438/11-1	COAL SAMPLE							0.8	6.3

sanas Testing Laboratory T 0478

Technical Signature

Page 1 of 1

Note :- Analysis marked with * are excluded from the schedule of accreditation

1. The results reported relate only to those items listed.
2. This analyses report may only be reproduced in full, unless prior written consent of Witlab (Pty) Ltd is obtained.
3. This document is not intended to relieve the parties from their contractual obligations or any sales contract.
4. This Document is issued in accordance with the Principal's instructions and is subject to the Standard Terms and Conditions of Business of Witlab (Pty) Ltd. (A copy is available on request)
5. Liability shall be limited to an amount equal to the fee paid for this service and claims in respect of this document will only be considered if based on proven gross negligence.

Figure 38: ALS laboratory group coal moisture determination analysis results

Appendix D – Results of Blank Runs to Quantify Equipment Leakage

Table 66 contains the results of the leakage test that was conducted the 31st July to the 1st August 2012 to adjust the results from the adsorption experimentation on particle S1. There is no data for the end of the first pressure step as the equipment stopped running and logging data. The run was restarted from the second pressure step, in line with the contingency plan for equipment stoppage. The leakage rate during the first pressure step was calculated from the leakage rate of the other pressure steps with correction for the reduced pressure in the first pressure step. This correction was performed as the pressure difference between the equipment and the atmosphere would be the driving force for the equipment leakage. It would have been preferable if the data had been logged, but in the absence of this, a leakage rate needed to be determined for the first pressure step of the experimental run.

Table 66: Blank Run to quantify leakage of the adsorption experimentation on particle S1

	Initial			Final				
	Pressure (bar)	**Temp (°C)**	**Moles CO_2 (mol)**	**Pressure (bar)**	**Temp (°C)**	**Moles CO_2 (mol)**	**Moles leaked:**	**Pressure leak:**
P Step 1	5.353	36.368	0.010					
P Step 2	17.173	37.275	0.036	15.022	36.626	0.031	0.005	2.151
P Step 3	30.474	37.148	0.067	25.523	36.350	0.055	0.012	4.951
P Step 4	45.927	36.884	0.113	37.630	36.107	0.087	0.026	8.297

Table 67 contains the results of the leakage tests conducted from the 11th to the 13th September 2012. The equipment had just returned from repair at NECSA and was operating with minimal leakage. The column of interest is the pressure in the sample cell. The gain in pressure from the first to second value would occur as a result of the system temperature increasing to the temperature of the constant temperature oven in which both the reference and sample cells are held. It can be seen that the equipment leakage is very low in comparison to other experimental runs.

Table 67: Leakage testing of the adsorption equipment from the 11th to 13th September 2012

Date and Time	Reference Cell (bar)	Sample Cell (bar)
11 September 15:30	47.5	47.9
12 September 10:00	47.3	48.9
12 September 12:30	47.3	48.8
13 September 10:00	47.0	48.6

Table 68 contains the results of the blank test that was conducted from the 21st to the 22nd September 2012. The equipment completed five pressure steps. The sixth pressure step was started but was not completed.

Table 68: Blank run to quantify leakage of the adsorption equipment conducted from 21st to 22nd September 2012

	Initial			Final				
	Pressure (bar)	Temp (°C)	Moles CO_2 (mol)	Pressure (bar)	Temp (°C)	Moles CO_2 (mol)	Initial - Final pressure	Leak rate (Bar/hr)
P Step 1	5.457	38.068	0.011	4.826	37.880	0.009	0.631	0.210
P Step 2	17.053	38.297	23.590	12.865	37.690	0.026	4.189	1.396
P Step 3	29.640	38.162	0.065	22.563	37.215	0.048	7.077	2.359
P Step 4	43.217	37.672	0.103	27.494	36.883	0.059	15.722	5.241
P Step 5	58.262	37.173	0.158	37.332	36.724	0.090	20.930	6.977

Table 69 contains the result of the blank run conducted to correct experimentation from the 30th October 2012 to the 4th November 2012. Due to time constraints with equipment availability the blank run could not be run for the full three hours equilibration time at each step. Thus a leakage rate in bar/hr has been determined for the equipment.

Table 69: Blank run to quantify leakage of the adsorption equipment during experimentation conducted from 30th October to 4th November 2012

	Initial			Final			
	Pressure (bar)	Temp (°C)	Moles CO_2 (mol)	Pressure (bar)	Temp (°C)	Moles CO_2 (mol)	Leak rate (Bar/hr)
P Step 1	6.699	35.693	0.013	6.747	35.995	0.013	-0.016
P Step 2	17.663	36.152	0.037	17.632	36.232	0.037	0.096
P Step 3	31.349	36.359	0.070	31.147	36.280	0.070	0.607
P Step 4	47.320	36.438	0.118	46.970	36.349	0.116	1.052
P Step 5	62.172	36.519	0.175	61.825	36.393	0.174	1.044
P Step 6	73.845	36.624	0.239	73.718	36.436	0.238	1.221
P Step 7	79.284	37.156	0.274	78.818	36.448	0.273	1.399